THE INFLUENCE OF DISSOLVED ORGANIC CARBON AND pH ON THE PHOTODEGRADATION OF METHYLMERCURY IN LAKE WATERS

Maya Spitz

Thesis submitted to the
Faculty of Graduate and Postdoctoral Studies
in partial fulfillment of the requirements
for the Master of Science degree in Biology

Department of Biology
Ottawa-Carleton Institute of Biology
Faculty of Science
University of Ottawa

ABSTRACT

Photodegradation rates of methylmercury (MeHg) were measured in water samples from several lakes in the Lake Berthelot region in Quebec in order to investigate the impact of drainage basin logging and associated changes in dissolved organic carbon (DOC) concentrations on MeHg levels in lake water. The lakes were selected on the basis of the amount of logging that had previously taken place in the drainage basin, and on DOC levels which were correspondingly higher in logged lakes due to increased runoff. Lakes DA9 and DF9 had DOC concentrations of 12.3 and 20.9 ppm, respectively and were designated as high DOC for the purposes of this study. Lakes N55 and N70 had DOC concentrations of 6.9 and 6.8 ppm, respectively and were designated as low DOC lakes. Experiments were conducted with both ambient and 2 ppt spiked MeHg levels in the high and low DOC lakes to determine whether the spiked levels reflect photodegradation patterns occurring in nature. The effect of different sized DOC fractions on photodegradation rates were also examined. Upon spiking, the binding of added MeHg reached equilibrium virtually immediately (within minutes) for all size fractions.

It was hypothesized that less photodegradation of MeHg would be found in high DOC lakes than in low DOC lakes. In contrast to expected results, no photodegradation was observed in the two lower DOC lakes, but there was photodegradation in the two higher DOC lakes. Hypothesizing that larger size fractions of DOC would result in lower methylmercury (MeHg) photodegradation

rates, water samples were fractionated into three DOC size fractions (300 kDa, 30 kDa, and 5 kDa). In the two high DOC lakes in which photodegradation was detected, DOC size fractions had an effect on photodegradation rates, though this effect varied. Average k values (hr^{-1}) for DA9 were -1.25×10^{-1} for the 5 kDa fraction, -1.16×10^{-1} for the 30 kDa fraction, and -9.21×10^{-2} for the 300 kDa fraction, indicating a decrease in photodegradation rates with larger fractions. For DF9, average k values were -1.69×10^{-1} for the 5 kDa fraction, -6.38×10^{-2} for the 30 kDa fraction, and -1.34×10^{-1} for the 300 kDa fraction, which does not indicate a clear trend in photodegradation rates with respect to DOC size fraction. A comparison of samples from a wetland outflow using ambient MeHg levels demonstrated that 300 kDa DOC fractions showed no photodegradation while 5 kDa DOC showed photodegradation with a k value of -9.12×10^{-2} (hr^{-1}). Overall, watershed logging status was found not to affect MeHg photodegradation rates in the lakes studied.

A possible contributor to the variation in photodegradation rates between lakes was postulated to be pH, with H^+ ions displacing MeHg from binding sites on DOC and rendering it available for photodegradation. To study the relationship between rates of photodegradation and pH, water samples were adjusted to pH values of approximately 4.5, 6.5, and 7.5 and incubated in sunlight. Rates of photodegradation increased with decreasing pH conditions in all lakes, except for one lake (N55) which also had no detectable photodegradation during the initial field trials. In the remaining three lakes studied, however, lower pH values (4.1-4.6)

resulted in greater photodegradation than higher pH values that resulted in little or no photodegradation. It appears that this effect only occurs in lakes with a potential for photodegradation.

As results suggested that the size of DOC controls rates of photodegradation, samples were analyzed for the size of DOC and corresponding MeHg content using tangential flow ultrafiltration (TFUF). The efficacy of the TFUF system as a means of both removing microbes as well as fractionating DOC into differing size fractions was evaluated. Results indicated that this is an effective field-portable method. Mass balances for MeHg recovery after filtering large volumes of water were found to be 96% for the 5 kDa filter, 81% for the 30 kDa filter, and 109% for the 300 kDa filter, while flow rates decreased by 26%, 17%, and 50% respectively. Potential artifacts of DOC fractionation using the TFUF were investigated. The amount of DOC passing through the filter was found to decrease with increasing volume of filtrate that passed through the membrane.

RESUME

Les niveaux de photodégradation du méthylmercure (MeHg) ont été mesurés dans des échantillons d'eau pris dans des lacs de la région du Lac Berthelot au Québec, afin d'étudier l'impact de l'exploitation forestière dans les bassin-versants et les concentrations de carbone organique dissous (COD), sur les niveaux de MeHg dans l'eau des lacs. Les lacs ont été sélectionnés en se basant sur le degré d'exploitation forestière dans les bassin-versants et sur les niveaux de COD, lesquels augmentent dans les lacs avec exploitation forestière en raison d'un plus grand écoulement de surface. Les lacs DA9 et DF9 avaient des concentrations de COD de 12.3 et 20.9 ppm respectivement, et ils ont été désignés, dans le cadre de cette étude, comme des lacs à haut niveau de COD. Les lacs N55 et N70 avaient des concentrations de COD de 6.9 et 6.8 ppm respectivement, et ont été désignés comme des lacs à bas niveau de DOC. Des expériences ont été menées sous des conditions ambiantes et avec des niveaux augmentées à 2 ppt de MeHg dans les lacs de haut et bas niveau de COD afin de comparer si les niveaux de pointe refletaient ce qui se produit sous les conditions ambiantes. L'effet des fractions sur les différents niveaux de COD et sur les taux de photodégradation a également été examiné. Nous avons observé qu'apres l'addition de MeHg un état d'équilibre était atteint presque immédiatement (en quelques minutes) pour toutes les fractions. L'hypothèse émise était que moins de photodégradation de MeHg serait trouvé dans des lacs à haut niveau COD, en comparaison avec les lacs à bas niveau de COD.

Contrairement aux résultats attendus, une photodégradation n'a pas été observée dans les deux lacs à bas niveau de COD, mais il y avait une photodégradation dans les

deux lacs à haut niveau de COD. En partant de l'hypothèse que les plus grandes fractions de COD vont résulter en un plus bas taux de photodégradation de méthylmercure (MeHg), les échantillons d'eau ont été fractionnés en trois niveaux de COD (300 kDa, 30 kDa et 5 kDa). Dans les deux lacs à haut niveau de COD où la photodégradation a été détectée, les fractions possédant différents niveaux de COD ont demontré un effet sur les taux de photodégradation, mais cet effet était variable. Les valeurs moyennes de k (hr^{-1}) pour DA9 étaient : 1.25×10^{-1} pour la faction de 5 kDa, -1.16×10^{-1} pour la fraction de 30 kDa et -9.21×10^{-2} pour la fraction de 300 kDa, ce qui démontre une diminution du taux de photodégradation avec les plus grandes fractions. Pour DF9, les valeurs moyennes de k étaient : 1.69×10^{-1} pour la fraction de 5 kDa, -6.38×10^{-2} pour la fraction de 30 kDa et -1.34×10^{-1} pour la fraction de 300 kDa, ce qui n'indique pas une tendance claire pour les taux de photodégradation en relation avec les fractions possédant différents niveaux de COD. Une comparaison a été effectuée avec des échantillons des écoulements de terrain marécageux à niveau ambiant de MeHg a démontré que les fractions de 300 kDa ne montraient pas de signe de photodégradation, alors que celles de 5 kDa montraient une photodégradation avec une valeur k de 9.12×10^{-2} (hr-1). Il semble que l'exploitation forestière dans les bassin-versants n'a pas un effet sur les taux de photodégradation dans les lacs qui étaient étudié.

Un contributeur possible de la variation des taux de photodégradation entre les lacs peut être le pH, car les ions de H^+ peuvent déplacer le MeHg des sites de liaison du COD et le rendre assimilable lors de la photodégradation. Afin d'étudier la relation entre les taux de photodégradation et le pH, des échantillons d'eau ont été ajustés à

des valeurs de pH d'environ 4.5, 6.5 et 7.5 et incubés sous la lumière solaire. Nous avons observé que les taux de photodégradation se sont accrus avec une diminution des conditions de pH dans tous les lacs, sauf un (N55), lequel n'avait pas de photodégradation détectable pendant les essais initiaux sur le terrain. Par ailleurs, il a été découvert que le pH jouait un rôle dans les trois autres lacs étudiés, les basses valeurs de pH (4.1-4.6) résultant en une plus grande photodégradation alors que les hautes valeurs de pH résultent en peu ou pas de photodégradation. Il semble que cet effet se produise seulement dans les lacs avec un potentiel de photodégradation.

Comme les résultats suggèrent que le niveau de COD est une variable contrôlant les taux de photodégradation, les échantillons ont été analysés pour observer le niveau de COD et le contenu de MeHg correspondant, en utilisant l'ultrafiltration tangentielle (TFUF). L'efficacité du système TFUF a été évaluée comme moyen d'enlever les microbes de nos échantillons et de fractionner le COD dans des fractions de différents niveaux. Les résultats ont indiqué que c'est une méthode portative efficace sur le terrain. Le bilan de masse pour la récupération de MeHg après la filtration de larges volumes d'eau était de 96% pour le filtre de 5 kDa, 81% pour le filtre de 30 kDa et 109% pour le filtre de 300 kDa, alors que les taux de débit ont diminué de 26%, 17% et 50% respectivement. Les potentiels d'artéfacts de fractionnement de COD en utilisant le TFUF ont été étudiés. La quantité de COD passant dans le filtre diminuait avec des volumes croissant de filtrat qui étaient passés à travers la membrane.

ACKNOWLEDGEMENTS

Funding for this project was provided by the Sustainable Forest Management Network, and is part of the sub-theme on Riparian Ecosystems for the Canadian Networks of Centres of Excellence for Sustainable Forestry.

I would like to thank my supervisor Dr. David Lean for his guidance and for giving me the opportunity to join his laboratory when I was coming in from a widely differing field. Thanks also to my research committee members Dr. Thor Arnason and Dr. Andy Rencz for their feedback and advice. Thanks also to Dr. Danielle Fortin for joining my defense committee and for providing feedback. My thanks to Steven Siciliano for his assistance with the initial project design as well as during the long hours of work in the field during my first summer. Many thanks to Dr. Scott Findlay for his patient assistance in the demystifying of statistics; his dedication under the most difficult of circumstances to the many students who have trooped to his door deserves all of our respect and gratitude. Thanks to Susan Winch and Jonathan Hill for their assistance and for being such effective sounding boards during this whole adventure. All members of the lab have made this a memorable experience in every way with camaraderie, support and humour throughout the trials and successes of research.

Ottawa Police Service Chief Vince Bevan also has my deepest regards and gratitude for seeing promise and possibility in this project, and for enthusiastically supporting

my plunge into unknown professional waters. My work supervisor Sgt. Ron Tucker has shown great support and understanding for me during this time, both with long talks and with endlessly juggling my shift schedule to suit my lab schedule. My deepest thanks to him.

Thanks to all those people in my personal life who have supported me in this endeavor and have provided ceaseless encouragement and enthusiasm each step of the way. My family has shown a constant interest in my research, and a willingness to hear all about the accompanying adventures. They have surmounted the many hurdles along with me. Last of all, my most heartfelt thanks to my now husband Mark Lowes. He has provided the substructure that has supported me throughout the last two years. Thanks for enthusiastically jumping into the world of toxicology with me, as well as for the "UN" food drops late at night in the lab. You have given me unceasing encouragement and support throughout this project, and during all my endeavours in life. I thank you for this, and hope that in our future to come I can give you as much as you have given me.

TABLE OF CONTENTS

LIST OF ABBREVIATIONS

CDOM .....coloured dissolved organic material
DAPI .....4′6-diamidino-2-phenylindole
DCM .....dichloromethane
DGM .....dissolved gaseous mercury
DIC .....dissolved inorganic carbon
DIW .....deionized water
DNA .....deoxyribonucleic acid
DOC .....dissolved organic carbon
DOM .....dissolved organic matter
F .....filtrate
FA .....fulvic acid
GC/AFS .....gas chromatography atomic fluorescence spectroscopy
HA .....humic acid
HS .....humic substances
ISC .....intersystem crossing
kDa .....kilodalton
PAR .....photosynthetically "available" radiation
ppb .....parts per billion
ppq .....parts per quadrillion
ppt .....parts per trillion
PSI .....pounds per square inch
R .....retentate
SCF .....sulfhydril cotton fibre
TFUF .....tangential flow ultrafiltrator
V_0 .....initial volume
Vr .....retentate volume

LIST OF TABLES

LIST OF FIGURES

1.0 INTRODUCTION AND LITERATURE REVIEW

1.1 INTRODUCTION TO THESIS

With mercury a pollutant of global concern, elucidation of the mercury cycle, particularly the fate of its most toxic form, methylmercury (MeHg), is crucial. MeHg is the only form which is biomagnified in the food chain. Most large fish in Canadian lakes exceed the human consumption guidelines for MeHg (Morel *et al.*, 1998). Knowledge of its sources and sinks is a prerequisite to developing methods to lower MeHg levels in aquatic systems.

There are a number of sources of MeHg in lake water, including watershed runoff. Watershed characteristics and perturbations therefore have an effect on MeHg levels in lake water. Logging and forest fire in particular have been investigated with respect to MeHg and DOC levels in lake systems. It was found that while logging increased both MeHg and DOC levels, forest fires did not lead to increased levels (Carignan *et al.*, 2000; Garcia and Carignan, 1999), indicating that factors other than solely the absence of trees were having an impact. Studies have also linked high levels of DOC and water colour with corresponding high levels of MeHg in general (Watras *et al.* 1995; Lee and Iverfeldt, 1991; Mierle and Ingram, 1991; Driscoll *et al.*, 1995; Faust, 1992). Along with the binding and transport of MeHg, DOC has also been cited as attenuating ultraviolet light (Scully and Lean, 1994; Crump *et al.*, 1999), which is responsible for the photodegradation of MeHg (Sellers and Kelly, 2001). In addition to this, the higher the

concentration of humic substances, the larger the proportion of MeHg present that is bound to it (Petersson *et al.*, 1995).

MeHg has been found to bind preferentially to larger size DOC (Gilmour and Henry, 1991; Hintelmann *et al.*, 1995; Hintelmann *et al.*, 1997). It was expected that due to the greater binding, MeHg associated with the larger size fractions would photodegrade less. This study explored this trend, and examined the effect of different size DOC fractions separated using tangential flow ultrafiltration (TFUF), on rates of photodegradation. The role of pH was also explored as a factor influencing photodegradation rates. H^+ ions can likely replace MeHg on binding sites on DOC, thereby rendering MeHg available to be degraded, or alternatively taken up the food chain. This process is important to elucidate, in view of acid rain impacts on lake systems. In support of this hypothesis, it has been found that with decreasing pH, the percentage of free MeHg compounds increases (Hintelmann *et al.*, 1995), and MeHg levels in fish are inversely related to pH (Winfrey and Rudd, 1990), indicating the increased mobilization and bioavailability of MeHg with decreased pH.

To further the research of MeHg, the effect of watershed logging on the photodegradation of MeHg in lakes was explored. In particular, the effects of both dissolved organic carbon (DOC) levels and of pH on this mechanism of MeHg removal from lake waters, were investigated. Lakes whose watersheds have and have not been logged were compared, as were differing size fractions of DOC. The appropriateness of tangential flow ultrafiltration for this research was also assessed, both for fractionating DOC into

different size categories, and for removing microbes from the samples examined. The following literature review provides background information for the research project, including sinks (focusing on photodegradation) and sources of MeHg, and an overview of DOC and its importance in the aquatic MeHg cycle.

1.2 LITERATURE REVIEW

1.2.1 Mercury Global Cycle

Mercury is a metallic element occurring naturally in the earth's crust. However it is also mobilized more quickly through human activities, including watershed logging as explored in Garcia and Carignan (1999). Its toxicity in the methylated form, along with its global transport in its gaseous form, makes it a pollutant of international concern. Anthropogenic sources of mercury include coal fuel generation stations, metal production, chlor-alkali and pulp industries, waste handling and treatment, and coal, peat, and wood burning (Lindqvist *et al.*, 1991). Natural sources are degassing and wind entrainment of dust particles from land, especially from mercuriferous areas, volcanic eruptions, forest fires, biogenic emissions and evasion from water surfaces (Rasmussen, 1994).

Though anthropogenic emissions have been drastically reduced since the early 1960's, mercury levels have not yet shown significant reductions in fish and wildlife (Pleijel and Munthe, 1995). It has been found in relatively high concentrations in the tissues of fish found in North American lakes with no obvious sources of mercury contamination (Sellers and Kelly, 2001). This may be at least partly due to the leaching of accumulated mercury of anthropogenic origins from the soil into the aquatic systems for re-cycling

(Pleijel and Munthe, 1995). Mercury in the atmosphere is primarily found (approximately 95%) in its elemental Hg^0 form. This form has a background concentration of 2 to 4 ng/m^3 in the northern hemisphere (Pleijel and Munthe, 1995). Hg^0 is slowly oxidized in the atmosphere to the mercuric (Hg^{2+}) state. This occurs at the solid-liquid interface in fog and cloud droplets, with ozone likely the main oxidant in this process. Oxidation by Cl_2 and H_2O_2 may also be significant (Morel *et al.*, 1998). The mercuric ion may then return to earth in precipitation. Hg^0 has an atmospheric lifetime of approximately 1-2 years, while Hg(II) has a lifetime of several days to weeks (Lindqvist and Rodhe, 1985).

Besides elemental mercury, the major forms of mercury in water are ionic mercury (bound to chloride, sulphide, hydroxyl ions, or organic acids) and organic mercury, particularly methylmercury (CH_3Hg^+) (Morel *et al.*, 1998). It was found in a study of Wisconsin lakes that Hg^0 averaged 3% of the measured total mercury. Chloride has a significant impact on mercury behaviour in aqueous solutions due to its ability to form stable complexes with Hg(II). It can complex with Hg adsorbed to the surfaces of sediments, resulting in its desorption and dispersal into the solution phase (Wang *et al.*, 1991). MeHg accounts for up to 25% of total mercury in surface waters, but is typically near 1%. Generally, the percentage of MeHg does not appear to be a function of total mercury levels. However the percentage does change with respect to surface versus anoxic bottom waters, with 37% in bottom waters of a pristine lake (Bloom, 1989), and 58% in the anoxic hypolimnion of a contaminated lake (Parks *et al.*, 1989). MeHg levels are found to be highest in the fall and lowest in the spring, and MeHg is found to be more particle-reactive than Hg (Watras *et al.*, 1995).

1.2.2 Methylmercury

In acidic, low salinity water, CH_3HgCl is the dominant MeHg species, but an increase in sulphide and thiol concentrations (one hundred-fold from lowest levels of 0.1nM) or an increase in pH to neutral or slightly alkaline conditions results in a total dominance of CH_3HgSH and CH_3HgSR (Dryssen and Wedborg, 1991). Faust (1992) has demonstrated that the octanol/water distribution coefficient of methylmercuric species shifts sharply from acidic pH to basic pH about the neutral point, with CH_3HgOH^0 predominant at basic pH, and CH_3HgCl^0 predominant at acidic pH. This, he states, is driven by the pH-dependent aqueous phase speciation shifts between CH_3HgCl^0 and CH_3HgOH^0. He speculates that the difference in partition coefficients is due to CH_3HgOH^0 forming stronger hydrogen bonds with water than 1-octanol, and also to the enhanced interaction with the "hydrocarbon tail" of 1-octanol by the Cl group. However note that the very high affinity of MeHg with sulfhydril groups (R-SH) could lead to greater bioaccumulation than that predicted by octanol/water distribution coefficients.

For lakes, Mason *et al.* (1995) postulated the following mechanism for MeHg biomagnification. It has been found that MeHg accumulates in the cytoplasm of phytoplankton, while Hg^{2+} is sequestered by the algal membranes, likely through binding with thiol groups. Zooplankton then digest the dissolved cytoplasmic contents, but excrete the membrane material, resulting in four times the accumulation of MeHg over inorganic mercury. The reactivity of MeHg with membrane components is lower than that of inorganic mercury, resulting in further favored uptake up the food chain (Mason *et al.*, 1995). The proportion of total mercury present as MeHg has been found to increase

from less than 1% in plants to 94% in piscivorous fish (Bowles *et al.*, 2001). Therefore, though the main discrimination occurs through the trophic transfer, the major enrichment occurs between the water and phytoplankton.

Methylmercury has a strong affinity for sulphur-containing amino acids, and as virtually all proteins contain sulfhydril groups (SH), methylmercury can inhibit the functioning of these proteins (Rand and Petrocelli, 1985; Chakrabarti *et al.*, 1997). In toxic doses, it causes neurological and developmental disorders in humans (Egeland and Middaugh, 1997; Pleijel and Munthe 1995). These disorders include enzyme inhibition, neurotransmitter binding, disruption of cell membranes, structural protein damage, and genetic mechanism alteration in a variety of tissues, including nervous tissues. The conventional explanation is that MeHg binds to protein which is consumed and transported, usually associated with cysteine at the target centers (ie. brain tissue).

1.2.3 Sinks of Methylmercury

The mercury levels in a system are a result of balances between uptake or production processes, and removal or degradation processes. There are a number of ways mercury is removed from aquatic systems. Hg^0 can volatilize from the surface of waters to the atmosphere (Amyot *et al.*, 1994). Sunlight has been found to enhance Hg^0 production in lake waters in general, via biological (Siciliano *et al.*, 2002) or photochemical processes, thereby removing mercury from the system (Amyot *et al.*, 1994; Amyot *et al.*, 1999). Experiments in the production of dissolved gaseous mercury (DGM) via the photoreduction of Hg(II) found that DGM concentrations up to 20 times higher than

natural levels could be achieved via the addition of Hg (II) complexes in sunlight exposed bottles. Therefore the evolution of DGM appears to be limited solely by substrate (photoreducible Hg) availability and light intensity (Amyot *et al.*, 1997). However, low levels of DGM production that were observed in high DOC lakes could be due to the DOC complexation of Hg, or to the attenuation of UV by the DOC (Amyot *et al.*, 1997). Studies have shown DGM production to be higher in July, while on a daily cycle a narrow peak occurred at sunrise. This suggests that photoreduction of Hg(II) occurred, but that the substrate wass rapidly depleted (Amyot *et al.*, 2000). The abiotic reduction of Hg(II) and Hg(I) into Hg^0 can also be via humic and fulvic acids (Costa and Liss, 1999). This process also appears to be photoenhanced (Allard and Arsenie, 1991), with UV radiation and fulvic acid reducing more Hg(II) than UV radiation alone. It is not clear if the fulvic acid acts as a photosensitizer initializing the reaction through electron or energy transfer, or if it is a complexing agent with photolysis acting on the humic-Hg complex directly (Xiao *et al.*, 1995).

Mercury-resistant bacteria also reduce the mercuric ion to volatile Hg^0 as their primary means of detoxification (Korthals and Winfrey, 1988). At the natural mercury concentrations in the low picomolar range, reduction to Hg^0 seems to be effected chiefly by photochemical processes, though microbial activity also plays a role, as recently demonstrated (Siciliano *et al.*, 2002). In polluted waters, when the mercury concentration exceeds 50pM, microbial processes (sulfate-reducing bacteria are likely forming several mercury species) are likely the predominant mechanism of Hg(II) reduction (Morel *et al.*, 1998).

1.2.4 Sources of Methylmercury

There are three important sources of MeHg in lakes: In-lake production, inputs from wetland-containing watersheds, and atmospheric deposition. The relative importance of different MeHg sources depends on the lake. Seepage lakes tend to have in-lake production as the major source of MeHg, while for drainage lakes, depending on catchment size and characteristics, approximately 50% may originate from the watershed. Input from precipitation is generally minor for both seepage and drainage lakes. However, if in-lake production is low and MeHg levels are high in precipitation, input can be important for seepage lakes and significant for drainage lakes (Rudd, 1995). While different sources may be important under different conditions, it appears that internal MeHg production in lakes is always very important.

Sulphate-reducing bacteria (which, as we have seen earlier, are also MeHg demethylators) are considered to be the principal methylators of mercury, and provide the major source of lake MeHg. Chemical inhibition studies of these bacteria have demonstrated significant reductions in methyl mercury production in freshwater sediments (Kerry *et al.*, 1991; Compeau and Bartha, 1985). The addition of organic carbon or sulfate may "fertilize" the sulfate-reducing bacteria, thus increasing their mercury methylation (Gilmour and Henry, 1991). Also, the oxidation of Hg^0 to Hg(II) fuels the methylation of Hg(II) (Amyot *et al.*, 2000).

It has been shown that wetlands are important sources of methylmercury, with yields from wetland-containing catchments yielding significantly more methylmercury than do

purely upland catchments (St. Louis *et al.*, 1994; Clair *et al.*, in press). High levels of DOC (dissolved organic carbon) are also typically found in wetlands. There has been found in numerous studies to be a positive relationship between DOC levels in run-off and lakes, and the levels of Hg and MeHg (Watras *et al.*, 1995; Lee and Iverfeldt, 1991; Mierle and Ingram, 1991; Driscoll *et al.*, 1995; Faust, 1992). The major fraction of DOC in surface waters originates from soil (Houle *et al.*, 1995). This is consistent with watershed characteristics having an important influence on mercury levels in rivers and lakes.

High DOC and low pH favour Hg methylation and retention over Hg^0 evasion from the water surface into the atmosphere (Watras *et al.*, 1995). In areas of similar deposition, a study by Gilmour and Henry (1991) of acidified lakes found that fish had higher MeHg over non-acidified lakes. They suggest that acidification may alter mercury methylation, increase bioaccumulation, or alter the distribution of mercury between organic and inorganic forms. Increased acidity could also cause increased Hg^{2+} mobilization from the watershed and sediments (Ramlal *et al.*, 1985). The pH of the lakes does not appear to affect the speciation of MeHg (versus other forms of mercury). In all lakes of a study, approximately one third was bound to particulate matter >0.8 μM in size, while another third was in the dissolved, chemically reactive form. (Bloom, 1991). A study of factors affecting MeHg accumulation in zooplankton found that MeHg levels were indeed best predicted by lake water colour and pH. Levels were positively correlated with water colour and inversely correlated with pH, though the effect of colour was greater than that of pH (Westcott and Kalff, 1996).

The impacts of logging and forest fire on watersheds and lakes have also been subjects of concern, as they are two major perturbations to watersheds. It has been found that there are significant increases in DOC and MeHg levels in lakes which have been logged, while no significant difference was found between levels in reference (not logged or burned) and burned lakes. DOC levels as well as light attenuation have been found to be up to threefold higher in logged lakes than in reference or burned lakes (Carignan *et al.*, 2000). Mercury levels in pike from logged lakes were found to be significantly higher than in reference lakes (Garcia and Carignan, 2000).

During high-intensity fires, most of the organic matter on the forest floor is mineralized or burned (Bormann and Likens, 1979). It has also been hypothesized that fire may change the speciation of mercury in soil, that certain elements including mercury may have been lost by volatilization, and that the productivity and nutrient pulse following a fire may dilute the mercury associated with the biota (Garcia and Carrignan, 1999). Wood ash also decreases soil acidity (Meiwes, 1995), while an increase in acidity, as mentioned above, could lead to increased mobilization of Hg^{2+} which could subsequently be methylated in lake water. If the organic material has been mineralized by fire, decreased acidity may help the mercury remain bound to it and prevent it from leaching into the lakes (Meiwes, 1995). In the presence of H^{+}, the metal ions are displaced and enter the aqueous phase (Baird, 1995).

The logging of trees could also lead to an increase in the level of the water table due to decreased removal of the water by the trees via transpiration. This rising of the water

table could bring mercury and other solutes in the soil to the surface, where it may then run off into the water system. A Swedish study has shown mercury and humic matter transport from catchments to be higher when the water table is higher (Johansson and Iverfeldt, 1994). However the same study also found that the content of mercury in organic material in run-off is site-specific, indicating that the source of humic matter may affect its structure and therefore how it behaves with respect to mercury. This sort of site specificity has been cited in many mercury studies. Experimental wetlands that were flooded were found to greatly increase MeHg production. There is a minimal estimate of a 26 fold increase in outflow, with a concurrent increase in levels in plant tissues and peat (Rudd, 1995). Periodic or intermittent natural flooding of wetlands associated with changes in water levels has also been found to enhance MeHg production (Snodgrass *et al.*, 2000). This would suggest another mechanism by which deforestation and the subsequent rising of the water table could contribute to the increased MeHg and DOC levels observed in lakes.

1.3 DISSOLVED ORGANIC CARBON

1.3.1 Background

There is a consistent, high correlation between mercury and DOC. This is likely due to the complexation of mercury to DOC. It is postulated that humic substances mobilize Hg deposited by precipitation (Melamed *et al.*, 2000). Humic substances do not have a precise chemical structure, but can be accorded the following general definition:

> A general category of naturally occurring, biogenic, heterogeneous organic substances that can generally be characterized as being yellow to black in colour, of high molecular weight, and refractory (Aiken *et al.*, 1985).

Three major fractions of humic substances are operationally defined by their solubilities:

Humin. That fraction of humic substances that is not soluble in water at any pH value.
Humic Acid. That fraction of humic substances that is not soluble in water under acid conditions (below pH 2), but becomes soluble at greater pH.
Fulvic Acid. That fraction of humic substances that is soluble under all pH conditions (Aiken *et al.*, 1985).

0.45 μm filters, as the nominal pore size of early membrane filters, have been designated as the boundary between dissolved and particulate organic carbon. However, bacteria, viruses and smaller colloidal particles are included in this "dissolved" fraction. It may be argued that the wide range of particle size may render any attempts to divide particulate from dissolved as arbitrary (Wangersky, 1993).

Dissolved organic matter (DOM) is made up of approximately 20% identifiable compounds including carbohydrates, carboxylic acids, amino acids, and hydrocarbons. The remaining 80% consists of complex, environmentally altered plant, bacterial, and fungal residues. DOM consists of thousands to millions of compounds as solutes in various aquatic systems (Leenheer, 1994). Attempts to characterize DOM may be summed up as follows:

> The quality of DOM is typically characterized by chemical and related optical properties. For example, DOM is characterized by its affinity to adsorb to synthetic resins, its elemental composition, its isotopic composition and 'age' (^{14}C activity), the density of different functional groups and double bonding, and spectral attenuation of light and subsequent fluorescence. These qualitative properties have been linked to different sources of DOM (allochthonous and autochthonous), and to in situ transformation.
>
> (Curtis 1998)

Humic substances have been found in every natural water sample that has been analyzed for their presence. The concentrations of dissolved humic substances in aqueous systems, such as surface water and shallow ground waters, have been cited to be generally in the range of 1-10 mgL^{-1}(Allard and Arsenie, 1991). However, another study stated that in coloured waters, DOC levels ranged from 5 mg C/L to more than 50 mg C/L. Concentrations below 5 mg C/L rarely have visible colour (Malcolm, 1985). The colour of a lake is a useful index of dissolved organic matter. However, measurements of water colour are likely most indicative of the presence of humic substances, while DOC measurements represent all sources of carbon. This would include carbohydrates and proteins, thus potentially giving high DOC values with relatively little colour in the water (Mierle and Ingram, 1991).

Stream humic acids were found to be composed of approximately 50% organic carbon (Malcolm, 1985). In the literature, there is a great range in the relative percentages of DOC constituents. Morel *et al.* (1998) found that humic acids constitute 50-90% of DOC in natural waters, while the surface DOC distribution in US rivers was found to be 45% fulvic acids, and 5% humic acids, and 25% low molecular weight acids (Malcolm, 1985). In the water column in general, dissolved fulvic acids are much more abundant than dissolved humic acid, with fulvics accounting for 40-60% of the dissolved organic material (Mcknight and Aiken, 1998), while 10% of the DOM is humic acid (Leenheer, 1994).

The composition and amount of these substances may vary depending on their origins in soil, surface water, or ground water. They occur in water in a size continuum varying from dissolved, through colloidal, through to particulate phases. The sizes of DOC are referred to as apparent molecular weights, since compounds of known molecular weights, not size, are used to calibrate separations, as discussed in the section on tangential-flow ultrafiltration (Logan and Jiang, 1990). Molecular weights range from approximately 500 to 1200 Daltons for fulvic acids, to more than 100,000 Daltons for humic acids (Mcknight and Aiken, 1998). As suggested earlier, the larger the size fraction, the greater the capabilities for adsorption and ion-exchange reactions are (Buffle *et al.*, 1978).

Since DOC is a ligand for trace metals, and organic contaminants, it may positively affect aquatic fauna by reducing the bioavailability of these metals and contaminants (Houle *et al.*, 1995). Fluorescence quenching has been used as an indicator of metal complexation

by naturally occurring organic matter (Seritti *et al.*, 1994). Two types of metal binding processes have been postulated: Strong, site-specific binding involving electron transfer interactions, and weak binding or "territorial binding" of counter ions in the vicinity of humic polyions (simple electrostatic attraction). Carboxylic acid functional groups are likely the dominant cause of this territorial binding, however the charge distribution about the molecule will depend on the structural arrangement of these groups (McNight, 1994). Their proximity to other functional groups is the major factor affecting binding. There is a lesser incidence of strong metal-binding sites, possible due to the wide variety in the structural nature of these sites, as well as the presence of non-oxygen-containing functional groups, including nitrogen and sulphur containing groups. Several biologically significant metals such as cadmium, copper, and iron may bind strongly to these groups (McNight, 1994). Mercury also strongly binds to sulphur-containing groups.

It has been found that fractions of DOC are lost from samples, commencing immediately upon sampling. Decay constants of 0.1 to 0.5 day^{-1} have been observed, with higher rates showing considerable decreases in DOC even with a 1 hour delay in processing (Wangersky, 1993). It appears that bacterial decomposition is a major cause of losses of the biologically labile fractions of the DOC. The composition of this labile fraction is not known; though some of it may be impervious to photochemical as well as chemical oxidation, all of it is available to biological degradation. A second fraction is somewhat more resistant to microbial degradation over periods of weeks to months, and is chemically resistant. Its composition is also unknown (Wangersky, 1993). However,

other authors have stated that despite the heterogeneity of DOC, both humic and fulvic acids are resistant to microbial decomposition unless it is facilitated by oxidative processes including photolysis (Wetzel *et al.*, 1995).

Humic material acts to a large extent as a complex acidic cation exchange resin (Lydersen, 1998). Experiments of controlled acidification have showed significant internal alkalinity generation (Sampson *et al.*, 1994). It was found that substantial fractions of sulfuric acid which were added to lower a lake's pH were not having an effect, and significantly more acid was required to maintain the target pH than predicted from the lake's initial pH and its volume. A process involved in this is cation production by ion exchange, in which H^+ replaces base cations (Ca^{2+}, Mg^{2+}, Na^+, K^+, NH_4^+) on exchange sites of organic and mineral sediments (Sampson *et al.*, 1994). The acid neutralizing capacity of the DOC depends on the number of functional groups which bind H^+ (Lydersen, 1998), and results in DOC having a significant buffering role in natural systems. This capacity however, is also dependant on the water chemistry, as sites available for proton exchange may be complexed by other reactants such as cations, clays, or colloids (Clair *et al.*, 1992). These factors, as well as the DOC chemistry itself may vary seasonally (Lyderson, 1998).

Aliphatic structures (generally short and branched) in fulvic acids are commonly terminated with carboxyl groups (Leenheer, 1994). Fulvic acids have the highest carboxylic acidity (Wang *et al.*, 2001), though carboxylic acids are the major acidic functional groups in both fulvics and humics (Mcknight and Aiken, 1998). The fact that

humic substances are not pure compounds, but are a heterogeneous mix of many compounds of similar chemical properties, coupled with a disparity in their sources and geochemical processes controlling their transport, may lead to significant differences in humic substances from different environments (Aiken *et al.*, 1985). Different species of phytoplankton have been found to release DOC in different amounts and of different biochemical composition. There are lysis products (including photolysis), and the bacterial utilization of DOC constantly alters its biochemical composition (Sundh, 1992). DOC exported into surface waters is mainly produced in the forest floor, but as water percolates through the soil profile, a significant fraction is adsorbed in the mineral horizons. Therefore, surface flow waters would be expected to be higher in DOC (Houle *et al.*, 1995).

1.3.2 Role of DOC in the Mercury Cycle

Upon the degradation of DOC, several low molecular weight sulphur compounds are formed, including H_2S and thiols. These form strong complexes with Hg^{2+} and CH_3Hg^+. Within DOC, humic substances are responsible for the vast majority of the binding capacity for mercury (Wallschlager *et al.*, 1996). Humic acids generally have a high metal-complexing capacity due to the presence of carboxylic groups. The presence of sulphidic groups in the humic substance may enhance the stability of Hg complexes in particular even further (Allard and Arsenie, 1991). Comparisons of the equilibrium binding constants of MeHg to thiol containing compounds suggests that at natural levels, MeHg is in fact primarily associated with the thiol groups when bound to humic acids (Amirbahman *et al.*, 2002). Studies have shown that the ratio of MeHg bound to humic substances to total MeHg in surface waters tends to approach one as the concentration of

humic substances increases. In other words, the more humic substances are present, the larger is the proportion of MeHg bound to it (Petersson *et al.*, 1995). It has also been found that with decreasing pH, the percentage of free methylmercury compounds increased, and the ratio of bound to unbound CH_3Hg^+ increased with decreasing total CH_3Hg^+ levels (Hintelmann *et al.*, 1995). Hintelmann *et al.* in their 1997 study however, found that virtually all MeHg in aerobic freshwaters is bound to humic material.

Binding of MeHg to DOC also appears to limit its bioavailability (Driscoll *et al.*, 1995). Despite the correlation of DOC levels with MeHg levels, increased levels of DOC in the water column produce lower rates of methylation, though there is an overall increase in bacterial activity (Winfrey and Rudd, 1990; Miskimmin *et al.*, 1992; Matilainen and Verta. 1995). This may be due to ligand formation between DOC and mercury, thus rendering it unavailable for methylation (Gilmour and Henry, 1991). In sediments however, DOC leads to increased methylation and increased bacterial activity (Gilmour and Henry, 1991). This could be due to differences between DOC in the water column and in the sediments. DOC in sediments may be older and therefore more degraded into compounds of lower molecular weight. This would make them more susceptible to further bacterial degradation. In addition, MeHg has been observed to bind preferentially to larger MW humics (Gilmour and Henry, 1991; Hintelmann *et al.*, 1995; Hintelmann *et al.*, 1997), resulting possibly in lower import to the sediments via DOC (Gilmour and Henry, 1991). This has been demonstrated in humic and fulvic acids isolated from various Ontario lakes, with much higher levels of MeHg bound to the humics compared to the fulvics. For a particular lake, a difference of 5.6 ng/g for fulvics and 108 ng/g for

humics was observed (Hintelmann *et al.*, 1997). It is postulated that sulfidic sulfur may be enriched in the high molecular weight fractions (Hintelmann *et al.*, 1997). A study by O'Driscoll and Evans (2000) found more specifically that MeHg binding to fulvic acids increased with molecular size, but binding to humic acids was not related to molecular size. Overall, they found that the binding of MeHg to humic acids was 1.9 to 14.4 times higher than binding to fulvic acids.

Abiotic methylation of mercury in soil has been observed, and appears to be associated with organic materials. Studies (Rogers, 1977) have shown that the methylating ability of the soil was lost upon exposure to ultraviolet radiation. This would be consistent with the photobleaching of humic substances. The absence of microbes in the soil was confirmed with plating soil extract on agar, resulting in no growth, yet upon amendment with $Hg(NO_3)_2$, methylmercury was produced. It was further determined that the fulvic acid fraction was methylating, while humic acids were not. Methylation was also greatest below pH 5.5, possibly due to the greater availability of the Hg ion (Rogers, 1977). Humic matter is considered the most likely potential methyl donor to Hg(II), likely through an electrophilic attack by $Hg^{2+}(aq)$ on fulvic acid (Weber 1993). MeHg production from Hg^{2+} in the presence of fulvic acid is highly dependent on the presence of catalytic metal ions, of which Fe^{2+}/Fe^{3+} are the most effective (Lee *et al.*, 1985). This process may be important with lakes whose watersheds have been logged, with the subsequent increased import of DOC and its associated MeHg.

1.3.3 Solar Radiation and DOC in the Mercury Cycle

Dissolved humic substances sorb or complex trace metals, and can catalyze certain photochemical and redox reactions (Steinberg and Muenster, 1985). Losses of humic substances under natural conditions may result from adsorption onto mineral surfaces, or by cleavage upon exposure to UV radiation (Steinberg and Muenster, 1985; Dahlén *et al.*, 1996). In addition to photolysis, photobleaching can occur whereby conjugated double bonds (aromaticity) are disrupted. This however may also lead to photolysis (Curtis, 1998), which causes a decrease in average molecular size. Generally, it has been found that cleavage by UV radiation is necessary for microbial decomposition of aquatic humic substances (Wang *et al.*, 2001). In general, it is evident that UV radiation can affect the content and function of DOC in surface waters.

Photochemical reactions between UV radiation and DOC occur at chromophores, or light-sensitive sites. These are mostly conjugated double bonds including aromatic rings and associated phenolic functional groups, carboxylic acids, and other functional groups which contain unbonded electrons (Thruman, 1985). Aromatic groups tend to absorb UV radiation more strongly than aliphatic groups. As fluorescence requires the absorption of UV-A, it is a measure of the aromatic proportion of DOC (Lean, 1998).

Solar radiation is operationally divided up into several fractions. UV radiation is subdivided into UV-A (320-400 nm), UV-B (280-320 nm), and UV-C (190-280 nm). Visible light is 400-700 nm and corresponds to photosynthetically "active" radiation (PAR) wavelengths (Vincent and Roy, 1993). UV-B is a small fraction (less than 1%) of

the total solar energy, but it is the highly active component that is absorbed quickly (Lean 1998). Because of low scattering at this wavelength, it can penetrate to biologically significant depths in lakes (Vincent and Roy, 1993; Willaimson, 1995). It triggers many photochemical processes (Amyot *et al.*, 1994), including mercury photoreduction. All plant, animal and microbial life appears to be susceptible to UV-B, with it exerting wide-ranging effects such as depressing photosynthesis, and causing mutagenesis and acute physiological stress that may ultimately lead to death (Vincent and Roy, 1993). At ground level on a sunny day, UV-B is about 20% of the UV-A levels, and 0.8% of the PAR. UV-C levels are negligible at ground level due to it being absorbed by molecular oxygen, which is subsequently photochemically converted to ozone, also a UV-C and UV-B absorber (Vincent and Roy, 1993). Direct spectral irradiance at ground level has been found to be a function of optical depth, including air scattering, aerosol scattering, ozone absorption, aerosol absorption, water vapour absorption, and mixed gas absorption (Green and Chai, 1988; Nemeth *et al.*, 1996). Cloudiness plays an important role, both in the amount of cloud cover and the type and height of the clouds. Sun elevation also affected radiation reflection by clouds, with lower elevations resulting in greater reflection (less reaching the earth's surface) (Nemeth *et al.*, 1996). Depletion of the ozone layer has caused great concern over increasing radiation levels reaching the earth's surface. Increases in UV-B radiation have been on the order of 10-20% in north-temperate regions from 1979-1992 (Madronich 1994).

DOC has been found to be the principle attenuating substance of UV-B and UV-A in temperate lakes (Scully and Lean, 1994). This makes it a key factor in determining the

depth to which biologically effective radiation can penetrate. This has been defined as a decrease to one tenth of its original value (Gáspár *et al.*, 1996). The 95% extinction depth of UV-B and photosynthetically active radiation (PAR- 400-700 nm) was found to be approximately 4 cm for a high (13 mg L^{-1}) DOC lake, and 50 cm for a low (3.5 mg L^{-1}) DOC lake (Kaczmarska *et al.*, 2000). In another study, it was found that when DOC concentrations declined below 2 mg C L^{-1}, the UV penetration undergwent an abrupt increase. Generally, in temperate lakes with DOC concentrations around 5 mg C L^{-1}, 99% of the UV-B radiation will be attenuated in approximately half a meter in depth (Crump *et al.*, 1999). This is supported by Sellers *et al.* (2001) who found that only in Teflon bottles incubated between 0 and 0.5 metres below the lake surface exhibited photodegradation of MeHg at rates of up to 27% per day.

Studies have shown that UV radiation absorption can be used as a quick measure of the concentration of dissolved organic matter in waters (Bannoub, 1973). Most of the energy absorbed by DOC occurs between 300 and 500 nm (Cooper *et al.*, 1989). It was also found in pond studies that the quality of the DOC influenced attenuation. The higher the fluorescence of the DOC, the greater the attenuation. Earlier in spring (May), there was more fluorescence, but by June, photobleaching may have quenched some of this (Crump *et al.*, 1999). UV can photoreduce high molecular weight humic materials to lower molecular weight ones (Vincent and Roy, 1993).

It has been found that UV/H_2O_2 treatments of water containing DOC produces strongly oxidizing hydroxyl radicals ($OH^{\cdot}$) in the presence of reduced iron (Wang *et al.*, 2001).

$$H_2O_2 \xrightarrow{h\nu} 2OH^{\cdot} \qquad (1)$$

Humics have the ability to reduce transition metals in natural waters (Skogerboe and Wilson, 1981). Hg (I) and Hg(II) are both reduced to Hg(0) by humic and fulvic acids (Costa and Liss, 1999), except at very low pH and/or high chloride concentrations (Wang *et al.*, 1991). The light absorption abilities of humics can enhance their reducing properties by transferring the absorbed energy to a suitable electron receptor (Nriagu, 1994). However, in one study the percentage of total Hg being photoreduced in low DOC Arctic and temperate lakes was found to be higher than in high DOC lakes. The authors concluded that in the high DOC lakes, it is likely that a larger fraction of total Hg is complexed to the DOC and therefore unavailable for reduction (Amyot *et al.*, 1997).

UV radiation also reduces the DOC content, likely through the loss of the reductive capacity of the humics, either by bleaching or by some other form of chemical aging, and through the photoproduction of low molecular weight compounds (Kieber *et al.*, 1990). Another study also found that photobleaching resulted in the decreased absorption in the UV and visible spectral region, along with the production of CO, dissolved inorganic carbon (DIC), and ammonium (NH_4^+). DIC was the most rapidly formed carbon-containing product, and with the removal of O_2, photobleaching was decreased (Gao and Zepp, 1998). Kieber's study also found the production of these compounds is strongly related to light absorbance by DOC and to loss of absorbance due to the photobleaching of DOC chromophores. The wavelengths responsible are in the UV-B region. Interestingly, despite disparate sources of DOC from natural water samples as well as

humic and fulvic extracts, photoproduction rates of the carbonyl compounds were linearly related to UV absorbance and rate of photobleaching. This suggests that similar chromophores and photochemical pathways are involved (Kieber *et al.*, 1990). When present at high concentrations, DOC seems to act as a competitive inhibitor for solar radiation, scavenging UV radiation before it can photoreduce Hg(II) . As a result, higher photoreduction rates have been observed in clear lakes containing little DOC, when it acts as a source of reducing agents for Hg photoreduction (Amyot *et al.*, 1997b). It has also been stated that water "stained brown by dissolved organic matter" reduces light penetration and MeHg photodegradation (Sellers *et al.*, 1996).

1.4 PHOTODEGRADATION OF METHYLMERCURY AND THE ROLE OF SINGLET OXYGEN

1.4.1 General

Methylmercury in lakes has been found to be photodegraded by sunlight, with reaction rates being first order with respect to concentrations of MeHg and to PAR levels (Sellers *et al.*, 1996). In their 2001 paper, Sellers *et al.* stated that MeHg is photodegraded primarily by ultraviolet "light", but also by visible light (quoting her 1997 thesis). The mechanism by which this occurs has yet to be elucidated, but two possibilities are as follows: The photodegradation process occurring via the hydrolysis of MeHg (Suda *et al.*, 1993):

$$CH_3\text{-}Hg^+ + H^+ \rightarrow CH_4 + Hg^{2+} \qquad (2)$$

Singlet oxygen generated by photochemical reactions has been cited as likely responsible for this degradation by Suda *et al.* (1993), however Bloom *et al.* in their 2001 study cite hydroxyl radicals (·OH) as MeHg oxidizers:

$$CH_3\text{-}Hg^+ + \cdot OH \rightarrow CH_3OH + Hg^+ \quad (3)$$

$$Hg^+ + \cdot OH \rightarrow Hg^{2+} + OH^- \quad (4)$$

Bloom *et al.* (2001) also demonstrate photolysis of MeHg in deionized water, indicating the direct photolysis of MeHg and postulating the following reaction:

$$CH_3Hg^+ \xrightarrow{h\nu} CH_3\cdot + Hg^+ \quad (5)$$

$$2Hg^+ \rightarrow Hg^0 + Hg^{2+} \quad (6)$$

Experiments examining the products of the photodegradation of MeHg appear to indicate that both reactions occur, as both Hg^0 and Hg^{2+} are produced (Bloom *et al.*, 2001). The dominant form of methylmercury in anoxic water is the methylmercuric sulfide ion (CH_3HgS^-), and it has also been shown to be readily decomposed by sunlight to CH_4 and HgS (Baughman *et al.*, 1973).

Singlet oxygen ($^1O_2$) exists in two exited states. The lowest or first exited singlet is that which is involved in many important processes (Larson, 1978). It has a lifetime of approximately 2 μs in water, and readily reacts with unsaturated organic compounds. A number of naturally occurring pigments are known to act as photosensitizing dyes, transferring energy from an excited triplet state to ground state triplet oxygen, thereby exciting it to the singlet state (Larson, 1978).

Specifically, reactive oxygen species in surface waters are primarily produced by *in situ* photochemical reactions (photooxidations) of naturally occurring chromophores. Coloured dissolved organic matter (CDOM) is the dominant source of these chromophores (Blough and Zepp, 1995). In fact, the only known source of singlet oxygen in natural waters is through energy transfer from an excited triplet state of CDOM to O_2, with UV being most effective at producing these reactions (Blough and Zepp, 1995; Haag and Hoigné, 1986). Zepp *et al.* (1985) proposed the following reaction,

$$^3DOC^* + O_2 \rightarrow DOC + {}^1O_2 \qquad (7)$$

thereby producing singlet oxygen from the photoexcitation of DOC, and subsequent energy transfer to oxygen. A two-electron reduction of $^1O_2$ produces hydrogen peroxide (H_2O_2) (Skurlatov and Ernestova, 1998; Larson, 1978). Light wavelengths of 400 nm or less cause photolysis of H_2O_2, most commonly producing two hydroxyl radicals. This process is catalyzed by metal-containing species. In the presence of reduced iron, the photochemically-produced hydrogen peroxide is converted into highly reactive hydroxyl radicals, which are powerful oxidants of organic compounds (Zepp *et al.*, 1992; Moffett and Zafiriou, 1993). Both hydroxyl and hydroperoxyl radicals can be efficiently produced from H_2O_2 by metal ions having two easily accessible valence states differing by one electron, ie. Fe^{2+}/Fe^{3+}. The following reactions have been postulated (Moffett and Zafiriou, 1993):

$$Fe(III) \xrightarrow{h\nu} Fe(II) \quad (8)$$

$$Fe(II) + HOOH \rightarrow Fe(III) + OH + OH^- \quad (9)$$

$$Fe(II) + OH \rightarrow Fe(III) + OH^- \quad (10)$$

The presence of both light and iron have an accelerating effect on the oxidation of humic substances by oxygen (Voelker *et al.*, 1997). However, iron has also been associated with the attenuation of both visible light and UV radiation, and high levels of iron have been also associated with high levels of DOC. Iron is among the most concentrated transition metals in natural waters (Blough and Zepp, 1995). Iron bound to humic substances as Fe(III) remains in solution, while Fe(III) itself is only sparingly soluble (Kwan and Voelker, 2002). Photochemical reduction reactions between UV and inorganic and organic ferric (Fe(III)) complexes (iron oxide) can release iron into the medium in the potentially more available ferrous (Fe(II)) form, which is biologically more available as well as chemically available for reactive oxygen species (O'Sullivan *et al.*, 1991, Blough and Zepp, 1995, Voelker *et al.*, 1997). It is believed that the absorption of a photon results in an excited ligand-to-metal charge transfer (LMCT), which may dissociate or be thermally deactivated. If it dissociates, Fe(II) and an oxidized organic radical are produced (Voelker *et al.*, 1997).

Superoxide (O_2^-) and H_2O_2 can interact to produce oxygen and ·OH, though the reaction is slow without metal catalysis. ·OH is the most powerful oxidizer known, and reacts with virtually all organic molecules (Larson, 1978). The half-life of hydrogen peroxide is, unlike other reactive oxygen species, relatively long at 4-24 hours (Kaczmarska *et al.*,

2000). The formation of superoxide ($O_2^{\cdot-}$) can result from the direct transfer of electrons from organic compounds in the triplet state. The formation of e_{aq}^- occurs with the subsequent reduction of O_2 to $O_2^{\cdot-}$ (Cooper *et al.*, 1989). General mechanisms are as follows:

$$^1HS \xrightarrow{\text{Light}} {}^1HS^* \xrightarrow{\text{ISC}} {}^3HS^* \quad (11)$$

$$HS^* \text{ or } {}^3HS^* \longrightarrow [HS^{+\cdot} + e^-] \longrightarrow HS^{+\cdot} + e_{aq}^- \quad (12)$$

$$O_2 + e_{aq}^- \longrightarrow O_2^{\cdot-} \quad (13)$$

$$^3HS^* + {}^3O_2 \longrightarrow HS^{+\cdot} + O_2^{\cdot-} \quad (14)$$

or

$$\longrightarrow {}^1HS^* + {}^1O_2 \quad (15)$$

$$^1HS + {}^1O_2 \longrightarrow HS^{+\cdot} + O_2^{\cdot-} \quad (16)$$

CDOM is also the principal source of hydroxyl radicals and superoxide, which is in turn the primary source of H_2O_2 via dismutation (Blough and Zepp, 1995). H_2O_2 originating mainly from the dissolved organic matter in natural waters through UV-induced transformations, could either act as an oxidizer or a reducer, depending on the pH of the system (Amyot *et al.*, 1994). Therefore, either Hg^0 or Hg^{2+} could be produced. In lakes, the diel variability in H_2O_2 concentration indicates its formation is photochemical in nature, with concentrations closely following solar radiation levels (Cooper and Lean, 1989). Studies have shown H_2O_2 levels to be highest around 1600 hrs on a sunny day, with levels lowest during early morning hours. On overcast days, generally none was detected at all, suggesting that it is produced primarily by photochemical reactions (Shtamm *et al.*, 1991). H_2O_2 concentrations also decrease with increasing depth to levels that are undetectable at the base of the mixed layer of lakes. (Moffett and Zafiriou, 1993).

Hydroxyl radical production by H_2O_2 reduction occurs in waters with sufficiently high metal levels. H_2O_2 photolysis is not significant due to the poor overlap between the surface spectrum and the absorption spectrum of H_2O_2 (Blough and Zepp, 1995).

Scully *et al.* (1996) have found that there is a calculable relationship between the concentration of DOC and the rate of formation of H_2O_2 under UV radiation, resulting in higher H_2O_2 production in lakes with higher DOC. However, another study found that lower concentrations of humic acid led to higher production of H_2O_2, likely due to the more dilute solution having increased light penetration (Draper and Crosby, 1983). Chromophores responsible for H_2O_2 formation are the same as those responsible to the attenuation of UV radiation (Scully *et al.*, 1995). Most H_2O_2 production is confined to the depth of UV radiation penetration, with lakes with a high extinction of UV by DOC exhibiting a concentration of H_2O_2 formation near the surface. In transparent lakes, H_2O_2 has been seen to be produced over a greater depth, resulting in a less marked near-surface maximum (Hermann, 1996). Various studies have also shown that the rate of H_2O_2 formation is greater for humic acids than for fulvic acids (Draper and Crosby, 1983; Shtamm *et al.*, 1991). UV radiation is absorbed by DOC, and superoxide is formed. This reacts with itself (dismutates), and produces H_2O_2. Cooper *et al.* (1994) proposed the following mechanism of H_2O_2 formation:

$$ {}^1DOC \xrightarrow{h\nu} {}_1{}^1DOC^* \xrightarrow{ISC} {}_1{}^3DOC^* \qquad (17) $$

$$ {}_1{}^3DOC^* + {}^3O_2 \rightarrow DOC^{+\cdot} + O_2^{-\cdot} \qquad (18) $$

$$ HO_2 + HO_2 \rightarrow H_2O_2 + O_2 \qquad (19) $$

$$ HO_2 + O_2^{-\cdot} + H_2O \rightarrow H_2O_2 + O_2 + OH^- \qquad (20) $$

Ground state DOC ($_0{}^1$DOC) is excited by UV to a singlet state ($_1{}^1$DOC*), and via intersystem crossing (ISC) is transformed to the excited triplet state ($_1{}^3$DOC*). Note that alternatively energy may also be released by fluorescence. This triplet state may then react with molecular oxygen to form superoxide ($O_2^{\cdot-}$) or its conjugate acid HO_2. This reacts with itself to give H_2O_2 and O_2. This step has alternately been described as follows (Petasne and Zika, 1987):

$$2O_2^{\cdot-} + 2H^+ \rightarrow H_2O_2 + O_2 \qquad (21)$$

HO_2 and $O_2^{\cdot-}$ react to produce OH- and additional H_2O_2 and O_2 (Cooper *et al.*, 1994). Note that not all superoxide radicals form H_2O_2, but also initiate other reactions (Petasne and Zika, 1987).

1.5 TANGENTIAL FLOW ULTRAFILTRATION

Tangential flow ultrafiltration (TFUF) is a filtration system whereby the solvent flow runs parallel to the filter membrane surfaces, as opposed to perpendicular as with traditional inline filtration systems. This has the advantage of minimizing clogging problems. A portion of the sample, the filtrate, passes through the membrane, while the remaining portion, the retentate, returns to the initial sample reservoir. This system has been previously used with success for freshwater trace metal studies of total mercury and methylmercury, as well as organic carbon (Babiarz *et al.*, 2000; Hoffman *et al.*, 2000). The predominant drive for flux across the membrane is an applied pressure gradient, with

smaller pore size requiring higher pressure to ensure that there is filtrate produced. Pressure is supplied by a peristaltic pump, which eliminates the higher pressure pulses of a piston-style pump. In the case of the smaller membrane pore sizes, backpressure may be applied by partially clamping the retentate line in order to ensure passing of sample through the membrane. The macromolecular separation is then achieved via the sieving through the membrane pores. Filtrate passing the membrane is theoretically below the membrane cutoff value, while the retentate which bypasses the membrane contains a mixture of solute which is above and below the cutoff value.

Solute rejection is based on the following properties: molecular size, shape, and flexibility, diffusional behavior of the solute within the solvent and the membrane pores, and the electrostatic or Van Der Waals forces between solute molecules and the membrane (Kilduff and Weber, 1992). The ionic strength of the solution however, also has an effect on the molecular weight cutoff value; at low ionic strengths, the specified cutoffs may be significantly higher than the actual experimental values (Kilduff and Weber, 1992). This suggests that membrane calibration should occur under conditions similar to those of the waters being tested. It has also been found that with lower pH values, a decrease in the fractions passing the membrane occurred, possibly due to changes in molecular configuration or to coagulation at low pH. This effect however is slight, particularly in the pH range of 4-9 (Buffle *et al.*, 1978).

TFUF membranes are generally characterized by molecular weight cutoff values. These are calibrated using globular molecules of known molecular weight. The accuracy of the

cutoff specifications depends primarily on how closely the molecules comprising the solution being fractionated resemble those used to calibrate the membrane (Kilduff and Weber, 1992). However, a study of river water found that though fractionation of their samples would differ from the separations obtained during commercial calibrations, they nonetheless achieved separations of differing chemical compositions (Quantum yields of CO and dissolved inorganic carbon (DIC) upon irradiation, absorption coefficients, etc.) (Gao and Zepp, 1998).

Limitations of TFUF include possible clogging and coagulation at the membrane surface, as well as membrane-colloid charge interactions (Hoffman *et al.*, 2000). These artifacts are more important in the freshwater systems studied here, than in marine systems. This is because these lower ionic strength water has fewer ions to screen the charges on the membrane (Babiarz *et al.*, 2000). There is also concentration polarization, or solute accumulation at the surface of the membrane which can decrease the advective flux through the membrane by as much as two orders of magnitude. This can lead to membrane rejection, or the exclusion of dissolved organics smaller than the membrane pores (Logan and Jiang, 1990). In other words, there is an "upgradient diffusive transport of solute away from the membrane in a direction opposite to permeate flow, due to the buildup of solute concentration at the membrane surface" (Kilduff and Weber, 1992). However, it has been found that the low DOC levels in water minimize mass accumulation at the membrane surface, leading to solvent flux through the membrane to be nearly constant during a batch analysis. In particular, mass accumulation at the membrane surface is minimized at DOM levels below 100 mg/L

(Logan and Jiang, 1990). In addition, the filter cassettes used in this experiment creates turbulence at the membrane surface, which minimizes both concentration polarization and clogging problems encountered with traditional inline filtration (Pall Filtron, product information). A concentration factor of two was used in this experiment, in order to avoid these problems as well as the "breaking" of larger molecules with excessive filtering and re-circulating, thereby allowing their passage through the membrane when they should have been excluded. Overall, it was found that ultrafiltration was the best method because target species may be concentrated, buffers are not required (may affect phase distribution of trace metals), and it allows the processing of large volumes of sample with a field-portable technique (Babiarz *et al.*, 2000).

2.0 HYPOTHESES

Previous studies have demonstrated that photodegradation may be a significant sink of MeHg in lake water (Sellers *et al.*, 1996; Delage 2000, unpublished results). The research group of Richard Carignan at the University of Montreal has been studying the effect of drainage basin logging on DOC and MeHg levels in lake ecosystems (Carignan *et al.*, 2000; Garcia and Carignan, 2000; Garcia and Carignan, 1999). This thesis explored the effect of drainage basin logging on the photodegradation rates of MeHg in lake water. It also investigated the effect of differing size fractions of DOC on MeHg photodegradation rates.

The principal hypotheses for this study are:

1) that photodegradation rates of MeHg will be higher in low DOC lakes than in high DOC lakes due to the greater depth of penetration of solar radiation in low DOC lakes;
2) since DOC increases with logging activities, MeHg photodegradation will be lower in lakes located in logged vs. non-logged drainage basins;
3) that MeHg will be photodegraded more slowly when associated with the larger DOC fraction due to greater binding of MeHg to larger size DOC fractions, thereby potentially rendering it unavailable for photodegradation;
4) that photodegradation rates will also increase at lower pH levels due to decreased binding of MeHg to DOC.

3.0 OBJECTIVES

This thesis investigated the relationship between DOC and MeHg photodegradation in lakes whose basins have and have not been logged in an exploration of the impact of logging on DOC and MeHg levels. TFUF was also used to fractionate lake DOC into three different size categories, in order to elucidate the effects of the different size fractions on photodegradation rates. DOC concentrations were also measured, with the expectation that the higher concentrations associated with logged drainage basins would result in lower photodegradation rates. Water collected from an inflow feeding directly from a wetland was also incubated at ambient MeHg levels. This was to compare MeHg photodegradation rates when associated with "fresh" DOC that has not been circulating in a lake, with the previous MeHg photodegradation results from the experiments on lake DOC. pH was monitored throughout all incubation experiments, and changes in pH and buffering capacity were measured to evaluate possible changes in DOC during incubation. A series of pH experiments was also performed to investigate the effect of different pH values on the photodegradation rates.

4.0 METHODS

4.1 Water Sample Collection and Preparation

Lakes in the Lake Berthelot region were chosen on the basis of their logging status and DOC levels. This region is in Quebec, and is in the process of having tracts of land clear-

cut, including those areas surrounding some of the many lakes to be found in the region. Lakes DF9 and DA9 were both logged, with DA9 logged on one side, and DF9 being completely clear-cut. DA9 is located at 48°09'59" latitude and 76°01'47" longitude, with a maximum depth of 9.2 m and 15.4% of the drainage basin logged. DF9 is located at 48°42'31" latitude and 75°01'03" longitude, with a maximum depth of 10.5 m and 66.6% of the drainage basin logged. N55 and N70 are "pristine", unlogged lakes. N55 is located at 47°59'23" latitude and 75°24'40" longitude, with a maximum depth of 7.8 m. N70 is located at 48°05'12" latitude and 75°29'09" longitude, with a maximum depth of 20.4 m. The waters of DF9 and DA9 were visibly browner than those of N55 and N70, and had higher measured levels of DOC, allowing a comparative study of high-DOC versus low-DOC content lake waters. Lake waters were pre-filtered through an in-line 100 μm filter to remove particulate matter that could clog the tangential flow ultrafiltrator membranes. Water samples were then filtered with the TFUF to produce filtrate fractions containing solutes <300 kDa, <30 kDa, and <5 kDa in size. Lakes K2 and K3 were sampled and water brought back to the laboratory for the pH experiments. K2 is located at 48°17'56" latitude and 75°10'08" longitude, with a maximum depth of 12.2 m and 1.7% of the drainage basin logged. K3 is located at 48°18'26" latitude and 75°16'18" longitude with a maximum depth of 7.2 m and 0.2% of the drainage basin logged. K2 and K3 water samples were pre-filtered through the 100 μm in-line filter, and then filtered with the TFUF fitted with a 2 μm cassette in order to remove microbes.

4.2 Field MeHg Photodegradation Experiments

These experiments were performed in order to evaluate MeHg photodegradation *in situ* on a lake verge. Water samples for the field trials were spiked with a 5 ppb standard of methylmercury chloride which was prepared daily, with 4 mL of the standard added per 10 L of filtered lake water, resulting in a 2 ng/L final spiking concentration. This concentration was chosen to bring MeHg levels sufficiently above our detection limits. Ambient levels of MeHg in the lakes of this region are often just above detection limits, thereby potentially leading to problems with photodegradation experiments. The spiked water was then incubated in the dark for 36 hrs before experiments were performed in order to allow maximal binding of the free MeHg to the DOC. A time course experiment was performed to verify binding during the dark incubation. Water samples were spiked to the 2 ng/L final MeHg concentration, and incubated in the dark for 12, 24, 36 and 48 hrs. At each incubation time, the water was fractionated into 300 kDa, 30 kDa and 5 kDa subfractions which were then analyzed for MeHg. This was to evaluate whether the concentration of MeHg associated with each DOC size fraction changed over time.

During the experiments, samples were incubated in one litre Teflon bottles, chosen for maximal transmission of UV radiation and minimal binding of MeHg to the walls of the container. Percent transmission of radiation was verified in the lab using a spectrophotometer. Dark controls were performed in black Teflon bottles. The bottles were floated at the unshaded lake verge in two large Tupperware trays with holes punched in the ends for water circulation. This helped keep the bottles and their contents from heating in the sun. Samples were analyzed for MeHg at times 0, 15 min, 30 min, 45 min, 60 min, 75 min, 90 min, 105 min, 120 min, 135 min, 150 min, 165 min, and 180

min. Due to limitations in the number of Teflon bottles available, and in order to examine the maximum number of incubation times, experiments were not done in duplicate. Instead, the entire experiment for each lake was run in the morning and then repeated in the afternoon. UVA, UVB, and visible light readings were taken every 15 minutes (Goldilux Oriel Ultraviolet meter, serial #70217/0109, UV-$\mu W/cm^2$; Goldilux Oriel UVB Probe, serial #70221/0110, $\mu W/cm^2$; Goldilux Oriel UVA Probe, model 70219, serial #0112, MFD 7/95; visible light meter, LI-COR Inc, model LI-185B, serial #QRPB1428-8207; Underwater Quantum Sensor, model LI-1925B, serial #UWQ2876). Each experiment was run in the morning, and then repeated in the afternoon. The temperature and pH of each sample were also recorded at the end of the incubation times. Measurements of pH (Corning pH meter, model 430, serial # 008503, IEC1010) were taken before and after the addition of HCl, and the volume of HCl added to bring the pH of the solution to approximately 3 was recorded. This allowed us to evaluate buffering capacity and any changes thereto with incubation. The pH was adjusted to 3 as necessitated by the MeHg extraction procedure outlined later in this Section.

The photodegradation reactions of MeHg are thought to be first order. Concentrations of MeHg were therefore log10 transformed to linearize the graphs plotting the concentration of MeHg versus time incubated. The resulting slopes were then transformed to ln by multiplying by 2.303 to give the photodegradation rate constant k values.

4.3 pH Experiments

Due to the variation in MeHg photodegradation rates obtained in the field, experiments were conducted in order to evaluate the effect of pH on MeHg photodegradation rates. All lake water used was again pre-filtered through a 100μm inline filter, and then through a 0.2 μm tangential flow filter to remove bacteria. Water samples from lakes DA9, N55, K2, and K3 were pH adjusted using 20% potassium hydroxide (KOH) and 20% perchloric acid ($HClO_4$). Perchloric acid was used to avoid problems with changing chloride ion concentrations (as would occur with hydrochloric acid), and possible problems of MeHg degradation by nitric acid. For each lake, the pH was adjusted to approximately 4.5, 6.5, and 7.5. The samples were then incubated on the rooftop of the biology building (Gendron) for 0, 4, and either 6 or 7 hours. A water tank with a circulating water source was used to float the Teflon sample bottles in, with a wire mesh under the bottles keeping them at the surface in a prone position. This was done to allow maximal exposure of the samples to sunlight. The Optikon 754-UWP Spectroradiometer system was used to measure solar radiation levels between 280 nm and 800 nm at 2 nm increments. This system was equipped with an Optikon OL 754-C Controller (Monochromator), Optronics Laboratories, Inc., the Spectroradiometer Optics Head, model 754-0-PMT, serial # 99203102, and the 3.5 m Quartz Fiber Optic Probe (waterproof, 250-800 nm).

4.4 Fractionation Experiments

Fractionation experiments were performed on DF9. This was in order to evaluate MeHg levels associated with particular DOC size fractions during the photodegradation process, and whether the MeHg degraded differentially when associated with different sized DOC.

Water samples filtered through the 30 kDa and 300 kDa filters were examined at incubation times of 0, 1, 2, and 3 hours. For each time examined, the 300 kDa fractions were re-filtered through the 30 kDa filter, and the resulting filtrate through the 5 kDa filter, while the 30 kDa fractions were re-filtered with the 5 kDa filter. Both the filtrate and retentate fractions were then analyzed for MeHg in order to determine how much each fraction degrades. Fractionation was then looked at for t=0 for lakes DF9, N55 and N70 to see if similar binding (and presumably degradation) patterns were observed. From these values, and using the curves obtained from DF9, fractionation for each lake was compared for differences that may account for any differences in photodegradation. The designations of samples used in these experiments involved the initial DOC size fraction of the sample, followed by the filter size then used to subfractionate it, followed by "R" or "F", depending on whether the filtrate or retentate was being examined. For example, 300K/5/F is the filtrate once the 300 kDa fraction was incubated, filtered through the 30 kDa and further filtered through the 5 kDa filter.

4.5 Determination of Hg^{2+} Levels

Almost 200 samples of 50 mL water samples from the field trials were brought back to the laboratory for analysis of Hg^{2+} levels in order to establish whether MeHg was being broken down to Hg^{2+} or to Hg^0 and being lost from the samples. For each sample of 50 mL, 250 μL of 18M HCl was added to acidify and preserve mercury speciation in the sample. These samples were then analyzed on a Tekran 2600 CVAFS.

4.6 Laboratory MeHg Photoproduction Experiments Under UV Lamps

Our field study showed possible MeHg photoproduction in unspiked one litre samples of high DOC water from lake DF9. Attempts to reproduce this photoproduction of MeHg with ambient initial MeHg levels were performed in the lab. Water samples were transported back from the field site and stored in a cool room at 4 °C for approximately two months prior to use. They were then filtered as per the field procedures, and then incubated under UV-B lamps. DA9 water samples were also spiked to produce a final concentration of 4 ppt of inorganic mercury (Hg^{2+}) prior to incubation under the UV-B lamps in order to provide a ready source of Hg^{2+} for methylation, in case MeHg levels decreased during storage.

4.7 Comparison of Inflow Incubations Under UV Lamps

Jack's Lake is located approximately 200 km northeast of Toronto (44°41′ 20″ N, 72°02′54″ W). Incubations of Jack's Lake water taken from the inflow off wetlands were performed in order to compare DOC fresh off a wetland, as opposed to circulating in a lake and therefore much more exposed to degradation processes. 5 kDa and 300 kDa fractions were examined, samples were unspiked, and incubation times examined were 0, 4, 8 and 10 hours. This experiment was a preliminary experiment; a more extensive experiment would be needed to verify results.

4.8 Dark Incubation Time Course Experiment

A time course experiment was performed with water samples from Lake Berthelot being used as a model. This was to establish that a 36-hour dark incubation was an appropriate time length for MeHg binding to DOC. The incubation times (dark, in cabin) tested were 12, 24, 36 and 48 hours. In detail, for each time, the following procedure was followed (similar to the fractionation experiment):

Four litres of previously filtered/ 2 ppt spiked 300 kDa sample were filtered through a 30 kDa filter. The 2 litres of retentate contained all size fractions. One litre of this was retained for analysis. The two litres of filtrate contained solutes <30 kDa in size. One litre was retained for analysis, while the remaining litre was passed through the 5 kDa filter. The 0.5 litre retentate contained the 30 kDa and 5 kDa size fractions (analyzed), and the filtrate contained the <5 kDa fraction (analyzed).

Two litres of previously filtered/spiked 30 kDa sample were then filtered though a 5 kDa filter. The one litre of retentate contained the <30 kDa and <5 kDa fractions, which was analyzed. The one litre of filtrate contained only the <5 kDa fraction, and was also analyzed.

4.9 Methylmercury Extraction

MeHg was extracted from water samples according to a procedure involving the preconcentration and separation of organic mercury compounds on a sulfhydril cotton column, followed by elution and quantification by GC/AFS (Cai *et al.*, 1996; Lee and Mowrer, 1989). The method for synthesizing sulfhydril cotton fiber (SCF) was followed as per Lee and Mowrer, with a few minor adjustments. Added to a round bottom flask in

the following order were 100 mL of thioglycolic acid (mercaptoacetic acid), 60 mL of acetic anhydride, 40 mL of 36% acetic acid, and 0.30 mL of concentrated sulphuric acid. The mixture was allowed to cool to approximately 45°C using a water bath. Fifteen grams of teased cotton wool were added to the flask, and the cotton thoroughly wetted. The flask was then sealed with a glass top, sealed with Teflon tape, wrapped in foil, and placed in an oven set at 40°C for 3-4 days. The cotton was then washed of traces of thioglycolic acid with 5000 mL of DIW using a Millipore filter assembly with suction. The cotton was then teased apart and placed in a shallow ceramic bowl loosely covered by foil in a 40°C oven to dry for approximately 24 hrs. It was then placed in a dark bottle in the fridge.

The water samples were adjusted to pH 3 using 20% HCl. A pH 3 buffer was then added at a ratio of 10 mL of buffer to 1L of sample. In each run, a procedural blank consisting of 1 L of DIW was run along with a 1 L matrix spike sample (1ppt spike in DIW). They were then passed over a SCF column made of a 5 mL Fisher Scientific screening column containing 160 mg (± 5mg) of SCF packed approximately 1 cm high. A system consisting of Teflon tubing, stoppers, and a blue disposable pipette tip was initially washed with 500 ml of 1% HCl using a peristaltic pump, and then rinsed with 500 mL of DIW. The SCF column was added to the system, and it was rinsed with 500 mL of DIW. The water samples were passed through the columns (12 columns were set up per pump). After the samples have passed, approximately 15 mL of DIW were passed over each column to rinse the system of any remaining MeHg. 6 mL of an acidic potassium bromide and copper sulfate (2:1) mixture were then pipetted onto the surface of the adsorbent two mL at a time, and the eluate was collected in a 7 mL glass vial. This

extracted the MeHg bound to the cotton. The eluate was then extracted with 300 μL of methylene chloride (dichloromethane, or DCM) on a shaker for 15 min, and then centrifuged for 10 minutes at 4500 rpm. This concentrated the DCM into a bubble at the bottom of the vial. The DCM was transferred through a layer of anhydrous Na_2SO_4 packed in a yellow pipette tip, to remove any of the aqueous fraction that may be mixed in. It was collected in a 2 mL sampling vial with a low volume glass insert. This was then subjected to GC-AFS analysis (HP 6890 Plus GC coupled via a pyrolysis oven at 800°C to a PSA Merlin Detector).

4.10 Tangential Flow Ultrafiltration System and Preparation

For the experiments examining DOC size fractions with respect to photodegradation, the TFUF (Pall Filtron Centramate Ultrafiltrator, constructed with ultra-high molecular weight polyethylene) was used to both remove microbes from the lake water samples and to fractionate water samples into the three fractions of differing DOC content: <300 kDa, <30 kDa, <5 kDa. This model of ultrafiltrator was chosen because its polyethylene internal contact surfaces bind MeHg minimally, making it ideal for trace level studies, and because it minimizes clogging problems associated with traditional inline filtration. The filter cassettes are designed such that water flow causes turbulence across the membrane surfaces, helping avoid clogging. It is also field portable and allows the filtration of the large volumes of water associated with these experiments. A peristaltic pump (Masterflex L/S standard drive peristaltic pump (Cole-Parmer Instrument Co, model No. 7520-00), ESA (Electrical Safety Approval) by Hydro on 01/07/27) was used to circulate solutions.

Filter cassettes (all are Pall Filtron Omega Centramate, 1 square foot, low protein-binding, modified polyethersulfone membrane; 300 kDa filter has a T-screen channel, the rest are suspended screen) were cleaned according to manufacturer's recommendations in order to remove preservative agents. The preservative mixture consisted of 15-18% glycerine, 0.05-0.1% sodium azide, and the balance was water. Initially, 5 litres of milli-Q water were circulated through the apparatus. This was followed in succession by 1 litre of 0.1 N HCl, 2 litres of milli-Q water, 1 litre of 0.1 N NaOH (to remove residual HCl), and lastly 5 litres of Milli-Q. This removed the NaOH. During this entire procedure, the retentate line was closed in order to push the solutions through the membranes. Flow rates for each filter size at designated pressures were calculated. The filters were then allowed to soak overnight in milli-Q water to allow any residual NaOH to dissipate out (dead volume of filters approximately 100 µl per cassette). Membranes were pre-conditioned in lake water for a minimum of 120 minutes before use, and a water sample concentration factor of 2 was used in order to minimize artifacts caused by excessive concentration of the samples. Tubing for filtration setup was standard fluoroethylene polymer (FEP, or Teflon®). Patches where needed (connections, clamps) were of Nalgene silicon premium tubing (Lab/FDA/USP/ VI Grade, ¼" diameter). Passing through the ultrafiltrator was approximately 20 cm of Pharmed® Masterflex® pump tubing consisting of a thermoplastic elastomer (polypropylene-based).

4.11 TFUF Evaluation Experiments

Mass balances of MeHg were calculated for DA9 after the DA9 spike test in order to determine if all mercury could be accounted for . This evaluated the adsorption of MeHg to the TFUF. Samples from lakes DA9, N70, and N55 were spiked and the mass balances calculated. For this, 2 litres of 0.1 N NaOH was passed through the filters (sampled), followed by 2 litres of milli-Q (sampled). Both filtrate and retentate were sampled. DOC mass balances could not be evaluated due to loss of samples from DOC coagulation.

Filtration rates were evaluated over the course of the experiments and approximately 168 hours of initial filtering. This was done with milli-Q water at specified pressures. The 5 kDa filter was run with an inlet pressure of 10 PSI, and a back pressure of 8 PSI on the retentate line in order to ensure the passing of sample through the filter cassette. The larger pore sizes of the 30 kDa and 300 kDa filters required no back pressure, and were operated at an inlet pressure of 8 PSI.

Permeability was evaluated in order to determine how much of the solute (MeHg and DOC) was passing the membrane. Eight estimates were taken per lake, covering the range of our concentration factor (2.00). One litre of lake water sample was run at 8 psi until the following volumes were achieved:

Volume in retentate (mL)	Concentration factor (V_0/V_r)
900	1.11
800	1.25
700	1.42
600	1.66

500	2.00
400	2.5
300	3.33
200	5

The concentration factor is defined here as the ratio of the initial volume (V_0) to the retentate volume (V_r).

4.12 Bacterial Enumeration Of Samples

In addition to fractionating DOC into different size fractions, the TFUF system removed microbes from the water samples. This allowed photodegradation results to be attributed to photochemical as opposed to microbial processes. Various 4 mL water samples were taken during the course of the field experiments, and 0.5 mL of glycerol was added to each as a cryoprotectant. These were frozen and retained for microbial enumeration using the DNA-staining fluorochrome 4′6-diamidino-2-phenylindole (DAPI) (Coleman, 1980). The dye binds almost exclusively to native DNA, and the DNA-dye complex has a much greater fluorescence than the unbound dye molecule, making nuclei clearly observable in cells still bathed in the dye solution (Coleman, 1980). Samples can then be observed using an epi-illumination system for fluorescence microscopy. With the filtration, minimal numbers of bacteria should be in the incubated samples, thus eliminating microbial processes as contributors to the observed results.

The method used is based on the procedure of Coleman 1980. In the lab, Nucleopore filters (0.2 μm pore size) that were pre-stained in Irgalan Black were used. The Irgalan Black is used to create a dark background against which to view the fluorescent bacteria.

These filters were removed from the dye and rinsed with autoclaved water prior to use. It is then placed on a wet Millipore filter, and they are clamped to the filter assembly. The 2 mg/L DAPI working solution was added to the samples in a 3:1 ratio (3 parts sample to one part DAPI). In adding it, the DAPI was filtered through a 0.2 μm filter fitted to a 5 cc syringe to remove any bacteria in the solution. They were then left under a duct-tape sealed cardboard box for the 10 min incubation period. This is done to allow time for binding of the DAPI to bacteria, and to prevent light from breaking down the photosensitive dye. The samples were then drawn through the filters under seven inches of Hg vacuum pressure. Once the sample was drawn through, the sides of the filter apparatus were rinsed with a small amount of sterile water (autoclaved and filtered through a 0.2 μm filter). The Nucleopore filter was then placed onto a microscope slide, one drop of low fluorescence immersion oil was added, and it was then covered with a coverslip. The samples were viewed with a fluorescence microscope (Carl Zeiss Jena fluorescence microscope, Model Jenamed 2, serial #750063), fitted with a grid pattern to assist with enumeration. The grid consisted of 10 squares on each side, each square covering 5μm, resulting in a total are of 2500 μm. Twelve grids were counted, chosen randomly from the entire field. The counts were averaged, and the total count for the volume filtered was calculated.

4.13 Teflon Transmittance

In examining radiation transmission through Teflon, both a newer and older bottle were used. The older bottles appear more opaque due to minor surface damages and abrading to the bottles. Pieces of the bottle were cut to approximately fit a quartz cuvette used in

the Spectrophotometer (Varian Cary 100 Bio UV-Visible Spectrophometer, serial #EL99033571), and then were shaved with a razor knife to a close fit. The cuvette was then filled with DIW in order to simulate the wetting of the Teflon as under field conditions. The absorbance was then evaluated at every 2 nm increment, and subsequently converted to % transmittance.

5.0 RESULTS

5.1 Field MeHg Photodegradation Results

Photodegradation rates of MeHg were examined *in situ*, with initial field incubation experiments of water samples from lakes DA9, DF9, N55 and N70. Water sample temperatures increased during the three hour incubations by, on average, approximately 6 degrees in the morning and 1.3 degrees in the afternoon experiments. The average pH values for filtered samples were as follows: DA9 was pH 6.9, DF9 was pH 6.2, N55 was pH 6.4, and N70 was pH 7.3. There were no significant changes in either pH or buffering capacity with incubation of the water samples.

The MeHg data for all four lakes are found in Appendices 18-21. When results from all lakes were pooled together and examined (General Linear Model, Systat 10), MeHg levels were found to be strongly influenced by several factors. Significant effects were found to be from the following factors: Inter-lake differences ($p<0.001$), indicating that MeHg concentrations were different among the four lakes; the size fraction of DOC ($p = 0.058$), indicating that different concentrations of MeHg were associated with different

size fractions; length of time incubated ($p<0.001$); and the time of day at which the incubations were performed ($p = 0.002$). The overall relationship which included the above factors had an R^2 value of 0.695. Concentrations of DOC and logging status were found to have no effect on photodegradation in the lakes studied.

Due to the great variability in photodegradation rates between lakes, the lakes were also examined individually. In DA9, MeHg was strongly affected by the length of the incubation period ($R^2 = 0.523$; $p < 0.001$) and the time of day incubations were performed ($p = 0.045$). Effects of DOC size fraction and time of day interactions were only marginal ($p=0.069$). Figures 1 to 3 show changes in $\log_{10}$MeHg concentration with time incubated in sunlight for lake DA9 spiked with 2 ppt MeHg, as examples of those graphs obtained for all four lakes. DF9 ($R^2 = 0.853$) showed a strong effect by time incubated, time of day incubated, and size fraction of DOC (all p values <0.001). It also had a size fraction and time of day interaction ($p=0.024$), and a marginal effect of size fraction and time incubated interaction ($p=0.063$). N70 showed no statistically significant photodegradation (or photoproduction), and no effects by DOC size fractions. The time of day incubated accounted for 78% of the MeHg variance observed. N55 showed no statistically significant effects by any of the variables on MeHg levels. Table 1 outlines the photodegradation rate constants (k) for each DOC size fraction. Actual linear photodegradation rates observed for lakes DA9 and DF9 are summarized in Table 2.

Table 1. Field photodegradation experiment data.

Lake	DOC fraction	AM		PM	
		k value (hr^{-1})	R^2	k value (min^{-1})	R^2
DA9	5 kDa	-1.36×10^{-1}	0.64	-1.14×10^{-1}	0.54
	30 kDa	-9.59×10^{-2}	0.46	-1.36×10^{-1}	0.64
	300 kDa	-8.51×10^{-2}	0.35	-9.91×10^{-2}	0.27
DF9	5 kDa	-1.38×10^{-1}	0.70	-2.00×10^{-1}	0.79
	30 kDa	-6.65×10^{-2}	0.79	-6.12×10^{-2}	0.17
	300 kDa	-1.00×10^{-1}	0.67	-1.67×10^{-1}	0.68
N55	5 kDa	-5.52×10^{-3}	0.002	-2.14×10^{-2}	0.040
	30 kDa	8.51×10^{-2}	0.057	-8.05×10^{-3}	0.002
	300 kDa	5.08×10^{-2}	0.029	4.58×10^{-2}	0.55
N70	5 kDa	1.33×10^{-1}	0.48	-1.93×10^{-2}	0.0055
	30 kDa	-3.96×10^{-2}	0.12	-2.65×10^{-2}	0.45
	300 kDa	-5.61×10^{-2}	0.34	3.86×10^{-2}	0.0071

Table 2. Actual field photodegradation rates observed (linear scale).

Lake	DOC Fraction	Photodegradation Rate (ppq/hr)	
		AM	PM
DA9	5 kDa	-241.2	-211.8
	30 kDa	-199.8	-234.4
	300 kDa	-162.2	-174.3
DF9	5 kDa	-98.6	-107.0
	30 kDa	-50.2	-38.9
	300 kDa	-60.7	-75.5

Figure 1. Field photodegradation of DA9 2 ppt MeHg spike (DOC size fraction <5kDa)

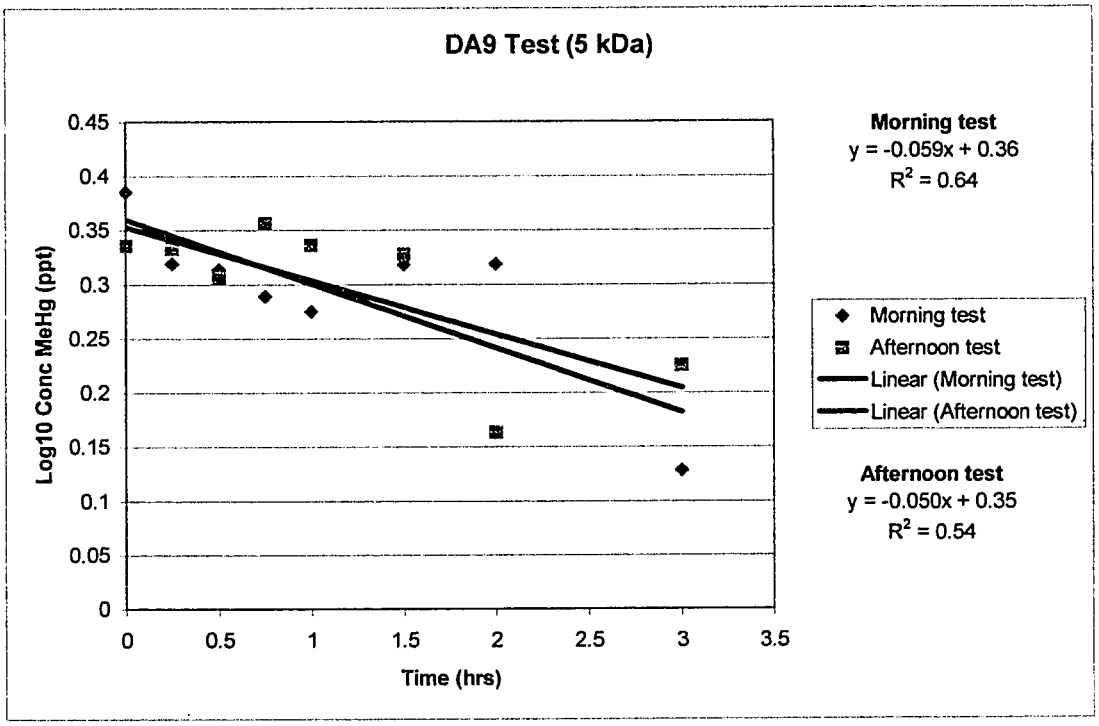
DA9 Test (5 kDa)
Log10 Conc MeHg (ppt)
0.45
0.4
0.35
0.3
0.25
0.2
0.15
0.1
0.05
0
0
0.5
1
1.5
2
2.5
3
3.5
Time (hrs)
Morning test
y = -0.059x + 0.36
R2 = 0.64
Morning test
Afternoon test
Linear (Morning test)
Linear (Afternoon test)
Afternoon test
y = -0.050x + 0.35
R2 = 0.54

Figure 2. Field photodegradation of DA9 2 ppt MeHg spike (DOC size fraction <30 kDa)

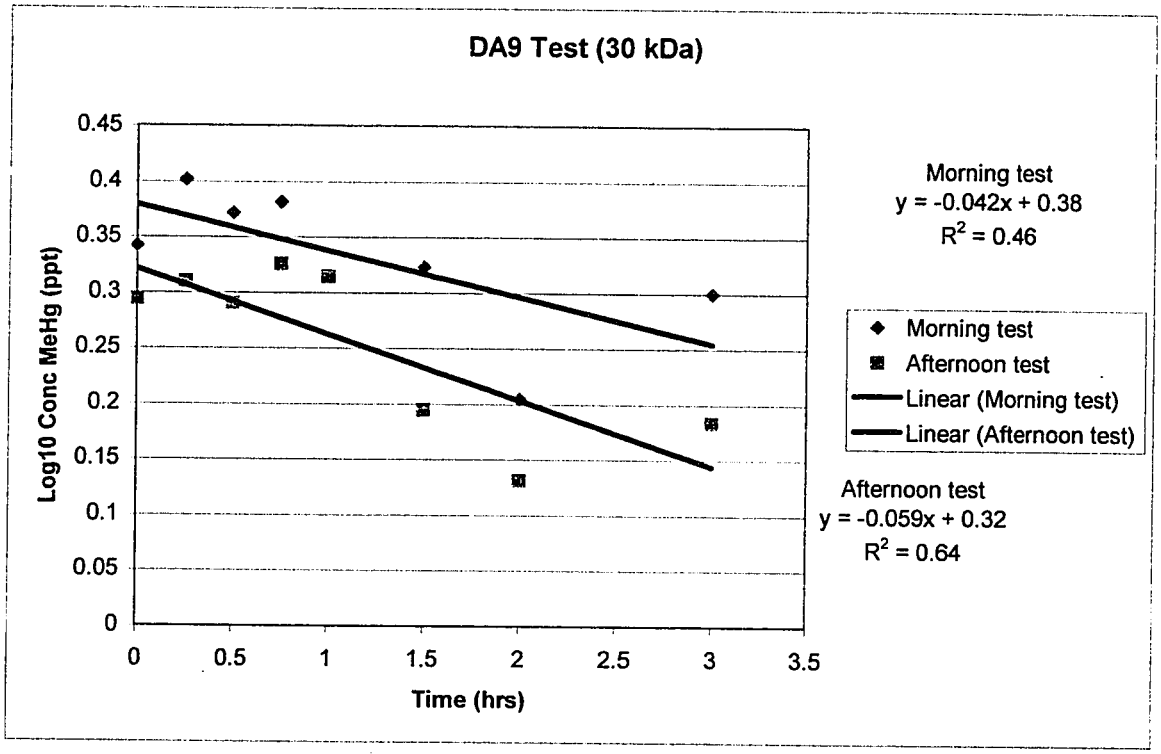
DA9 Test (30 kDa)
Log10 Conc MeHg (ppt)
0.45
0.4
0.35
0.3
0.25
0.2
0.15
0.1
0.05
0
0
0.5
1
1.5
2
2.5
3
3.5
Time (hrs)
Morning test
y = -0.042x + 0.38
R2 = 0.46
Afternoon test
y = -0.059x + 0.32
R2 = 0.64
Morning test
Afternoon test
Linear (Morning test)
Linear (Afternoon test)

Figure 3. Field photodegradation of DA9 2 ppt MeHg spike (DOC size fraction <300 kDa)

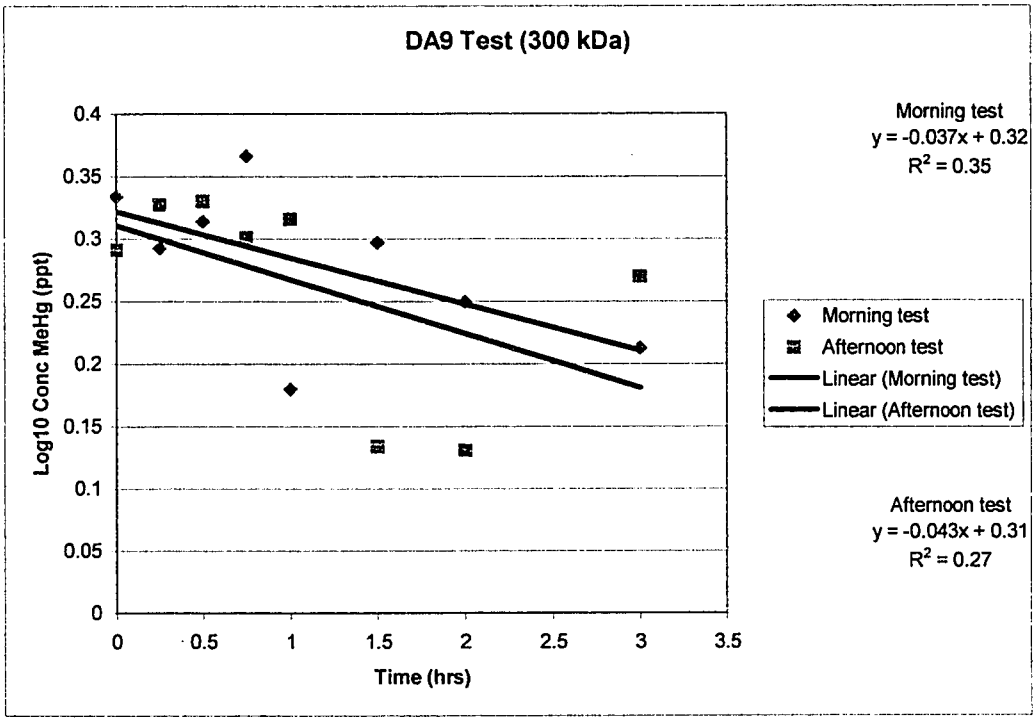
DA9 Test (300 kDa)
Log10 Conc MeHg (ppt)
0.4
0.35
0.3
0.25
0.2
0.15
0.1
0.05
0
0
0.5
1
1.5
2
2.5
3
3.5
Time (hrs)
Morning test
y = -0.037x + 0.32
R2 = 0.35
Afternoon test
y = -0.043x + 0.31
R2 = 0.27
Morning test
Afternoon test
Linear (Morning test)
Linear (Afternoon test)

The series of incubations with ambient level MeHg were done in the field using water samples from lake DF9. This was to evaluate MeHg photodegradation rates at natural MeHg levels. Figures 4 to 6 show $\log_{10}$MeHg concentration plotted versus time incubated. These preliminary experiments demonstrate that after an initial 1–1.5 hour time span of degradation, there may have been some production of MeHg in the later portions of the incubations. Due to the small sample size, conclusions should be limited, however the possibility of the photoproduction of MeHg led to another series of experiments that attempted to reproduce these results. These are discussed in Section 5.4.

Figure 4. Ambient MeHg field incubation of DF9 (DOC size fraction <5 kDa)

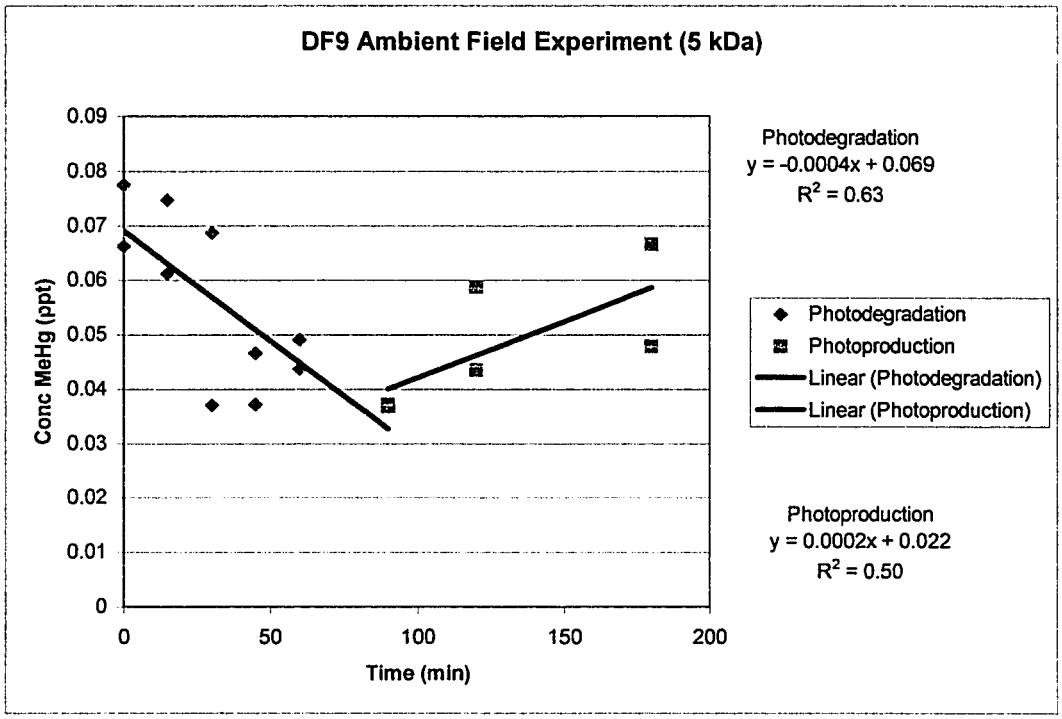
DF9 Ambient Field Experiment (5 kDa)
Conc MeHg (ppt)
0.09
0.08
0.07
0.06
0.05
0.04
0.03
0.02
0.01
0
0
50
100
150
200
Time (min)
Photodegradation
y = -0.0004x + 0.069
R2 = 0.63
Photodegradation
Photoproduction
Linear (Photodegradation)
Linear (Photoproduction)
Photoproduction
y = 0.0002x + 0.022
R2 = 0.50

Figure 5. Ambient MeHg field incubation of DF9 (DOC size fraction <30 kDa)

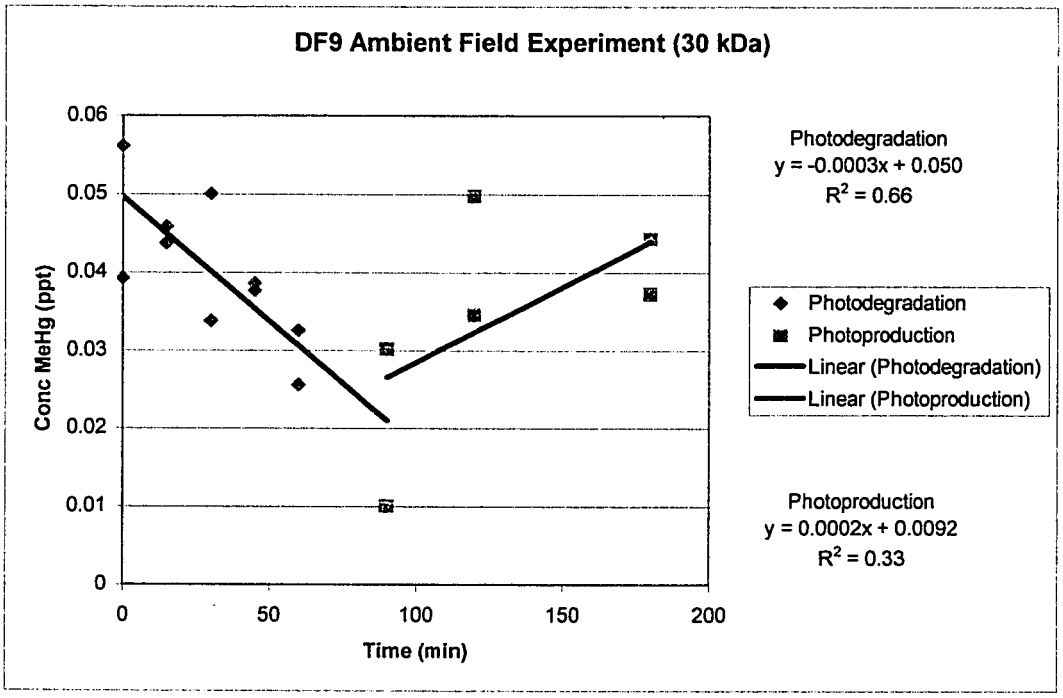
DF9 Ambient Field Experiment (30 kDa)
Conc MeHg (ppt)
0.06
0.05
0.04
0.03
0.02
0.01
0
0
50
100
150
200
Time (min)
Photodegradation
y = -0.0003x + 0.050
R2 = 0.66
Photodegradation
Photoproduction
Linear (Photodegradation)
Linear (Photoproduction)
Photoproduction
y = 0.0002x + 0.0092
R2 = 0.33

Figure 6. Ambient MeHg field incubation of DF9 (DOC size fraction <300 kDa)

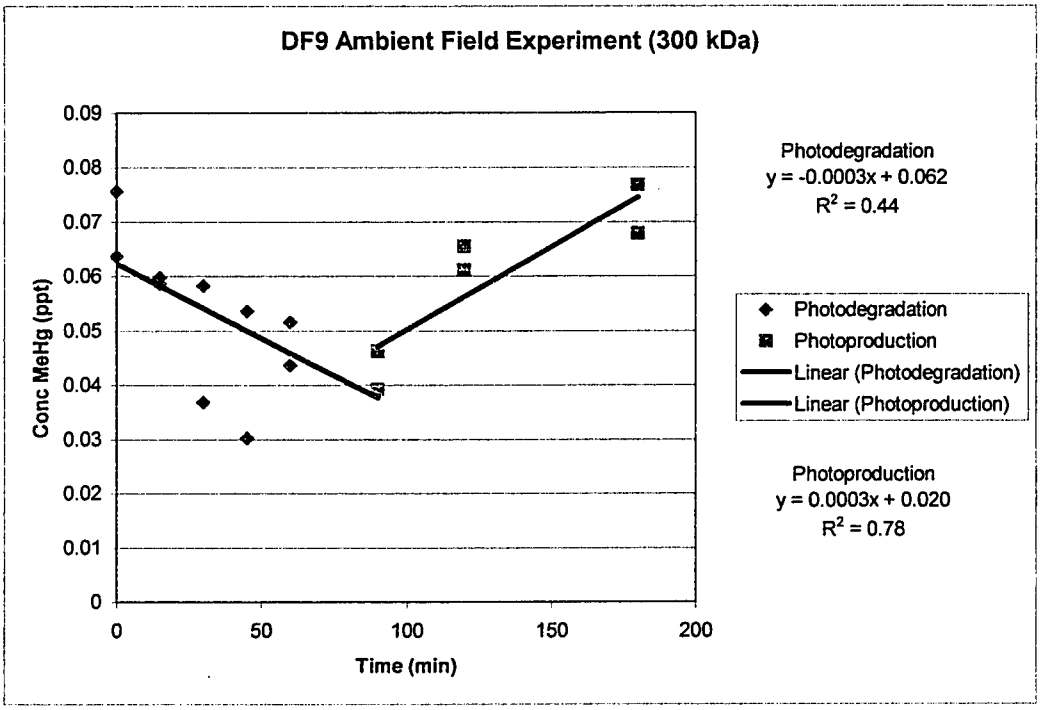
DF9 Ambient Field Experiment (300 kDa)
Conc MeHg (ppt)
0.09
0.08
0.07
0.06
0.05
0.04
0.03
0.02
0.01
0
0
50
100
150
200
Time (min)
Photodegradation
y = -0.0003x + 0.062
R2 = 0.44
Photodegradation
Photoproduction
Linear (Photodegradation)
Linear (Photoproduction)
Photoproduction
y = 0.0003x + 0.020
R2 = 0.78

5.2 pH Experiments

For the rooftop pH experiments, the exact adjusted pH values for the lakes were as follows:

Lake	pH Values		
DA9	4.53	6.49	7.66
N55	4.42	6.44	7.61
K2	4.46	6.53	7.44
K3	4.06	6.41	7.50

A preliminary experiment to this one compared pH 7.5 and 6.5, and no changes in MeHg photodegradation were found. A study by Amirbahman *et al.* (2002) demonstrated a decrease in adsorption of MeHg to dissolved humic acids when the pH was adjusted to below 5.2. Therefore, the pH values chosen for this experiment went down to approximately 4.5, while the higher pH values were within the range of natural values spanned by the lakes studied. The lowest pH of K3 was dropped to near 4 due to buffering of the lake waters tending to return the adjusted pH's towards the natural values.

Results of the experiments are depicted graphically in Figures 7 to 10, with the log10MeHg concentration plotted versus time incubated. A general linear model was applied to the entire set of data obtained (Systat 10), with 47% of the variability of the model being explained by lake effects ($p=0.014$), pH ($p=0.001$), time incubated

($p<0.001$), and pH/time interactions ($p=0.001$). DOC concentrations had no effect on photodegradation rates observed.

Again due to the differences in photodegradation among lakes, each lake was also analyzed separately. N55 (Figure 7) had showed no photodegradation in the initial field experiments, and again showed no photodegradation despite the pH adjusting. DA9 (Figure 8) showed an effect of pH ($p=0.012$), time ($p=0.002$), and of pH/time interactions ($p=0.005$), giving an R^2 value of 0.552. K2 (Figure 9) showed a strong pH effect with MeHg levels ($p=0.016$), which accounted for 42% of the variability in MeHg levels. Time did not appear to have an effect ($p=0.509$), but the effect may not have been detected statistically due to the low power of the test because of low sample sizes. K3 (Figure 10) showed an effect of time ($p=0.002$), indicating that photodegradation was occurring, but pH was found not to have a significant effect (8% of variability of MeHg observed). Again, this may be due to low power of the test.

Figure 7. Rooftop pH incubations of N55.

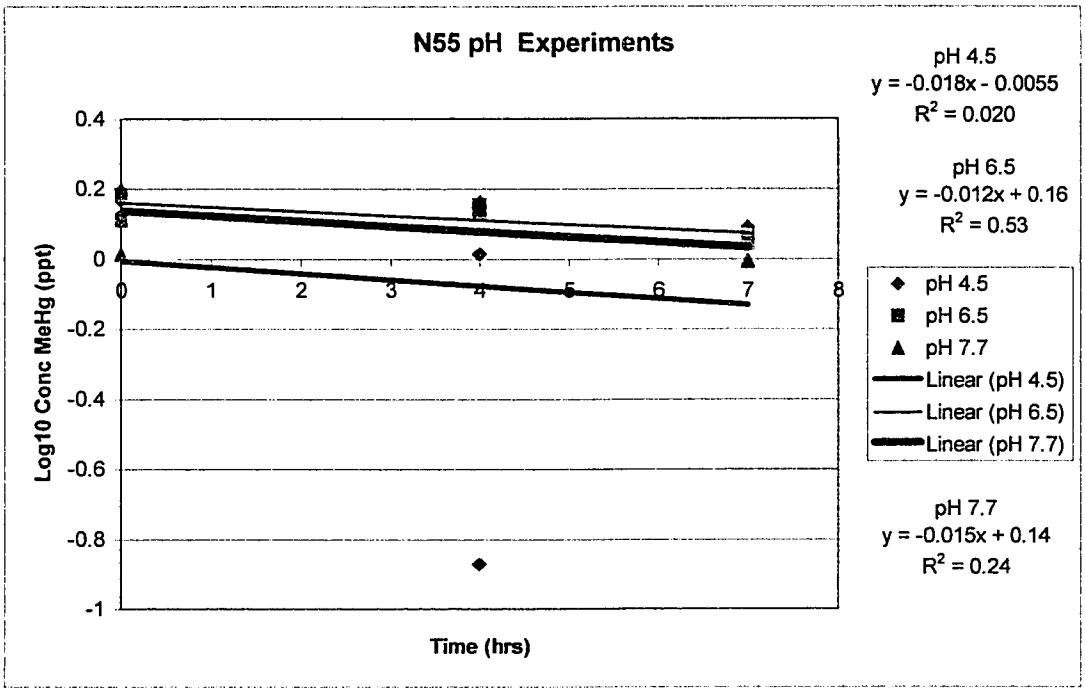
N55 pH Experiments
pH 4.5
y = -0.018x - 0.0055
R2 = 0.020
pH 6.5
y = -0.012x + 0.16
R2 = 0.53
pH 7.7
y = -0.015x + 0.14
R2 = 0.24
pH 4.5
pH 6.5
pH 7.7
Linear (pH 4.5)
Linear (pH 6.5)
Linear (pH 7.7)
Log10 Conc MeHg (ppt)
Time (hrs)
0.4
0.2
0
-0.2
-0.4
-0.6
-0.8
-1
0
1
2
3
4
5
6
7
8

Figure 8. Rooftop pH incubations of DA9.

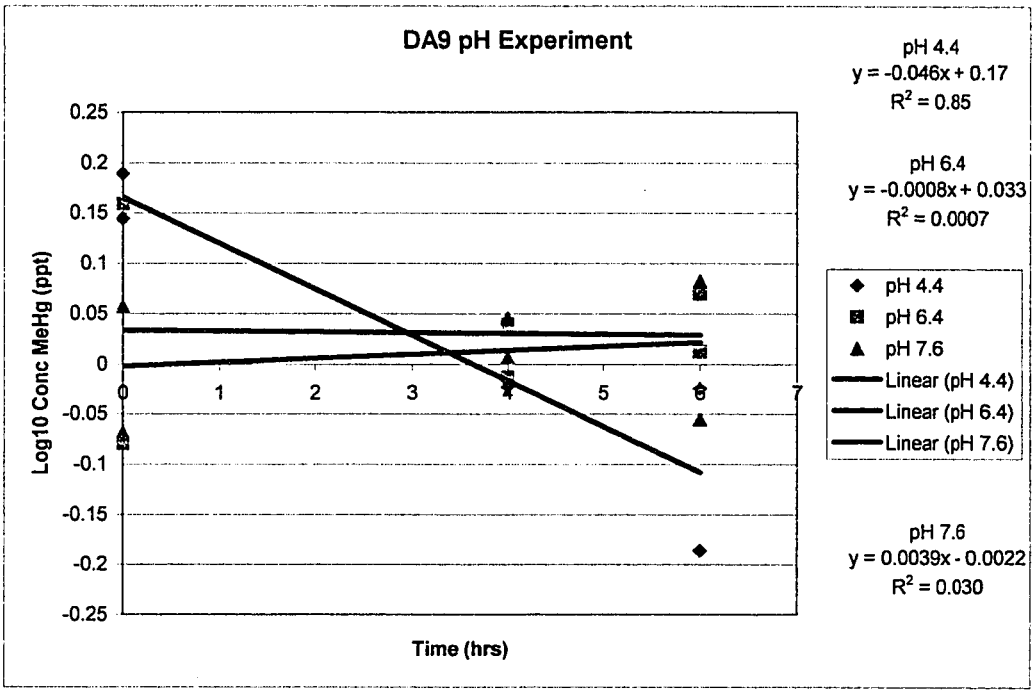
DA9 pH Experiment
Log10 Conc MeHg (ppt)
Time (hrs)
0.25
0.2
0.15
0.1
0.05
0
-0.05
-0.1
-0.15
-0.2
-0.25
0
1
2
3
5
7
pH 4.4
y = -0.046x + 0.17
R2 = 0.85
pH 6.4
y = -0.0008x + 0.033
R2 = 0.0007
pH 7.6
y = 0.0039x - 0.0022
R2 = 0.030
pH 4.4
pH 6.4
pH 7.6
Linear (pH 4.4)
Linear (pH 6.4)
Linear (pH 7.6)

Figure 9. Rooftop pH incubations of K2.

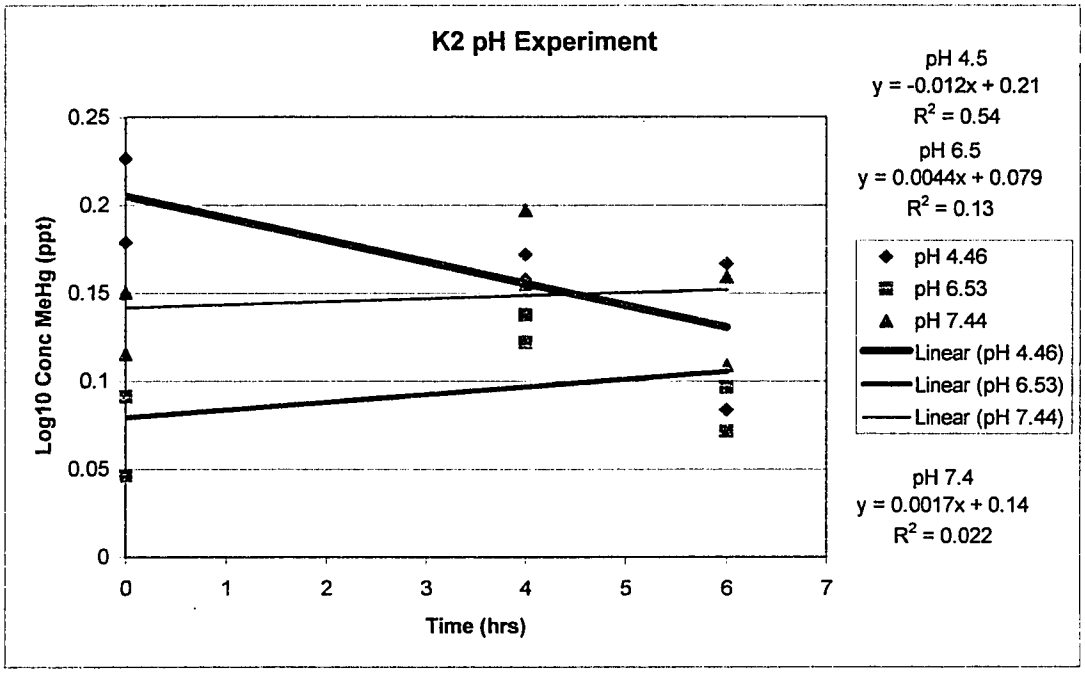
K2 pH Experiment
Log10 Conc MeHg (ppt)
0.25
0.2
0.15
0.1
0.05
0
0
1
2
3
4
5
6
7
Time (hrs)
pH 4.5
y = -0.012x + 0.21
R2 = 0.54
pH 6.5
y = 0.0044x + 0.079
R2 = 0.13
pH 7.4
y = 0.0017x + 0.14
R2 = 0.022
pH 4.46
pH 6.53
pH 7.44
Linear (pH 4.46)
Linear (pH 6.53)
Linear (pH 7.44)

Figure 10. Rooftop incubations of K3.

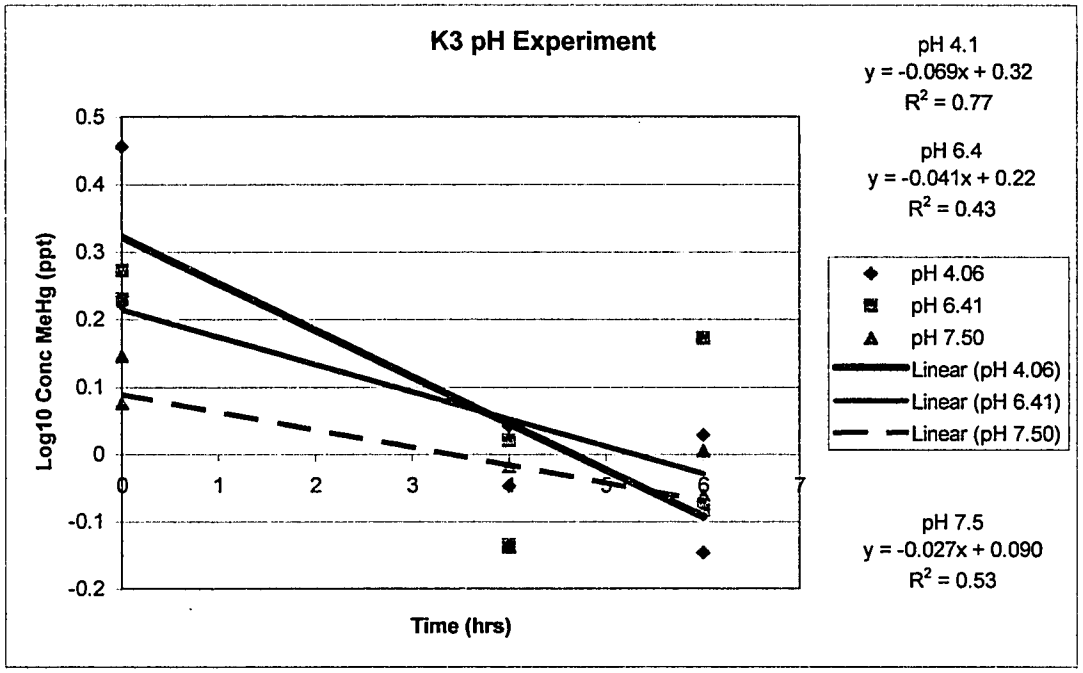
K3 pH Experiment
Log10 Conc MeHg (ppt)
0.5
0.4
0.3
0.2
0.1
0
-0.1
-0.2
0
1
2
3
Time (hrs)
pH 4.1
y = -0.069x + 0.32
R2 = 0.77
pH 6.4
y = -0.041x + 0.22
R2 = 0.43
pH 4.06
pH 6.41
pH 7.50
Linear (pH 4.06)
Linear (pH 6.41)
Linear (pH 7.50)
pH 7.5
y = -0.027x + 0.090
R2 = 0.53

5.3 Determination of Hg^{2+} Levels

Many samples showed no detectable levels of Hg^{2+}, and those that did showed no trends between time irradiated and levels of Hg^{2+}. Data not shown.

5.4 Laboratory MeHg Photoproduction Experiments Under UV Lamp

Results of the laboratory ambient level MeHg photoproduction experiments were negative, with no detectable increases in MeHg concentrations with time incubated. Samples spiked with 4 ppt of inorganic mercury also demonstrated no photoproduction of methylmercury. Figure 11 shows the changes in $\log_{10}$MeHg concentrations with time incubated for both the ambient and spiked samples. There was, however, photodegradation of what appears to be the ambient levels of methylmercury present in the spiked samples, with initial levels of MeHg in unspiked samples being similar to those of spiked samples. The rate constant for the degradation of MeHg in the ambient samples showed a slightly greater loss rate than that of the spiked samples ($-0.069\ hr^{-1}$ compared to $-0.055\ hr^{-1}$, respectively). A general linear model analysis was applied, examining the effect of spiking, incubation time, and whether or not it was a dark control. Time of incubation had a strong effect ($p<0.001$), indicating MeHg loss with time. Whether or not it was a dark control had a marginal effect ($p=0.061$), and spiking with Hg^{2+} had no significant effect on MeHg levels ($p=0.260$).

Figure 11. Comparison of MeHg levels for ambient DA9 and 4 ppt inorganic mercury spike. Experiment performed under UV-B lamp (average UV-A intensity 74.1 $\mu W/cm^2$, UV-B intensity 168.3 $\mu W/cm^2$)

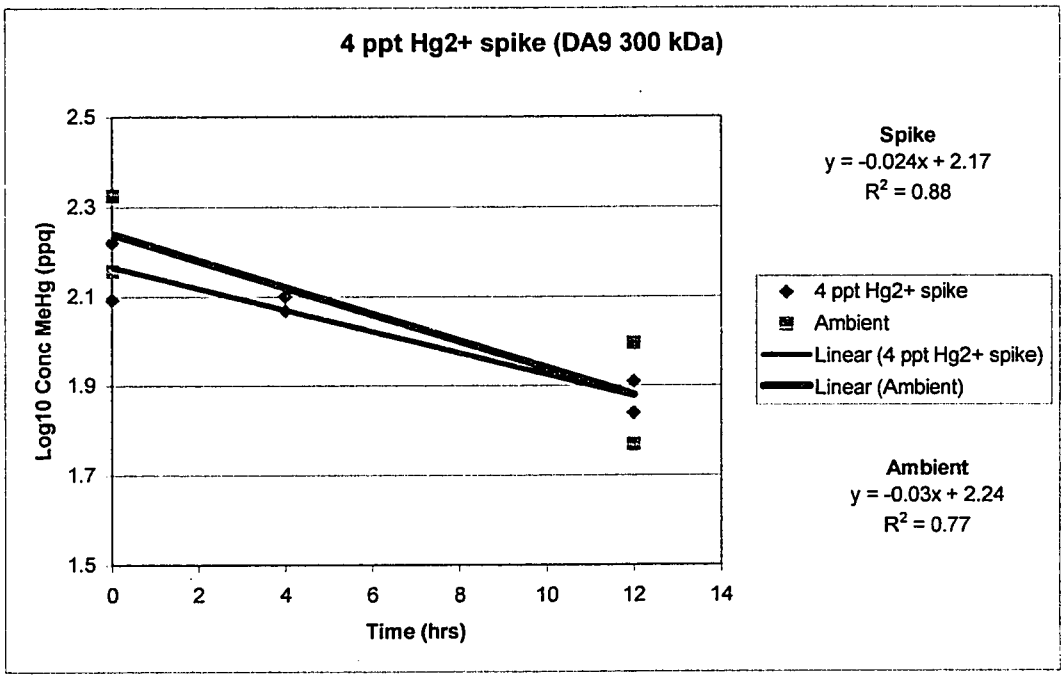
4 ppt Hg2+ spike (DA9 300 kDa)
Log10 Conc MeHg (ppq)
2.5
2.3
2.1
1.9
1.7
1.5
0
2
4
6
8
10
12
14
Time (hrs)
Spike
y = -0.024x + 2.17
R2 = 0.88
4 ppt Hg2+ spike
Ambient
Linear (4 ppt Hg2+ spike)
Linear (Ambient)
Ambient
y = -0.03x + 2.24
R2 = 0.77

5.5 Comparison of Inflow Incubations Under UV Lamp

This experiment is depicted graphically in Figure 12, showing the changes in $\log_{10}$MeHg concentration with time incubated. It demonstrates, with an R^2 value of 0.88, an effect of time ($p=0.034$), and of size fraction/time interactions ($p=0.003$). It was found that there was photodegradation of the 5 kDa samples, with a k value of -9.21×10^{-2} (hr^{-1}), while the 300 kDa samples showed no signs of degradation. As a preliminary experiment, sample sizes are very low, but it is included because it appears that inflow waters have different results from lake water. A more extensive experiment would be recommended to explore the differences between inflow and lake water samples.

Figure 12. Incubation of 300 kDa and 5 kDa DOC fractions of ambient Jack's Lake inflow water.

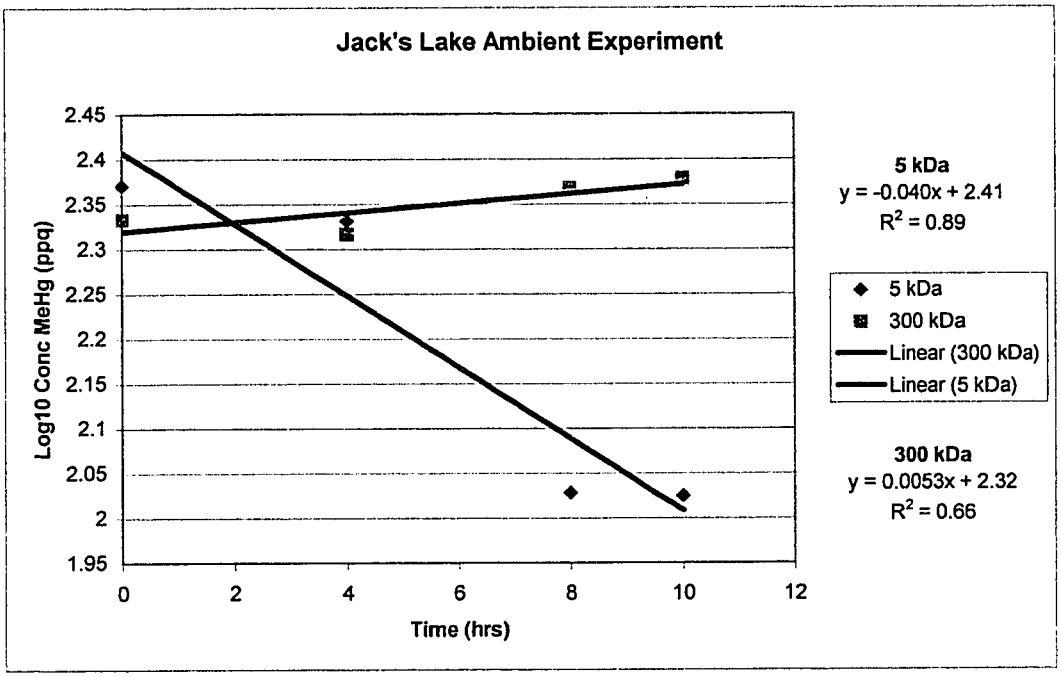
Jack's Lake Ambient Experiment
Log10 Conc MeHg (ppq)
2.45
2.4
2.35
2.3
2.25
2.2
2.15
2.1
2.05
2
1.95
0
2
4
6
8
10
12
Time (hrs)
5 kDa
y = -0.040x + 2.41
R2 = 0.89
5 kDa
300 kDa
Linear (300 kDa)
Linear (5 kDa)
300 kDa
y = 0.0053x + 2.32
R2 = 0.66

5.6 Fractionation Experiments

MeHg showed marked concentration patterns when associated with different DOC size fractions (Figures 13-17). As shown in Figure 13, at time zero, the retentate portions of each size fraction for all lakes examined showed much higher concentrations of MeHg than the filtrate portions. However, in Figure 14 these larger fractions also showed significant MeHg photodegradation over the first hour of incubation in sunlight. At time one hour, the 300 kDa sample showed a large decrease in MeHg in the 30 kDa retentate, but a small increase in the filtrate. The filtrate portions did not show photodegradation from their initial lower values. At time two hours (Figure 15), those fractions passing through the 5 kDa filter both showed an increase in MeHg. Figure 17 shows the trends of the retentate and filtrate MeHg levels for the fraction 300K/30 over all the incubation times. With the three remaining lakes, only time zero was examined for fractionation (Figures 20-22). In each case, the pattern of greater amounts of MeHg being bound to larger portions of the DOC size fractions was followed without exception.

There were no significant changes in DF9 DOC concentrations of each fraction examined over time, with the exception possibly of 300K/5/F (Figures 18 and 19). DOC concentrations for the filtrate and retentate portions of each size fraction were all close and in cases slightly higher in the filtrate. The highest DOC concentration was in the 300K/30/R fraction, with an average of approximately 20 mg/L. This showed no significant changes with incubation. The lowest concentration was found in the 30K/5/F fraction, which again did not significantly change with incubation time.

Figure 13. Field photodegradation of DF9 fractionation experiment. MeHg values at time 0 hrs. Error bars indicate range of duplicate values. In sample designations, the first number signifies in kDa the DOC size fraction of the initial sample, the second number the filter size that the sample was filtered through, and "R" or "F" signifies the retentate or filtrate portions of the filtered sample, respectively.

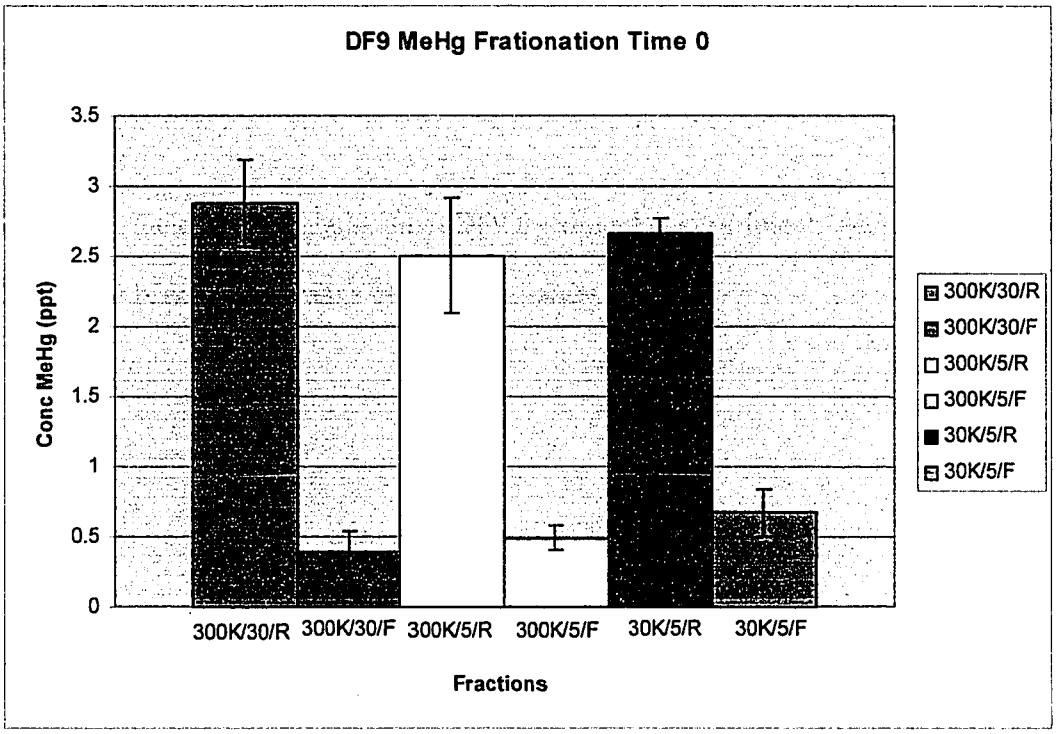
DF9 MeHg Frationation Time 0
Conc MeHg (ppt)
3.5
3
2.5
2
1.5
1
0.5
0
300K/30/R
300K/30/F
300K/5/R
300K/5/F
30K/5/R
30K/5/F
Fractions

Figure 14. Field photodegradation of DF9 fractionation experiment. MeHg values at time 1 hr. Error bars indicate range of duplicate values.

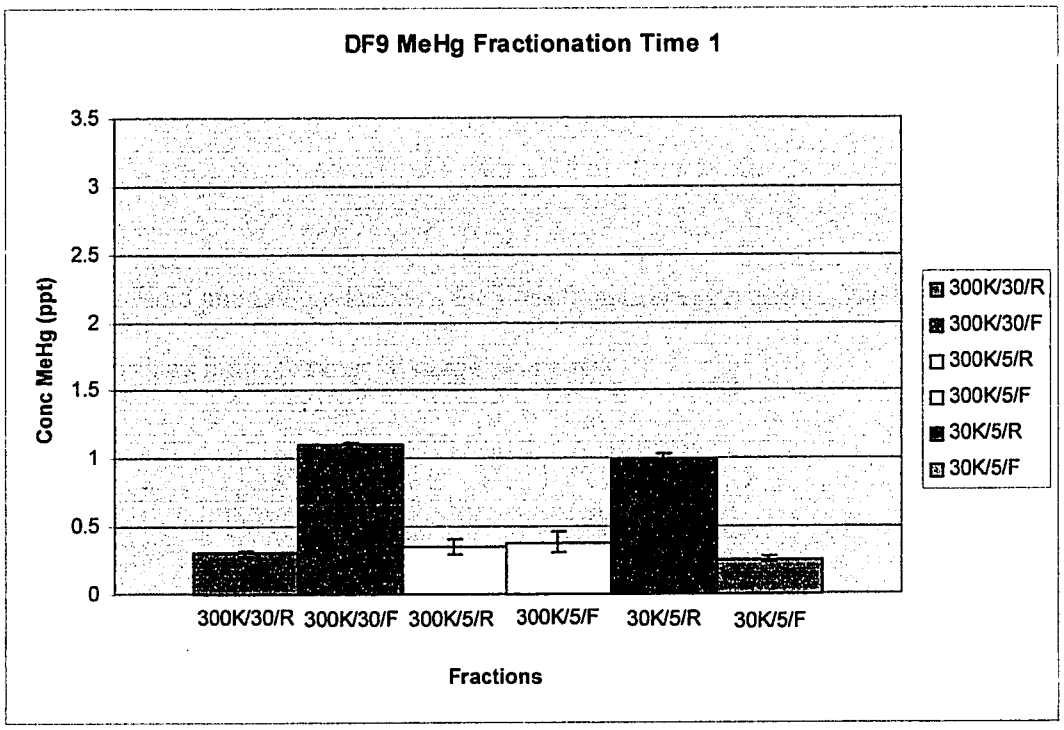
DF9 MeHg Fractionation Time 1
Conc MeHg (ppt)
3.5
3
2.5
2
1.5
1
0.5
0
300K/30/R
300K/30/F
300K/5/R
300K/5/F
30K/5/R
30K/5/F
Fractions

Figure 15. Field photodegradation of DF9 fractionation experiment. MeHg values at time 2 hrs. Error bars indicate range of duplicate values.

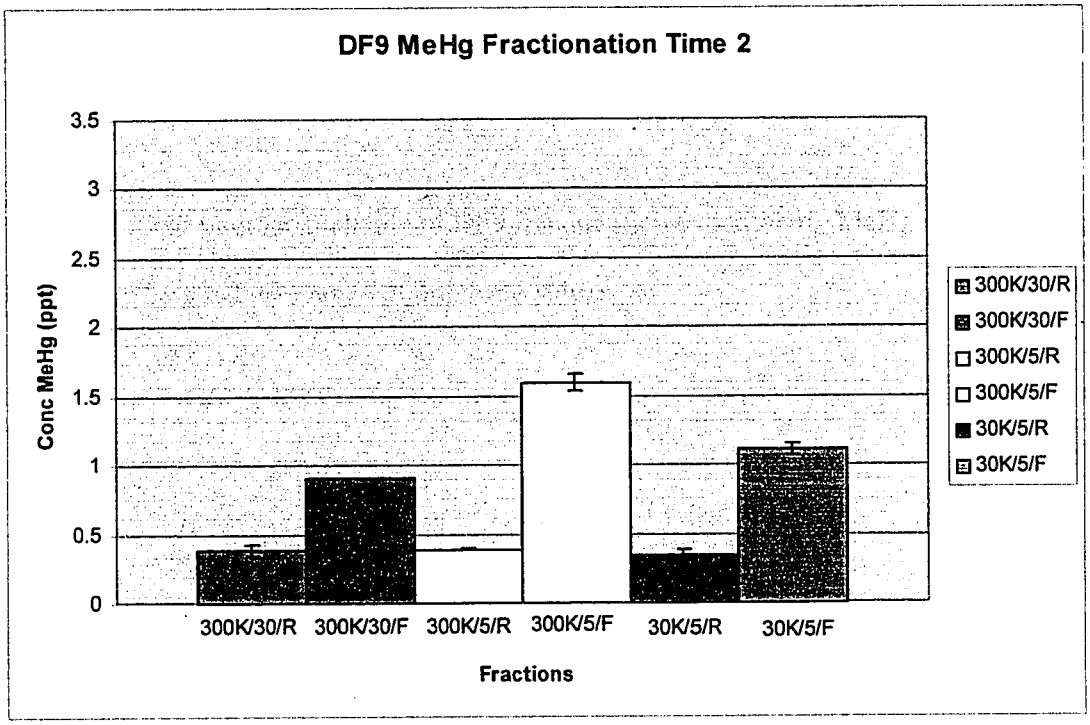
DF9 MeHg Fractionation Time 2
Conc MeHg (ppt)
3.5
3
2.5
2
1.5
1
0.5
0
300K/30/R
300K/30/F
300K/5/R
300K/5/F
30K/5/R
30K/5/F
Fractions

Figure 16. Field photodegradation of DF9 fractionation experiment. MeHg values at time 3 hrs. Error bars indicate range of duplicate values.

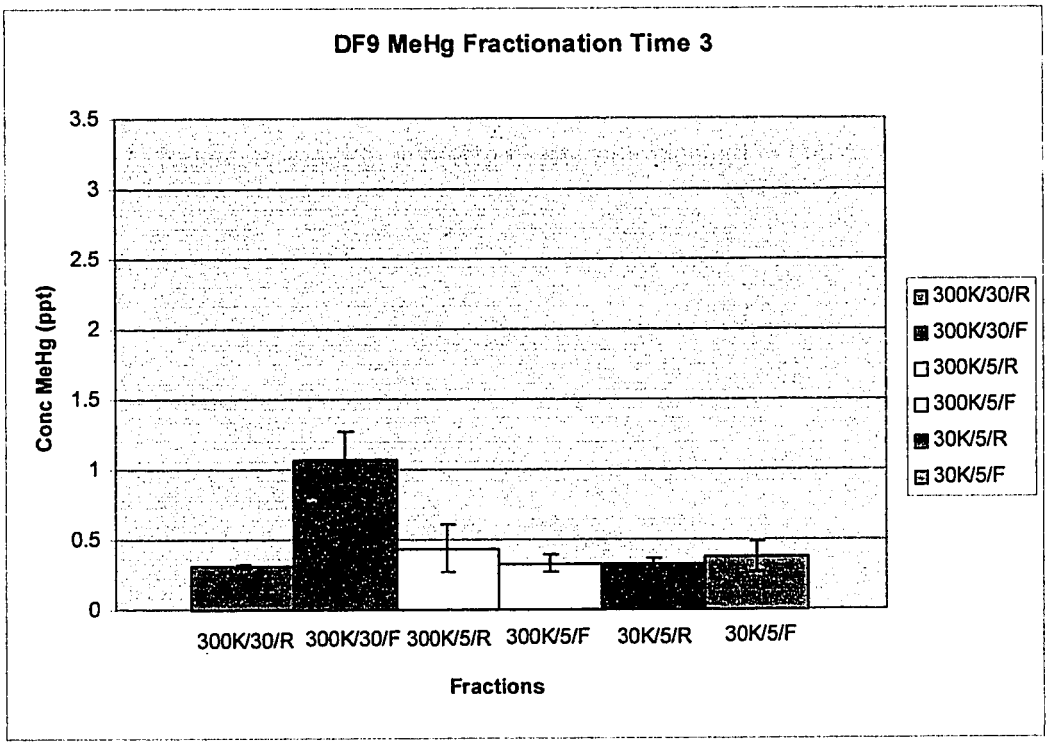
DF9 MeHg Fractionation Time 3
Conc MeHg (ppt)
3.5
3
2.5
2
1.5
1
0.5
0
300K/30/R
300K/30/F
300K/5/R
300K/5/F
30K/5/R
30K/5/F
Fractions

Figure 17. Retentate and filtrate MeHg trends with incubation (300K/30).

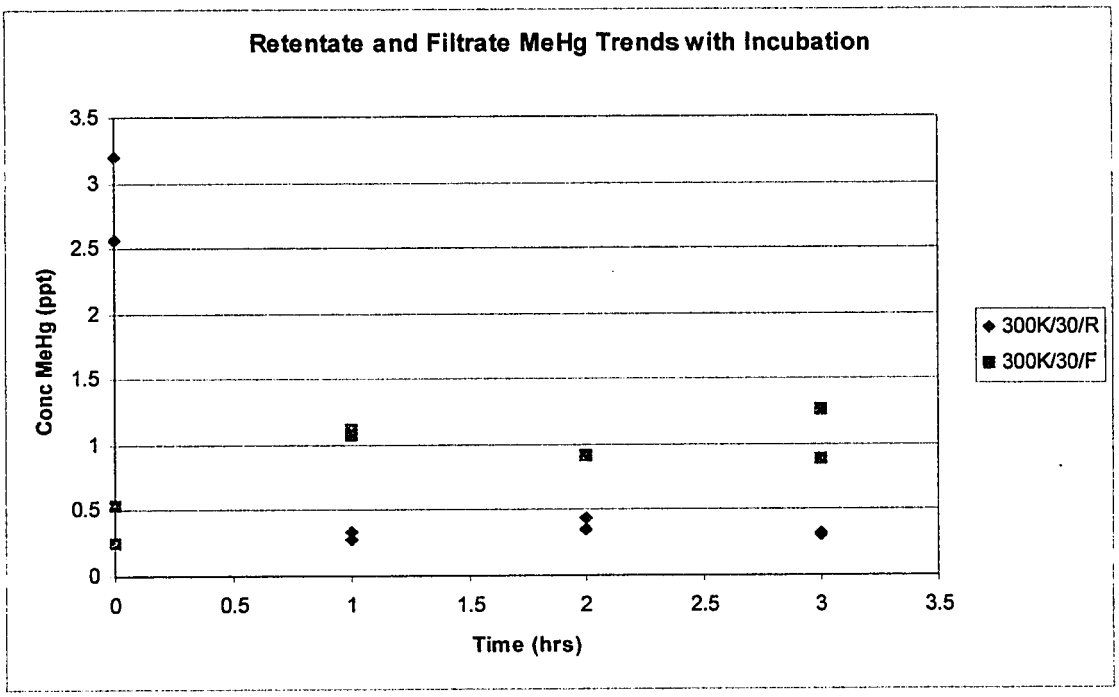
Retentate and Filtrate MeHg Trends with Incubation
Conc MeHg (ppt)
3.5
3
2.5
2
1.5
1
0.5
0
0
0.5
1
1.5
2
2.5
3
3.5
Time (hrs)
300K/30/R
300K/30/F

Figure 18. DOC fraction trends with incubation time (retentates).

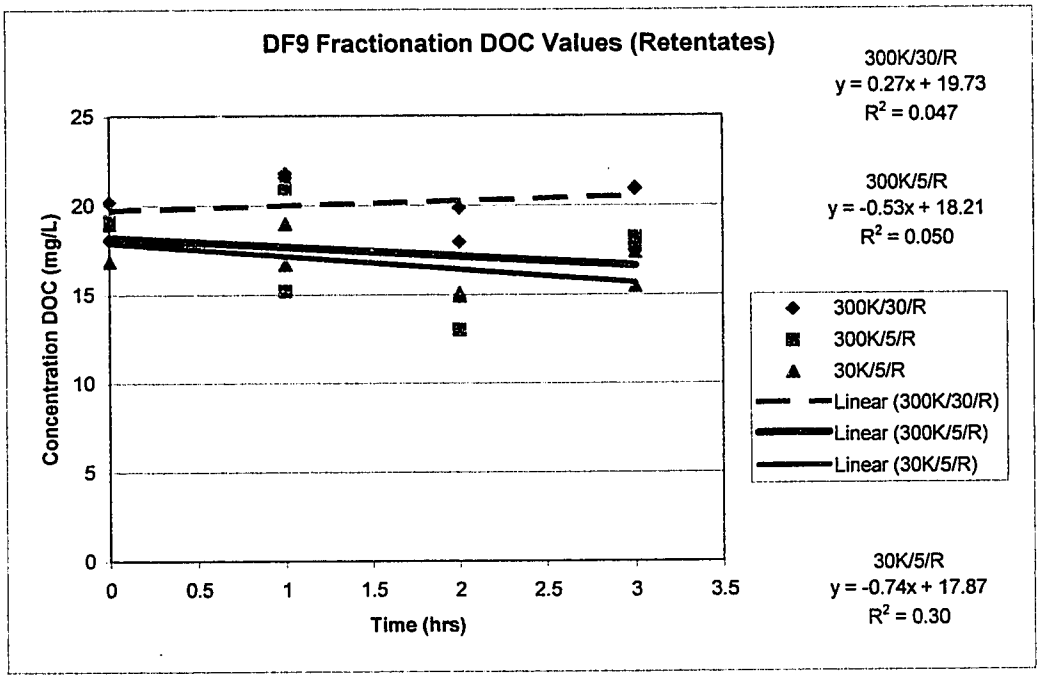
DF9 Fractionation DOC Values (Retentates)
Concentration DOC (mg/L)
Time (hrs)
0
5
10
15
20
25
0
0.5
1
1.5
2
2.5
3
3.5
300K/30/R
y = 0.27x + 19.73
R2 = 0.047
300K/5/R
y = -0.53x + 18.21
R2 = 0.050
30K/5/R
y = -0.74x + 17.87
R2 = 0.30
300K/30/R
300K/5/R
30K/5/R
Linear (300K/30/R)
Linear (300K/5/R)
Linear (30K/5/R)

Figure 19. DOC fraction trends with incubation time (filtrates).

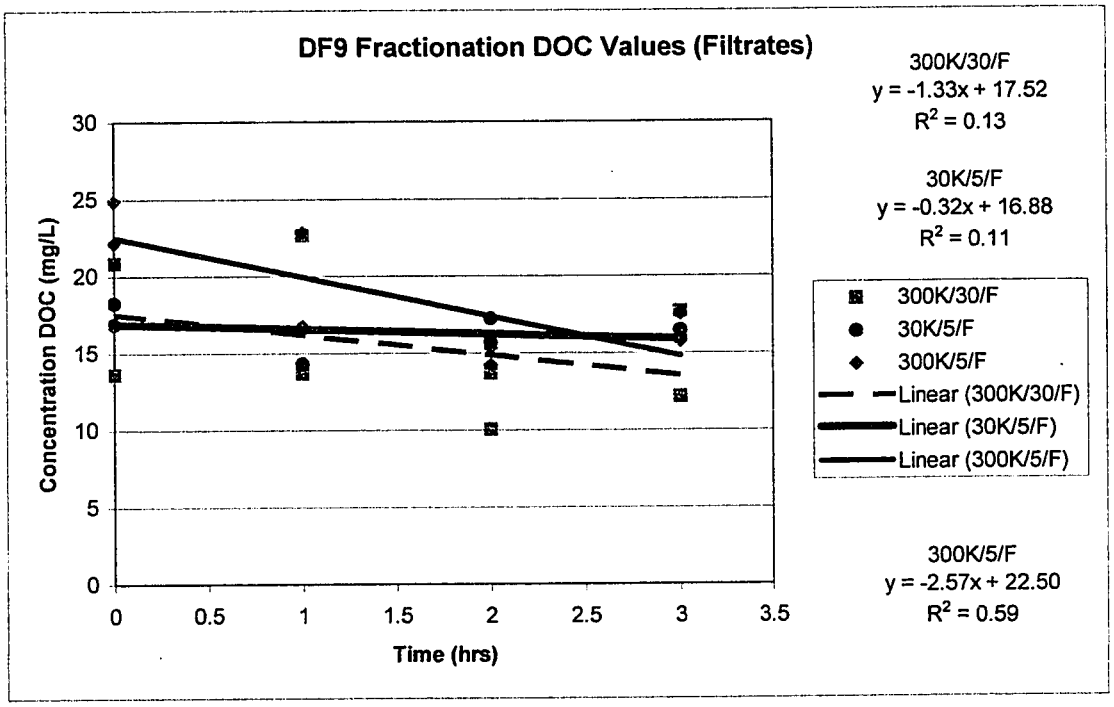
DF9 Fractionation DOC Values (Filtrates)
Concentration DOC (mg/L)
Time (hrs)
0
5
10
15
20
25
30
0
0.5
1
1.5
2
2.5
3
3.5
300K/30/F
y = -1.33x + 17.52
R2 = 0.13
30K/5/F
y = -0.32x + 16.88
R2 = 0.11
300K/5/F
y = -2.57x + 22.50
R2 = 0.59
300K/30/F
30K/5/F
300K/5/F
Linear (300K/30/F)
Linear (30K/5/F)
Linear (300K/5/F)

Figure 20. Field DA9 fractionation experiment. MeHg values at time 0 hrs.

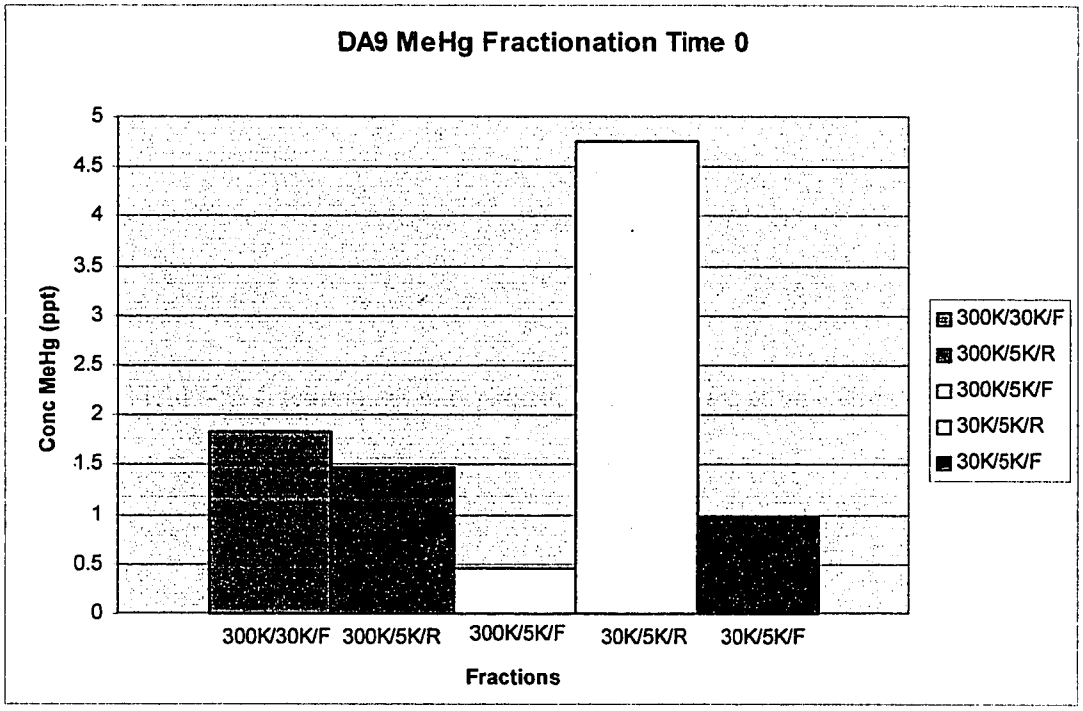
DA9 MeHg Fractionation Time 0
Conc MeHg (ppt)
5
4.5
4
3.5
3
2.5
2
1.5
1
0.5
0
300K/30K/F
300K/5K/R
300K/5K/F
30K/5K/R
30K/5K/F
Fractions
300K/30K/F
300K/5K/R
300K/5K/F
30K/5K/R
30K/5K/F

Figure 21. Field N55 fractionation experiment. MeHg values at time 0 hrs.

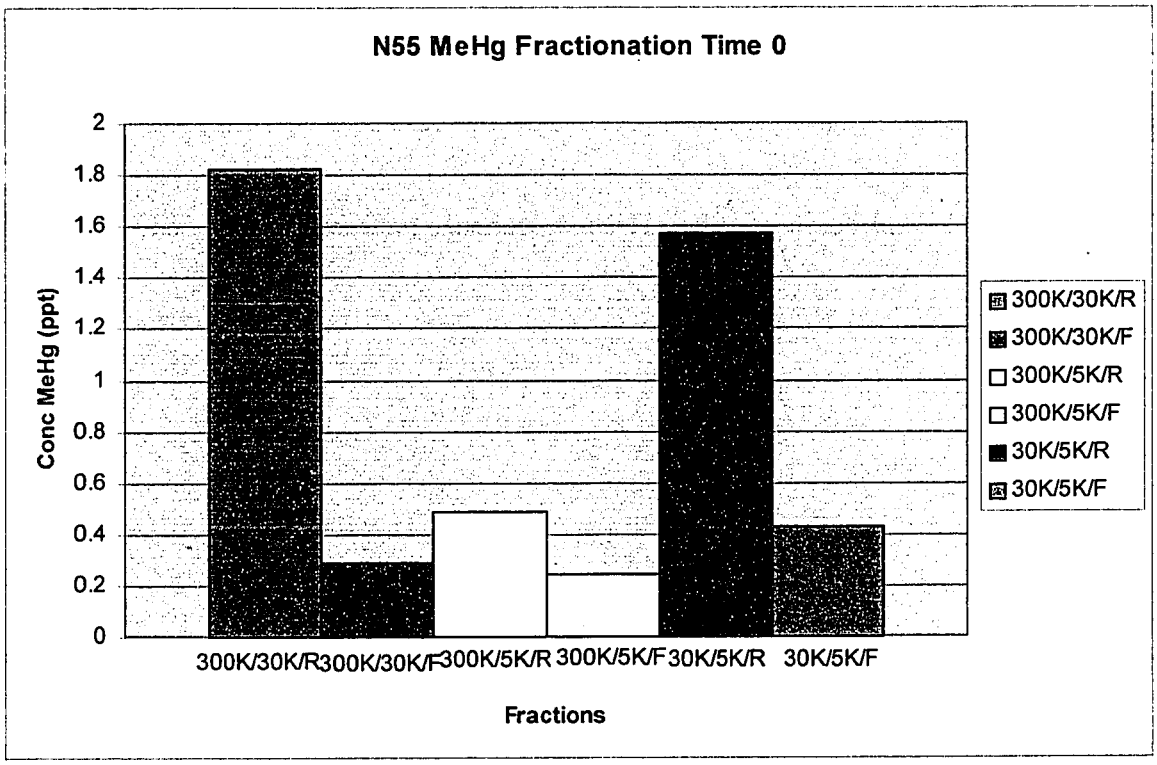
N55 MeHg Fractionation Time 0
Conc MeHg (ppt)
2
1.8
1.6
1.4
1.2
1
0.8
0.6
0.4
0.2
0
300K/30K/R
300K/30K/F
300K/5K/R
300K/5K/F
30K/5K/R
30K/5K/F
Fractions

Figure 22. Field N70 fractionation experiment. MeHg values at time 0 hrs.

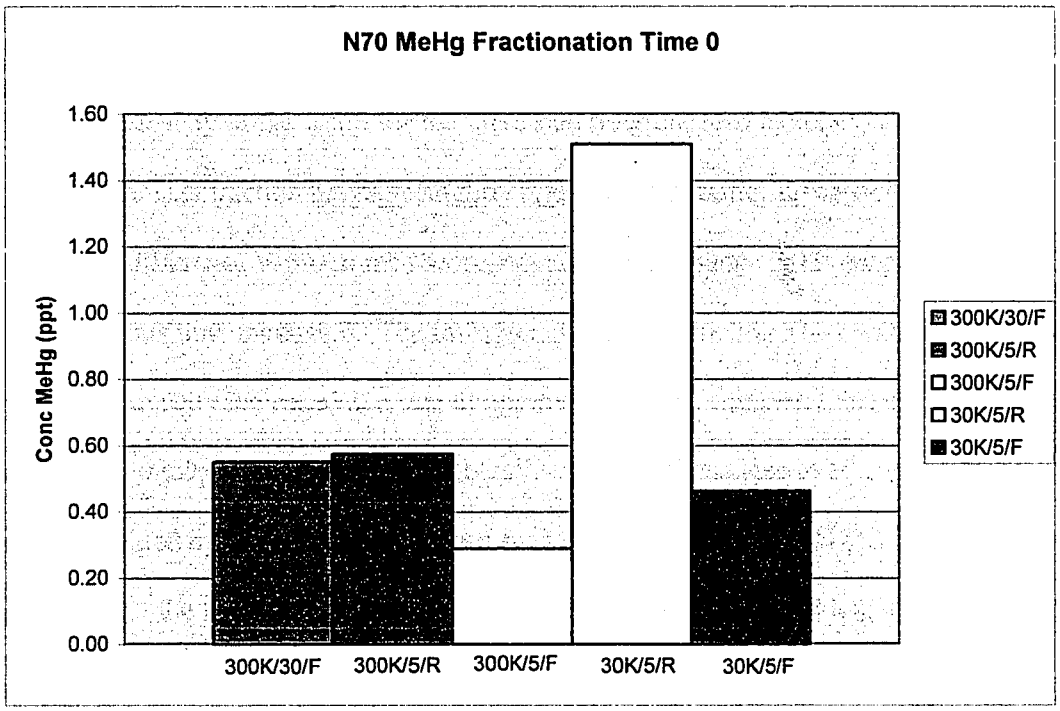
N70 MeHg Fractionation Time 0
Conc MeHg (ppt)
1.60
1.40
1.20
1.00
0.80
0.60
0.40
0.20
0.00
300K/30/F
300K/5/R
300K/5/F
30K/5/R
30K/5/F
300K/30/F
300K/5/R
300K/5/F
30K/5/R
30K/5/F

5.7 Changes in Buffering Capacity and pH With Incubation

The four lakes examined in the initial field experiments were evaluated for changes in pH and buffering capacity during the incubations. There were no significant changes in either factor for any of the Northern Quebec lakes. However, Jack's Lake water that was taken directly from the wetlands outflow showed significant changes. Changes in pH for all three DOC size fractions were virtually identical, with all three showing increases in pH from approximately 6 to 7 over the eight hour incubation time (Figure 23). The buffering capacity of the water for the three size fractions also increased over time, with the 300 kDa size fraction having a slightly higher overall buffering capacity. Figure 24 shows the difference between the theoretical and actual change in H^+ concentration plotted versus time incubated. The raw data is in Appendix 28. The 5 kDa fraction's buffering capacity increased at a rate of approximately 0.2 mmoles/L/hr, and both the 30 kDa and 300 kDa increased at 0.1 mmoles/L/hr. Actual changes in H^+ ion concentration were evaluated by measured pH changes for a given volume of 3.6 N HCl added, and was compared to the theoretical change in H^+ concentration with HCl added.

Figure 23. Trends in pH change over time incubated for three size fractions of DOC.

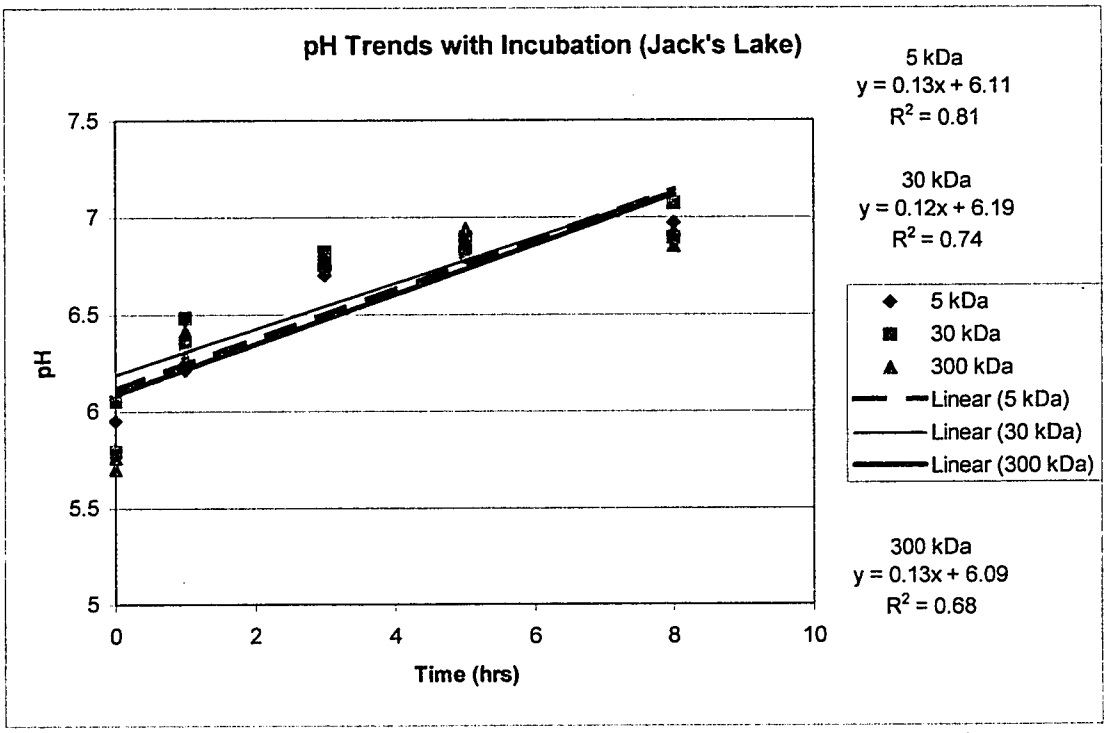
pH Trends with Incubation (Jack's Lake)
5 kDa
y = 0.13x + 6.11
R2 = 0.81
30 kDa
y = 0.12x + 6.19
R2 = 0.74
300 kDa
y = 0.13x + 6.09
R2 = 0.68
5 kDa
30 kDa
300 kDa
Linear (5 kDa)
Linear (30 kDa)
Linear (300 kDa)
pH
Time (hrs)
7.5
7
6.5
6
5.5
5
0
2
4
6
8
10

Figure 24. Trends in buffering capacity over incubation time for three DOC size fractions.

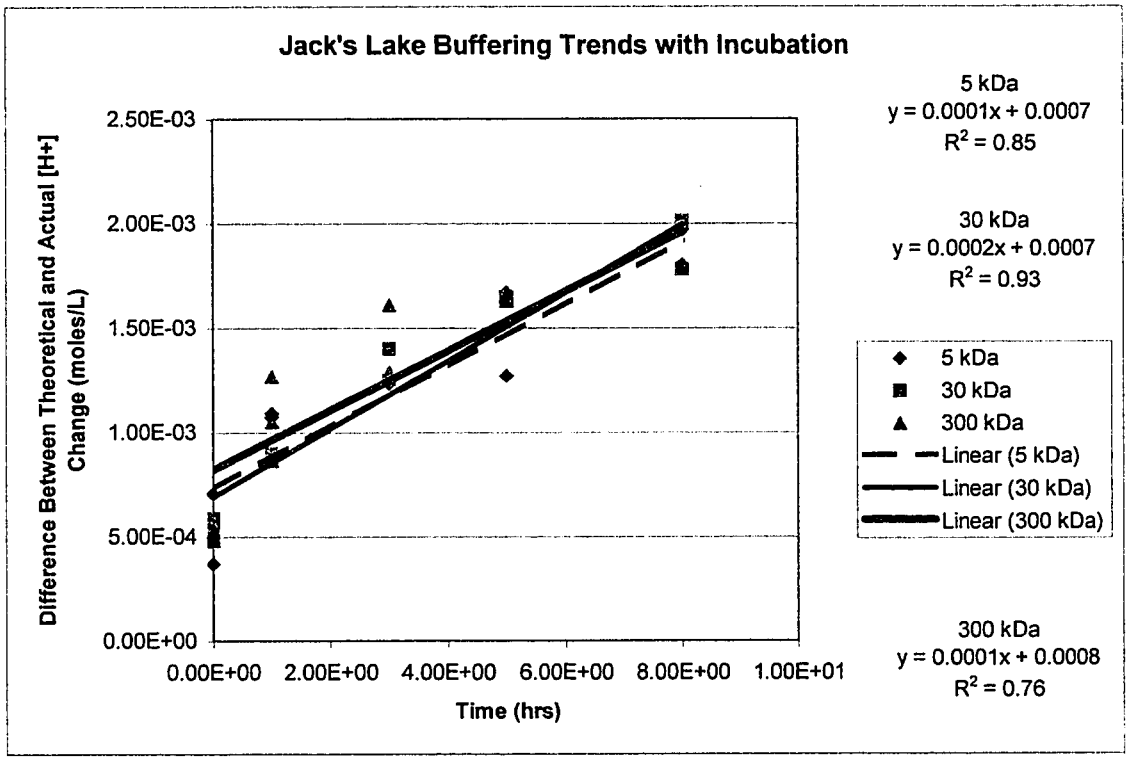
Jack's Lake Buffering Trends with Incubation
Difference Between Theoretical and Actual [H+] Change (moles/L)
2.50E-03
2.00E-03
1.50E-03
1.00E-03
5.00E-04
0.00E+00
0.00E+00
2.00E+00
4.00E+00
6.00E+00
8.00E+00
1.00E+01
Time (hrs)
5 kDa
y = 0.0001x + 0.0007
R2 = 0.85
30 kDa
y = 0.0002x + 0.0007
R2 = 0.93
300 kDa
y = 0.0001x + 0.0008
R2 = 0.76
5 kDa
30 kDa
300 kDa
Linear (5 kDa)
Linear (30 kDa)
Linear (300 kDa)

5.8 Dark Incubation Time Course Experiment

Results from the time course experiment indicate that a dark incubation period is not necessary for equilibrium binding of MeHg to DOC. MeHg values for each DOC size fraction were not found to be correlated with incubation time. The raw data for this experiment is found in Appendix 35.

5.9 DAPI Microbial Enumeration

DAPI microbial enumeration of 23 lake water samples that had been incubated in the field for the full three hours showed no detectable bacteria in 20 of the samples. In samples from N55 (30 kDa filter at three hour incubation), 1.0×10^6/L of cocci were observed, from N70 (300 kDa filter at three hour incubation), 9.0×10^6/L cocci were observed, and from N70 (5 kDa filter at three hour incubation), 9.1×10^4/L cocci were observed. Note that the only samples in which cocci were observed were at the three hour incubations. Due to equipment constraints, while traveling from the field site to the laboratory, samples for microbial analysis thawed for approximately 8 hours, during which time bacteria present would have had time to proliferate. It can be expected that bacterial levels would have been significantly lower during the actual experiments.

5.10 Tangential Flow Ultrafiltrator

The initial filtration rates for the filters were 112 ml/min (10 psi inlet/8 psi retentate line pressure), 254 ml/min (8 psi inlet pressure) , and 200 ml/min (8 psi inlet pressure) for the 5 kDa, 30 kDa and 300 kDa, respectively . Evaluation of filter performance after the

filtering of approximately 200 litres of lake water through each filter found that the filtration rates decreased by 26%, 17%, and 50% for the 5 kDa, 30 kDa, and 300 kDa filters, respectively. The 300 kDa filter, as an older model T-screen filter, has less space between the filter surface layers within the cassette, and showed the greatest decrease in filtration rate, possibly due to increased clogging. Mass balances (n=3) for MeHg under the above noted conditions were 96%, 81%, and 109% for the 5 kDa, 30 kDa, and 300 kDa filters, respectively. Mass balances for DOC could not be calculated due to the coagulation of DOC out of higher concentration samples.

The partitioning of DOC in the retentate and filtrate portions of water samples as filtering progresses gives an indication of how much DOC passes a particular filter. Due to problems with the DOC coagulating out of the retentate fractions of both the 5 kDa and 300 kDa fractions, and therefore not being able to be run on the DOC analyzer at the University of Montreal, no retentate values were obtained. Therefore, for these two filters, only the change in DOC concentration in the filtrate could be evaluated. The relationship between the percent of the sample passing the filter with the amount of DOC in only the filtrate fraction is not as strong as that with the ratio of the filtrate over the retentate. The 5 kDa filter showed only a weak relationship (R^2=0.013), as shown in Figure 25. It demonstrated no decrease in the concentration of DOC passing the filter with percent of initial sample filtered. The 30 kDa filter (Figure 26) showed a very strong relationship (R^2=0.92) between the log10 transformed ratio of the DOC concentration of the filtrate over the retentate, and the percent of the initial sample volume which had passed through the filter. The slope produces a k value of –0.14 mg/L

per every 10% of sample passing through the filter. The 300 kDa filter (Figure 25) had an R^2 value of 0.40. If plotted linearly, the slope produces a k value of –0.015 mg/L per every 10% of 1000 mL sample passing through the filter. However note that the DOC concentration passing the filter plateaus when approximately 30% of the sample has been filtered, therefore suggesting a power relationship. Using the Systat 10 General Linear Model, it was found that filter size accounted for 74% of the variability in DOC concentration passing the filters, while percent of sample filtered accounted for only 7% of the variability.

Figure 25. Comparison of DOC in filtrate to volume of filtrate from a 1000 mL Lake Berthelot sample, with DOC sampled every 100 mL.

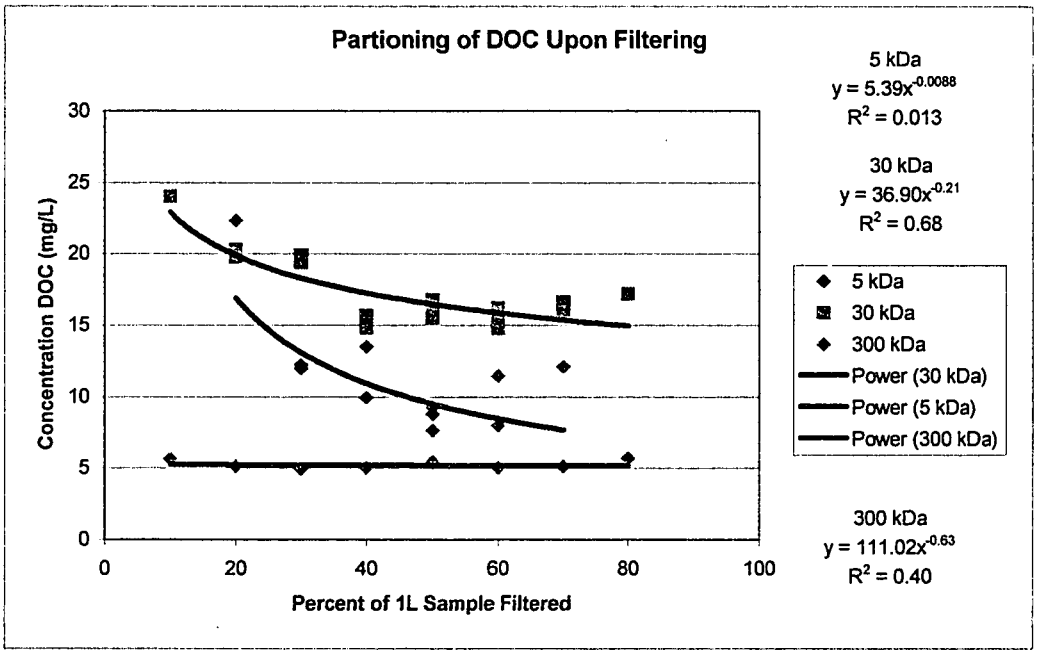
Partioning of DOC Upon Filtering
Concentration DOC (mg/L)
Percent of 1L Sample Filtered
0
5
10
15
20
25
30
0
20
40
60
80
100
5 kDa
y = 5.39x^-0.0088
R² = 0.013
30 kDa
y = 36.90x^-0.21
R² = 0.68
300 kDa
y = 111.02x^-0.63
R² = 0.40
5 kDa
30 kDa
300 kDa
Power (30 kDa)
Power (5 kDa)
Power (300 kDa)

Figure 26. Comparison of DOC in 30 kDa filtrate and retentate as filtering of 1000 mL Lake Berthelot sample progresses, with DOC sampled every 100 mL.

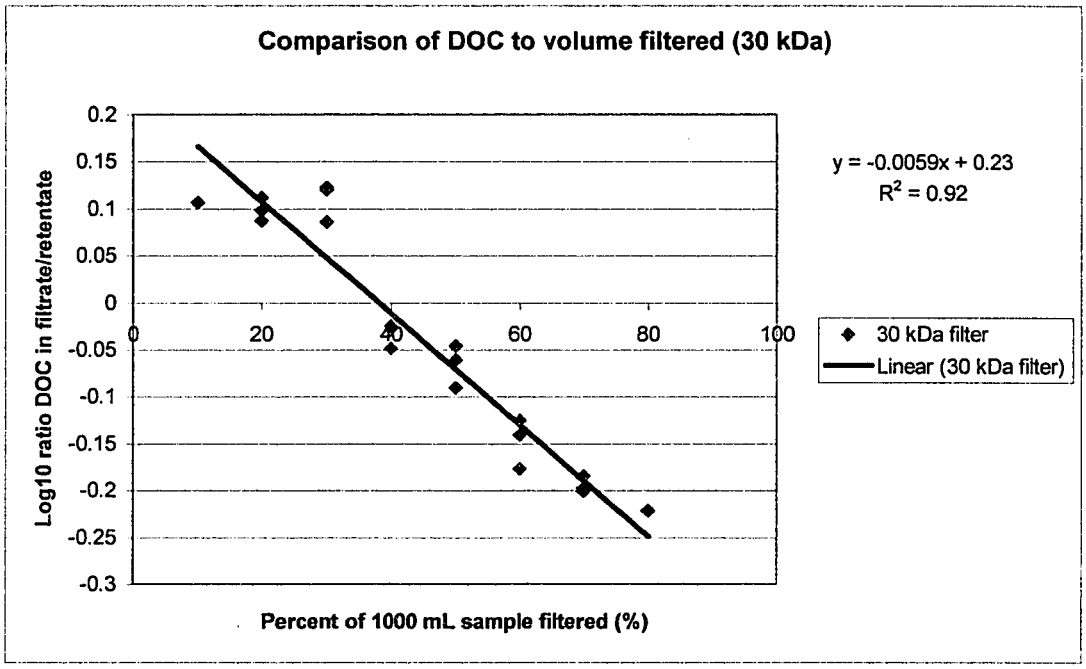
Comparison of DOC to volume filtered (30 kDa)
Log10 ratio DOC in filtrate/retentate
0.2
0.15
0.1
0.05
0
-0.05
-0.1
-0.15
-0.2
-0.25
-0.3
0
20
40
60
80
100
Percent of 1000 mL sample filtered (%)
y = -0.0059x + 0.23
R2 = 0.92
30 kDa filter
Linear (30 kDa filter)

5.11 Teflon UV Radiation Transmittance

For an old Teflon bottle, it was found that wet Teflon (see Figure 27, Table 3) transmitted 36.76% of UV-A and 13.69% of UV-B. For a new Teflon bottle (more similar to the majority of bottles used in the experiments), 48.96% of UV-A and 22.46% of UV-B were transmitted. There is a sharp decrease in transmittance between approximately 600 nm to 250 nm when it drops from approximately 90% for newer Teflon to less than 1%.

Figure 27. Comparison of percent transmittance of radiation through wetted older (more opaque) and newer Teflon.

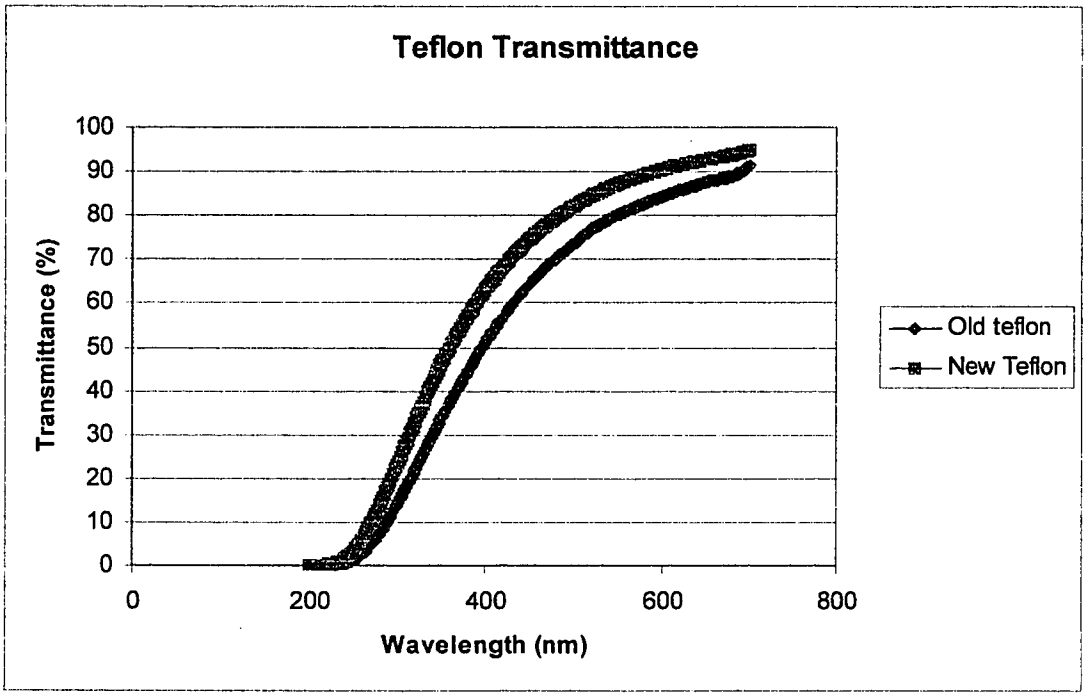
Teflon Transmittance
Transmittance (%)
100
90
80
70
60
50
40
30
20
10
0
0
200
400
600
800
Wavelength (nm)
Old teflon
New Teflon

Table 3. Percent cumulative transmittance of UVA and UVB through wet Teflon.

	Average Transmittance (%)	
	UVB	UVA
Older Teflon	13.69	36.76
Newer Teflon	22.46	48.96

6.0 DISCUSSION

6.1 Photodegradation Rates in High Versus Low DOC Lakes

Results from field photodegradation experiments were not consistent with the hypothesis that higher DOC levels in lake water would lead to lower photodegradation rates. The concentrations of DOC in the samples studied were found in fact to have no effect on photodegradation rates, though both high DOC lakes were found to demonstrate photodegradation while the low DOC lakes did not. However, out of the two high DOC lakes, DA9 with the lower DOC concentration showed higher photodegradation rates than DF9. DA9 had a concentration of DOC approximately half that of DF9, and showed a degradation rate on a linear scale of approximately 10% per hour from the initial 2 ppt spiked concentration, as shown in Table 2. DF9, however showed a degradation rate of approximately 2.5-5% per hour for the different size fractions. These two lakes in isolation appear to support the hypothesis that higher DOC lakes would have lower rates of MeHg photodegradation. The differences in response between the high and low DOC lakes may be due to other hydrochemical differences between the lakes, or to differences in DOC quality as opposed to quantity. Perhaps DA9 and DF9 with logged watersheds had more recent and higher DOC inputs than N55 and N70, resulting in more "photoactive" DOC.

Previous photodegradation experiments with lake water spiked with 7.5 ng/L MeHg resulted in a significant decrease in MeHg to the approximately 3-4 ng/L level during the initial 20-40 mins of incubation for lake water exposed to UVA and UVB. At that point

the MeHg level would plateau (Delage, 2000, unpublished results). That initial photodegradation rate is approximately 9 times greater than the rate observed for DA9. The results from the present experiments could be in keeping with the previous results of Delage in that the 2 ng/L spike concentration examined in this study falls below the previously reported "plateau" section of her photodegradation curve. However, 7.5 ng/L MeHg spikes are far above natural ambient levels and may depict photodegradation rates not consistent with those of natural MeHg levels. The 2 ppt MeHg spike was chosen for this thesis in order to keep levels as close to those found in natural systems as possible, but to bring the concentrations above the ambient levels which are often close to the detection limit.

As mentioned in the introduction, it has been previously found that the ratio of bound to unbound MeHg increased with decreasing total MeHg levels (Hintelmann *et al.*, 1995). Thus with the higher initial spikes used in Delage's experiments, there may be more free MeHg to be immediately photodegraded. The dark incubation experiments performed in this thesis indicated that at the MeHg levels used, MeHg did not require the time allotted to allow binding to DOC. This corroborates the results obtained in a study examining MeHg binding to dissolved humic acids. The authors found that the diffusion of MeHg through a dialysis membrane was the rate limiting step, not the formation of the complex (Amirbahman *et al.*, 2002).

Over the time span examined for the ambient level MeHg experiments, it is difficult to predict how the levels would change with longer incubation times. As it stands, it is clear

that levels would not continue to increase indefinitely, but would either plateau or decrease again. The possibility of MeHg photoproduction however, led to another series of experiments which were performed in the laboratory. Lake water samples with ambient MeHg levels incubated under UV lamps in an attempt to produce increased MeHg concentrations had negative results. As noted in the introduction, Hg^{2+} is reduced to Hg^0 by both humic and fulvic acids (Costa and Liss, 1999). This could have left low Hg^{2+} levels in solution to be photomethylated after the water for the laboratory experiments had been stored. Also, Hg^{2+} present in the water could have become tightly bound to DOC during the storage time, rendering it unavailable for methylation. This may be with a shift from weak or territorial binding to strong, site-specific binding of MeHg with DOC (McNight, 1994). The ambient experiment was therefore followed by the Hg^{2+} spike test. Due to its low power, conclusions other than the lack of photoproduction of MeHg would require a more extensive experiment. However, there appears to be photodegradation of ambient levels of MeHg, with Hg^{2+} spikes having no significant effect on MeHg levels compared to unspiked controls.

For all experiments, $\log_{10}$MeHg concentrations were plotted against time incubated, and the slopes for particular DOC size fractions for each lake were compared for morning and afternoon field incubations (differing UV intensity). It was found that the average UV intensities measured over the times incubated were not related to the final photodegradation rates. This indicates that time incubated in the sun was more important than the UV intensity ranges measured in these experiments. This could be due to differences in UVB intensity causing greater differences in H_20_2 and singlet

oxygen production in lower DOC (uncoloured) lakes versus higher DOC (coloured) lakes (Scully *et al.*, 1997). All lakes studied in this thesis had visibly coloured water, with DOC concentrations ranging from 6.8 to 20.9 ppm. Uncoloured waters generally have DOC levels less than 5 ppm (Malcolm, 1985).

The results of the Teflon transmittance experiments, shown in Figure 27 and Table 3, demonstrate that only 13.7-22.5% of UV-B is transmitted. Much of this highly active component of solar radiation is therefore being blocked during the photodegradation experiments. This indicates that actual photodegradation rates under natural conditions may be significantly higher than those measured in these experiments, due to the water being irradiated by the full intensity of the solar spectrum. This may be despite the relative greater importance observed in this study of time incubated as opposed to UV intensity. These experiments were conducted over three hour time spans, while under natural conditions greater UV levels over much greater time spans could have significant effects. Note also that Sellers reported in her 2001 paper a personal communication with Amyot who stated that 78% and 66% of UV-A and UV-B are transmitted through one litre Teflon bottles, which is significantly higher than the percentages found to be transmitted in this study.

In general, as with other studies of lake DOC, there is great variability in results between lakes, allowing few conclusions about lakes in general to be drawn. Though in this study higher DOC lakes showed photodegradation of MeHg, this may not reflect what is happening in lake systems as a whole. These studies essentially investigated what occurs

at the surfaces of lakes, and does not take into account the effect of depth and the subsequent UV attenuation in lakes. In natural systems, with DOC as the principal attenuator of solar radiation, lakes with less DOC may overall have higher photodegradation rates as the radiation penetrates the water to greater depths. DOC also acts as a methyl donor (Lee, 1985; Weber, 1993), suggesting that with the higher concentrations having more methyl groups available to donate, more mercury may be methylated. This effect would be enhanced by the protective role DOC itself plays in ultraviolet radiation attenuation, thereby minimizing the photodegradation of MeHg. This along with the initial influx of MeHg associated with DOC in runoff could contribute to the higher MeHg levels observed in high DOC lakes. With a large fraction of ultraviolet radiation being blocked by the Teflon bottles used in these experiments, it is also likely that observed degradation rates are underestimated.

Though there was no measurable photodegradation in the low DOC lakes of this study, but this may not be the case with all low DOC lakes. The removal of DOC fractions larger that 300 kDa in all these incubations could also be affecting MeHg photodegradation. A series of experiments that filters samples only through a 0.2 μm filter to remove microbes would be recommended. Examining a range of lower DOC (clear) lakes is also recommended, as all the lakes in this study had relatively high DOC levels and were visibly brown in colour. With a greater DOC concentration range, differences in photodegradation trends may be seen with respect to DOC concentration and watershed logging.

6.2 Photodegradation [of MeHg] When Associated With Different DOC Size Fractions

These results indicate a strong preference for MeHg to bind to larger size DOC fractions, as greater MeHg concentrations do not parallel greater DOC concentrations.

The DF9 fractionation experiments show a clear pattern of MeHg associating to a greater extent with the larger size DOC fractions in the retentate portions of each sample as opposed to the filtrates. As shown in Figure 13, the retentates have MeHg concentrations of approximately 2.7 ppt at time zero, while the filtrates have MeHg concentrations between approximately 0.4 and 0.7 ppt. In addition to this, upon one hour of incubation in sunlight, Figure 14 shows that the concentration of MeHg associated with the larger size DOC drops to between 0.3 and 0.4 ppt, approximately the same levels maintained in the filtrate. This demonstrates that MeHg associated with larger size DOC fractions is being photodegraded. The filtrate MeHg concentrations remain fairly constant at 0.3 ppt. As shown in Figure17, the 300K/30/F fraction is the exception. It increases from 0.4 to 1.1 ppt after one hour of incubation and then the concentration remains relatively constant. It is possible that even though there are no corresponding shifts in the DOC concentration from the retentate to the filtrate (levels remain similar to each other throughout incubation), some of the MeHg may have been cleaved from the retentate fraction of the DOC, and subsequently bound to the filtrate. When the 300K/30/F MeHg increases in an apparent shift from 300K/30/R, these levels do not drop back down to the 0.3 level, suggesting that once associated with smaller sized DOC, MeHg does not photodegrade over the time span examined. This appears to be contrary to the hypothesis that MeHg associated with larger size DOC fractions would photodegrade less

than that associated with smaller size DOC fractions. The larger size DOC has a greater potential for adsorption and ion-exchange reactions (Buffle *et al.*, 1978), and may also be more photochemically active.

From the preliminary inflow experiment, it is apparent that water samples from a lake inflow off a wetland have very different results than circulating lake water. As shown in Figure 12, this experiment demonstrated that with incubation under a UV lamp, there was a decrease in MeHg associated with the 5 kDa fraction, but no corresponding decrease with that associated with the 300 kDa fraction. With "fresher" DOC, larger size fractions of DOC may protect MeHg from photodegradation. DOC off a wetland would be less degraded, by photochemical and other means, than DOC circulating within a lake. Field experiments also demonstrated that MeHg binds preferentially to larger size fractions of DOC, thus the 300 kDa fraction possibly protected the MeHg more, through rendering it chemically unavailable via binding, or by blocking the sunlight. However, due to the low sample size because of limitations in space under the UV lamps, no replicates were done for each incubation time. Therefore, conclusions should be treated as tentative until a more extensive experiment is conducted.

6.3 Photodegradation Rates With Adjusted pH Values

The lake which showed high levels of photodegradation in previous studies (Delage, 2000) had a much lower pH than the lakes examined in this study, a factor which is explored in the pH experiments of this study. These experiments indicated that, in lakes

where photodegradation of MeHg occurs, pH has an effect on rates. However, this appears to be the case only in lakes with a potential for photodegradation. Lake N55 showed no photodegradation in the initial field trials. As shown in Figure 7, it again showed no photodegradation, even upon pH manipulation. There did appear to be pH effects for the other three lakes examined. The low pH samples in these lakes showed rates of photodegradation which were higher than those of higher pH. In the cases of DA9 (Figure 8) and K2 (Figure 9), there was no detectable photodegradation at the two higher pH values studied, but there was photodegradation when pH values were dropped to approximately 4.5. As shown in Figure 10, K3 showed a more stepwise response, with photodegradation rates increasing with each progressive decrease in pH.

DOC concentrations had no effect on photodegradation rates observed. However, as mentioned earlier, the differences in concentration are not very large among the lakes studied, so it is possible that larger differences would have an effect. The lake effects when the entire data set is analyzed are quite small (8% of variability), but the differences in photodegradation between lakes may be due to differing water chemistry including different structures and therefore activities of the DOC.

In an acidic lake, methylmercury bound to DOC may be displaced by H^+, thus resulting in more free MeHg which can then be photodegraded. The study by Amirbahman *et al.* (2002) demonstrated a decrease in adsorption of MeHg to dissolved humic acids when the pH was adjusted to below 5.2. Also note the importance of an acidic environment for the actual photodegradation process as outlined in equation 2 of this paper. The series of

pH experiments performed in this study support the hypothesis that MeHg is more readily photodegraded when it is not bound to DOC. With decreasing pH, photodegradation rates increase in all lakes examined except for N55, which showed no photodegradation in initial field trials. This indicates that differences in DOC quality or other differences in water chemistry besides pH also influence photodegradation.

There was a difference[s] between lake water and inflow water with respect to pH and buffering trends with incubation in sunlight. The differences in results [~~is~~] [are] not surprising. The lake water has already been irradiated for extensive lengths of time (up to one year), and no changes in pH and buffering trends were observed during the course of incubations. The inflow water would not have been subjected to the same levels of cumulative irradiation, and did show trends. As shown in Figures 23 and 24, both pH and buffering capacity for inflow water increased with incubation time. Possible photolysis of the Jack's Lake DOC during the course of the incubation may result in H^+ binding sites being made available (either by cleaving of smaller molecules from DOC, creating more H^+ binding sites, or removal of steric hindrance to binding). This is also interesting in light of a study which showed MeHg having a higher adsorption affinity for Suwannee River humic acid than for peat humic acid which is expected to be less degraded than that from a river source (Amirbahman *et al.*, 2002). Again, this would be in keeping with degradation of humic substances possibly producing more binding sites.

Acid rain could have very significant effects on MeHg levels in fish, especially in logged lakes with high DOC and MeHg. With higher levels of MeHg being found in fish from

lower pH lakes (Winfrey and Rudd, 1990), the possibility of MeHg being displaced from DOC binding sites by H^+, thereby rendering it available for uptake in the food chain appears to be supported. As mentioned earlier, Amirbahman's 2002 study did demonstrate a decrease in adsorption of MeHg to dissolved humic acids when the pH was adjusted to below 5.2. In acidic environments, CH_3HgCl is the predominant form of MeHg (Dryssen and Wedborg, 1991), and this is the form most readily taken up in the food chain (Morel *et al.*, 1998). Our studies also indicate that with decreasing pH, MeHg bound to DOC may be released, making it available for photodegradation. In addition to this, it has been found that pH 6 is the threshold to use in critical load modeling for zooplankton community changes with acidification in south-central Ontario lakes (Holt *et al.*, 2003). This could exacerbate MeHg problems in already negatively impacted lake systems. By using perchloric acid in our pH experiments, we did not change the sulphate concentrations in the water, but with acid rain, the primary strong acid is sulphuric acid. Sulphate has been shown to stimulate sulphate-reducing bacteria and their subsequent methylating activities (Gilmour *et al.*, 1992, Branfireun *et al.*, 1999), thereby potentially compounding the MeHg problem in lakes with no point source of contamination.

6.4 Photodegradation Rates Related to Watershed Logging Activities

The hypothesis that photodegradation would [~~be found to~~] decrease with logging activities was not statistically supported by the data. Despite this lack [of] statistical support, only the logged lakes showed photodegradation. Larger sample sizes may result in differences between logged and not logged watersheds being detected due to higher power of the statistical tests. In addition, as mentioned previously, logging watersheds

has been found to increase lake DOC levels (Carignan *et al.*, 2000). All DOC levels of the lakes examined in this study are relatively high, and do not represent a wide range in concentrations. With a greater difference in DOC concentrations associated with logging status, photodegradation rates may be found to vary. Greater percentages of each watershed studied being logged may also lead to greater differences between logged and unlogged lakes.

In addition, it is clear from the results of this study that photodegradation rates may vary significantly among different lakes. Therefore, logging may have affected rates in individual lakes, but this could not be determined in this study. A future study should be undertaken with photodegradation rates being measured for a series of lakes prior to and after logging of the watershed.

6.5 Permeability of DOC [the DOC is not permeable or impermeable] Across TFUF Filters

The permeabilities of the filters as evaluated over the examined concentrations factors generally showed a relationship between the amount of filtrate passing the filter and the volume filtered. The amount of DOC passing through the membrane decreases with the amount of filtrate produced. However, it is difficult to say precisely what these relationships indicate. To determine if there is an unbiased passage of DOC smaller than the cutoff value through the membrane, one would have to know the concentration of that fraction within the water sample (in the initial sample reservoir) at each stage of filtering. Due to the retentate being a mixture of all size fractions, this could not be determined.

The decrease in the amount of DOC passing the filter membrane with progressive filtering could be due to the corresponding decrease in the amount of DOC below the cutoff value remaining in the retentate, or due to solute exclusion due to the progressively higher fraction of larger size DOC in the retentate "blocking" the passage of the target fraction, or concentration polarization at the membrane surface. As filtering continues, larger size fractions of DOC may also be getting broken, and the smaller fragments passing through the filter. It is likely a combination of all these effects. However note that the DOC concentration passing the 300 kDa filter plateaus when approximately 40% of the sample has been filtered, while the 30 kDa filter plateaus at approximately 50% sample filtered. This could be due to larger size fractions breaking and fragments passing through the filter after most of the actual fraction below the membrane cutoff has passed. It could also be because the larger size filter concentrates the DOC in the retentate less, leading to a more constant passing of DOC through the filter. The amount of DOC in the filtrate of the 5 kDa filter remains fairly constant and lower than those of the larger filters. This is expected as the smaller membrane pore size results in less DOC passing the filter.

7.0 CONCLUSIONS

Field trials showed that the higher DOC lakes demonstrated photodegradation while the lower DOC lakes did not. As there were different rates among the same size DOC fractions from different lakes while there was no effect by different concentrations, there appears be a qualitative difference between the DOC of different sources, leading to differences in photochemical behaviour.

In the case of Jack's Lake incubation with fresh input DOC, it appears that the larger DOC size fraction is protecting the MeHg from photodegradation. This may be due to the effect we observed in our fractionation experiments as well as previous studies (Gilmour and Henry, 1991; Hintelmann *et al.*, 1995; Hintelmann *et al.*, 1997) which indicate that MeHg binds preferentially to larger size fractions. The MeHg in the 5 kDa fraction may not be binding as much as the 300 kDa fraction, thus making it more available for photodegradation. Also there may be higher levels of DOC in the 300 kDa fraction blocking more of the UV radiation.

Fractionation experiments demonstrated a greater preference of MeHg to bind with larger size DOC fractions. Concentrations were approximately 4-7 times higher when associated with the retentate versus filtrate. However upon incubation, it was the MeHg associated with the larger sized DOC that exhibited photodegradation.

pH appears to play a key role in photodegradation of MeHg. With decreasing pH to below 5, there is an increase in photodegradation rates that are either low or nonexistent at higher pH values. Certain lakes however, whether due to differences in DOC or other hydrochemical factors, do not appear to demonstrate photodegradation under any of the examined conditions. Lake N55 showed no photodegradation in the field, nor upon pH manipulation. DOC concentrations in the pH experiments again had no effect on photodegradation rates. Further investigations into the effect of DOC size fractions from lake input sources of DOC and the concurrent effect of pH would be valuable to elucidate the results obtained in this study.

Currently all policy is based on total mercury only. These studies demonstrate that MeHg, the form which accumulates in food chains, is a small percent of total mercury but is very dynamic. Although MeHg levels are higher in correspondingly high DOC lakes, it is nevertheless being degraded, while in slightly lower DOC lakes no degradation is detectable. DOC however also attenuates UV radiation so may provide some "shading" to MeHg not near the lake surface. It is clear that more data is needed on MeHg loading rates coupled with degradation and other losses throughout the lake column in order to better assess the impacts of watershed uses.

8.0 WORKS CITED

Aiken, G., *et al.* 1985, in G. R. Aiken, D. M. McKnight, and R. L. Wershaw (eds), Humic Substances in Soil, Sediment and Water, John Wiley & Sons, New York, p.4-5.

Allard, B. and Arsenie, I. 1991. Abiotic reduction of mercury by humic substances in aquatic system - An important process for the mercury cycle. Water Air Soil Pollut. 56: 457-464.

Amirbahman, A., Reid, A.L., Haines, T.A., Kahl, J.S. and Arnold, C. 2002. Association of methylmercury with dissolved humic acids. Environ. Sci. Technol. 36: 690-695.

Amyot, M., Mierle, G., Lean, D. and McQueen, D.J. 1997. Effect of solar radiation on the formation of dissolved gaseous mercury in temperate lakes. Geochim. Cosmochim. Acta. 61: 975-987.

Amyot, M., *et al.* 1999. Mercury in Lake Ontario and the St. Lawrence River. Great Lakes Research Review. 4(2): 1-4.

Amyot, M., Lean, D.R.S. and Mierle, G. 1997b. Photochemical formation of volatile mercury in high arctic lakes. Environ. Toxicol. Chem. 16: 2054-2063.

Amyot, M., Mierle, G., Lean, D.R.S. and McQueen. 1994. Sunlight-induced formation of dissolved gaseous mercury in lake waters. Environ. Sci. Technol. 28 (13): 2366-2371.

Amyot, M., Lean, D.R.S., Poissant, L. and Doyon, M.-R. 2000. Distribution and transformation of elemental mercury in the St. Lawrence River and Lake Ontario. Can. J. Fish. Aquat. Sci. 57 (Suppl. 1) : 155-163.

Babiarz, C.L., Hoffman, S.R., Shafer, M.M., Hurley, J.P., Andren, A.W. and Armstrong, D.E. 2000. A critical evaluation of tangential-flow ultrafiltration for trace metal studies in freshwater systems. 2. Total mercury and methylmercury. Environ. Sci. Technol. 34 : 3428-3434.

Baird, C. 1995. Environmental Chemistry. W.H. Freeman and Company, New York.

Bannoub, M.W. 1973. Ultra violet absorption as a measure of organic matter in natural waters in Bodensee. Arch. Hydrobiol. 71(2): 159-165.

Baughman, G.L., Gordon, J.A., Wolfe, N.L., and Zepp, R.G. 1973. Chemistry of organomercurials in aquatic systems. Ecol. Res. Ser. U.S. Environmental Protection Agency.

Bloom, N.S. 1989. Determination of picogram levels of methylmercury by aqueous phase ethylation followed by cryogenic gas chromatography with cold vapour atomic fluorescence detection. Can. J. Fish. Aquat. Sci. 46: 1131-1140.

Bloom, N.S., Watras, Carl, J., and Hurley, J.P. 1991. Impact of acidification on the methylmercury cycle of remote seepage lakes. Water, Air, and Soil Pollution. 56: 477-491.

Bloom, P.R., Brezonik, P.L., and Khwaja, A.R. 2001. Photochemical reactions and organic matter binding of mercuric ion and methylmercury in surface water. WRC Research: 7-13.

Blough, N. V. and Zepp, R. G. 1995. Reactive oxygen species in natural waters, in C.S. Foote, J.S. Valentine, N. Greenberg, and J.F. Liebman (eds), Chapman and Hall, New York, p 280-333.

Bormann, F.H. and Likens, G.E. 1979. Pattern and process in a forested ecosystem. Springer-Verlag, New York.

Bowles, K.C., Apte, S.C., Maher, W.A., Kawei, M., and Smith, R. 2001. Bioaccumulation and biomagnification of mercury in Lake Murray, Papua New Guinea. Can. J. Fish. Aquat. Sci. 58: 888-897.

Branfireun, B.A., Roulet, B.A., Kelly, C.A. and Rudd, W.M. . 1999. In situ sulphate stimulation of mercury methylation in a boreal peatland : Toward a link between acid rain and methylmercury contamination in remote environments. Global Biogeochemical Cycles. 13(3): 743-750.

Buffle, J., Deladoey, P., and Haerdi, W. 1978. The use of ultrafiltration for the separation and fractionation of organic ligands in fresh waters. Analytica Chemica Acta. 101: 339-357.

Cai, Y., Jaffé, R., Alli, A. and Jones, R. 1996. Determination of organomercury compounds in aqueous samples by capillary gas chromatography-atomic fluorescence spectrometry following solid-phase extraction. Anal. Chim. Acta. 334: 251-259.

Carignan, R., D'Arcy, P., and Lamontagne, S. 2000. Comparative impacts of fire and forest harvesting on water quality in Boreal Shield lakes. Can. J. Fish. Aquat. Sci. 57(Suppl. 2): 105-117.

Chakrabarti, S., *et al.* June 1997. Development of biological markers for monitoring neurotoxicity to methylmercury exposure. Prepared by Universite de Montreal for Canadian Electrical Association.

Clair, T.A., Pollock, T.L., Collins, P.V. and Kramer, J.R. 1992. How brown waters are influenced by acidification : The Humex Lake case study. Environment International. 18: 589-596.

Coleman, A.W. 1980. Enhanced detection of bacteria in natural environments by fluorochrome staining of DNA. Limnol. Oceanogr. 25(5): 948-951.

Compeau, G. C. and Bartha, R. 1985. Sulfate-reducing bacteria: Principal methylators of mercury in anoxic estuarine sediment. Applied and Environmental Microbiology 50(2): 498-502.

Cooper, W.J., and Lean, D.R. S. 1989. Hydrogen peroxide concentration in a northern lake: Photochemical formation and diel variability. Environ. Sci. Technol. 23(11): 1425-1428.

Cooper, W.J., Shao, C., Lean, D.R.S., Gordon, A. and Scully, F.E. 1994. Factors affecting the distribution of H_2O_2 in surface waters, p. 393-422. *In* Environmental chemistry of lakes and reservoirs. Adv. Chem. Ser. 237. ACS.

Cooper, W.J., Zika, R.G., Petasne, R.G. and Fischer, A.M. 1989. Sunlight-induced photochemistry of humic substances in natural water: Major reactive species, in I.H. Suffet and Patrick MacCarthy (eds), "Aquatic Humic Substances: Influence of Fate and

Treatment of Pollutants", Advances in Chemistry Series. 219, American Chemical Society, Washington DC, p 334-362.

Costa and Liss. 1999. Photoreduction of mercury in sea water and its possible *implications for Hg° air-sea fluxes. Marine Chemistry. 68: 87-95.*

Crump, D., Lean, D., Berrill, M., Coulson, D. and Toy, L. 1999. Spectral irradiance in pond water: Influence of water chemistry. Photochemistry and Photobiology. 79(6): 893-901.

Curtis, P.J. 1998. Climatic and hydrologic control of DOM concentration and quality in lakes, in D.O. Hessen, and L.J. Tranvik (eds), "Aquatic Humic Substances: Ecology and Biogeochemistry", Ecological Studies. 133, Springer-Verlag, Germany, p 93-105.

Dahlén, J., Bertilsson, S., and Pettersson, C. 1996. Effects of UV-A irradiation on dissolved organic matter in humic surface waters. Environment International. 22(5): 501-506.

Delage, D., 2000. Photodegradation of Methylmercury. Honours Thesis, Supervisor Dr. Lean, Department of Biology, University of Ottawa (unpublished).

Dillon, P.J., Reid, R.A., and de Groisbois, E. 1987. The rate of acidification of aquatic ecosystems in Ontario, Canada. Nature. 329: 45-48.

Draper, W.M., and Crosby, D.G. 1983. The photochemical generation of hydrogen peroxide in natural waters. Arch. Environ. Contam. Toxicol. 12: 121-126.

Driscoll, C.T., et al. 1995. The role of dissolved organic carbon in the chemistry and bioavailability of mercury in remote Adirondack lakes. Water, Air and Soil Pollution. 80: 499-508.

Dryssen, D., and Wedborg, M. 1991. The sulphur-mercury(II) system in natural waters. Water, Air, and Soil Pollution. 56: 507-519.

Egeland, G. M. and Middaugh, J.P. 1997. Balancing fish consumption benefits with mercury exposure. Science. 278: 1904-1905.

Faust, B.C. 1992. The octanol/water distribution coefficients of methylmercuric species: The role of aqueous-phase chemical speciation. Environ. Toxicol. And Chem. 11:1373-1376,

Gao, H. and Zepp, R.G. 1998. Factors influencing photoreactions of dissolved organic matter in a coastal river of the southeastern United States. Envir. Sci. and Technol. 32(19): 2940-2946.

Garcia, E. and Carignan, R. 1999. Impact of wildfire and clear-cutting in the boreal forest on methyl mercury in zooplankton. Can. J. Fish. Aquat. Sci. 56: 339-345.

Garcia, E. and Carignan, R. 2000. Mercury concentrations in northern pike (*Esox lucius*) from boreal lakes with logged, burned, or undisturbed catchments. Can. J. Aquat. Sci. 57(Suppl.2): 129-135.

Gáspár, S., Bérces, A., Rontó, Gy. and Gróf, P. 1996. Biological effectiveness of environmental radiation in aquatic systems, measurements by T7-phage sensor. Journal of Photochemistry and Photobiology B: Biology. 32: 183-187.

Gilmour, C.C., and Henry, E.A. 1991. Mercury methylation in aquatic systems affected by acid deposition. Environ. Pollut. 71: 131-169.

Gilmour, C.C., Henry, E.A. and Mitchell, R. 1992. Sulfate stimulation of mercury methylation in freshwater sediment. Environ. Sci. Technol. 26: 2281-2287.

Green, A.E.S. and Chai, S.-T. 1988. Solar spectral irradiance in the visible and infrared regions. Photochemistry and Photobiology. 48(4): 477-486.

Haag, W. R. and Hoigné, J. 1986. Singlet oxygen in surface waters. 3. Photochemical formation and steady-state concentrations in various types of waters. *Environ. Sci. Technol.* **20**(4): 341-348.

Hermann, R. 1996. The daily changing pattern of hydrogen peroxide in new Zealand surface waters. Environ. Toxicol. Chem. 15(5) : 652-662.

Hintelmann, H., P.M. Melbourne, and Evans, R.D. 1995. Binding of methylmercury compounds by humic and fulvic acids. Water, Air and Soil Pollution. 80: 1031-1034.

Hintelmann, H., Welbourn, P.M., and Evans, R. D. 1997. Measurement of complexation of methylmercury(II) compounds by freshwater humic substances using equilibrium dialysis. Environ. Sci. Technol. 31: 489-495.

Hoffman, S.R., Shafer, M.M., Babiarz, C.L. and Armstrong, D.E. 2000. A critical evaluation of tangential-flow ultrafiltration for trace metal studies in freshwater systems. 1. Organic carbon. Environ. Sci. Technol. 34 : 3420-3427.

Holt, C.A., Yan, N.D., and Somers, K.M. 2003. pH 6 as the threshold to use in critical load modeling for zooplankton community change with acidification in lakes of south-central Ontario: Accounting for morphometry and geography. Can. J. Fish. Aquat. Sci. 60: 151-158.

Houle, D., Carignan, R., and Lachance, M. 1995. Dissolved organic carbon and sulfur in southwestern Quebec lakes : Relationships with catchment and lake properties. Limnol. Oceanogr. 40(4): 710-717.

Johansson, K., and Iverfeldt, A. 1994. The relation between mercury content in soil and the transport of mercury from small catchments in Sweden, in Carl J. Watras and John W. Huckabee (eds), "Mercury Pollution: Integration and Synthesis", Lewis Publishers, Boca Raton, p 323-328.

Kaczmarska, I., Clair, T.A., Ehrman, J.M., MacDonald, S.L., Lean, D. and Day, K.E. 2000. The effect of ultraviolet B on phytoplankton populations in clear and brown temperate Canadian lakes. Limnol. Oceanogr. 45(3): 651-663.

Kelly, C.A., Rudd, J.W.M., Furutani, A. and Schindler, D.W . 1984. Effects of lake acidification on rates of organic matter decomposition in sediments. Limnol. Oceanogr. 29(4): 687-694.

Kerry, A., Welbourn, P.M., Prucha, B. and Mierle, G. 1991. Mercury methylation by sulphate-reducing bacteria from sediments of an acid stressed lake. Water, Air, and Soil pollution. 56: 565-575.

Kieber, R.J., Zhou, X., and Mopper, K. 1990. Formation of carbonyl compounds from UV-induced photodegradation of humic substances in natural waters: Fate of riverine carbon in the sea. Limnol. Oceanogr. 35(7):1503-1515.

Kilduff, J., and Weber, W.J., Jr. 1992. Transport and separation of organic macromolecules in ultrafiltration processes. Environ. Sci. Technol. 26(3) : 569-577.

Korthals, S., and Winfrey. 1988. Appl. Environ. Microbiol. 54: 2003-2009.

Kwan, W.P. and Voelker, B.M. 2002. Decomposition of hydrogen peroxide and organic compounds in the presence of dissolved iron and ferrihydrite. Environ. Sci. Technol. 36: 1467-1467.

Larson, R. A. 1978. Environmental chemistry of reactive oxygen species. CRC Critical Reviews in Environmental Control. 8(3): 197-246.

Lean, D. 1998. Attenuation of solar radiation in humic waters, in D.O. Hessen, and L.J. Tranvik (eds), "Aquatic Humic Substances: Ecology and Biogeochemistry", Ecological Studies. 133, Springer-Verlag, Germany, p 109-124.

Lee, Y.-H., and Iverfeldt, A. 1991. Measurement of methylmercury and mercury in run-off, lake and rain waters. Water, Air and Soil Pollution. 56: 309-321.

Lee, Y.-H., Hultberg, H., and Andersson, I. 1985. Catalytic effect of various metal ions on the methylation of mercury in the presence of humic substances. Water, Air, and Soil Pollution. 25: 391-400.

Lee, Y.H., and Mowrer, J. 1989. Determination of methylmercury in natural waters at the sub-nanograms per litre level by capillary gas chromatography after adsorbent preconcentration. J. Anal. Chim. Acta. 221: 259-268.

Leenheer, J. A. 1994. Chemistry of dissolved organic matter in rivers, lakes, and reservoirs, in Lawrence A Baker (ed), "Environmental Chemistry of Lakes and Reservoirs", Advances in Chemistry Series. 237, American Chemical Society, Washington, DC, p 195-221.

Lindqvist, O., *et al.* 1991. Mercury in the Swedish environment. Water Air Soil Pollution. 55: 23-30.

Lindqvist, O., and Rodhe, H. 1985. Atmospheric mercury- a review. Tellus 27B: 136-159.

Logan, B.E., and Jiang, Q. 1990. Molecular size distributions of dissolved organic matter. Journal of Environmental Engineering. 116(6), Nov/Dec: 1046-1062.

Lydersen, E. 1998. Humus and acidification, in D.O. Hessen, and L.J. Tranvik (eds), "Aquatic Humic Substances: Ecology and Biogeochemistry", Ecological Studies. 133, Springer-Verlag, Germany, p 64-92.

Madronich, S. 1994. Increases in biologically damaging UV-B radiation due to stratospheric ozone reductions: A brief review. Arch. Hydrobiol. Beih. Ergebn. Limnol. 43: 17-30.

Malcolm, R. 1985. "Geochemistry of Stream Fulvic and Humic Substances", in G.R. Aiken, D.M. McKnight, and R.L. Wershaw (eds), Humic Substances in Soil, Sediment and Water, John Wiley & Sons, New York, p 181-209.

Mason, R.P., Reinfelder, J.R., and Morel, F.M.M. 1995. Bioaccumulation of mercury and methylmercury. Water, Air, and Soil Pollution. 80: 915-921.

Matilainen, T. 1995. Involvement of bacteria in methylmercury formation in anaerobic lake waters. Water, Air and Soil Pollution. 80: 757-764.

Matilainen, T., and Verta, M. 1995. Mercury methylation and demethylation in aerobic surface waters. Can. J. Fish. Aquat. Sci. 52: 1597-1608.

McKnight, D.M. 1994. Structural components and proposed structural models of fulvic acid from the Suwannee River, in "Humic Substances in the Suwannee River, Georgia: Interactions, Properties, and Proposed Structures", United States Geological Survey Water-Supply Paper 2373.

McKnight, D.M., and Aiken, G.R. 1998. Sources and age of aquatic humus, in D.O. Hessen, and L.J. Tranvik (eds), "Aquatic Humic Substances: Ecology and Biogeochemistry", Ecological Studies 133, Springer-Verlag, Germany, p 9-39.

Meiwes, K.J. 1995. Application of lime and wood ash to decrease acidification of forest soils. Water, Air and Soil Pollution. 85: 143-152.

Melamed, R., Trigueiro, F.E., and Villas Boas, R.C. 2000. The effect of humic acid on mercury solubility and complexation. Appl. Organometal. Chem. 14: 473-476.

Mierle, G., and Ingram, R. 1991. The role of humic substances in the mobilization of mercury from watersheds. Water, Air and Soil Pollution. 56: 349-357.

Miles, C.J., and Brezonik, P.L. 1981. Oxygen consumption in humic-colored waters by a photochemical ferrous-ferric catalytic cycle. Environmental Science and Technology. 15(9): 1089-1095.

Miskimmin, B.M., Rudd, J.W.M., and Kelly, C.A. 1992. Influence of dissolved organic carbon, pH, and microbial repiration rates on mercury methylation and demethylation in lake water. Can. J. Fish. Aquat. Sci. 49:17-22.

Moffett, J.W., and Zafiriou, O.C. 1993. The photochemical decomposition of hydrogen peroxide in surface waters of the eastern Caribbean and Orinoco River. Journal of Geophysical Research. 98(C2): 2307-2313.

Morel, F.M.M., Kraepiel, A.M.L. and Amyot, M. 1998. The chemical cycle and bioaccumulation of mercury. Annu. Rev. Ecol. Syst. 29: 543-566.

Nemeth, P., Toth, Z. and Nagy, Z. 1996. Effect of weather conditions on UV-B radiation reaching the earth's surface. Journal of Photochemistry and Photobiology B: Biology 32: 177-181.

Nriagu, J.O. 1994. Mechanistic steps in the photoreduction of mercury in natural waters. The Science of the Total Environment. 154: 1-8.

O'Sullivan, D.W., Hanson, A.K., Miller, W.L., and Kester, D.R. 1991. Measurement of Fe(II) in surface water of the equatorial Pacific. Limnol. Oceanogr. 36: 1727-1741.

Parks, J. W., Lutz, A., Sutton, J.A. and Townsend, B.E. 1989. Water column methylmercury in the Wabigoon/English River-Lake system : Factors controlling concentrations, speciation and net production. Can. J. Fish. Aquat. Sci. 46: 2184-2202.

Petasne, R.G., and Zika, R.G. 1987. Fate of superoxide in coastal sea water. Nature. 325(6104): 516-518.

Pettersson, C., Bishop, K., Lee, Y.-H. and Allard, B. 1995. Relations between organic carbon and methylmercury in humic rich surface waters from Svartberget catchment in northern Sweden. Water, Air, and Soil Pollution. 80: 971-979.

Pleijel, K., and Munthe, J. 1995. Modelling the atmospheric mercury cycle-chemistry in fog droplets. Atmospheric Environment. 29(12): 1441-1457.

Ramlal, P.S., Rudd, J.W.M., Furutani, A. and Xun, L. 1985. The effect of pH on methyl mercury production and decomposition in lake sediments. Can. J. Fish. Aquat. Sci. 42: 685-691.

Rand, G.M. and Petrocelli, S.R. 1985. Fundamentals of aquatic toxicology. HPC, New York. 666p.

Rasmussen, J.B., Godbout, L., and Schallenberg, M. 1989. The humic content of lake water and its relationship to watershed and lake morphometry. Limnol. Oceanogr. 34(7): 1336-1343.

Rasmussen, P.E. 1994. Current methods of estimating atmospheric mercury fluxes in remote areas. Environ. Sci. Technol. 28: 2233-2241.

Rogers, R.D. 1977. Abiological methylation of mercury in soil. J. Environ. Qual. 6(4): 463-467.

Rudd, J.W. M. 1995. Sources of methyl mercury to freshwater ecosystems: A review. Water, Air, and Soil Pollution. 80: 697-713.

Sampson, C.J., Brezonik, P.L., and Weir, E.P. 1994. Effects of acidification on chemical composition and chemical cycles in a seepage lake, in Lawrence A Baker (ed), "Environmental Chemistry of Lakes and Reservoirs", Advances in Chemistry Series. 237, American Chemical Society, Washington, DC, p 121-159.

Scully, N.M. and Lean, D.R.S. 1994. The attenuation of ultraviolet radiation in temperate lakes. Arch. Hydrobiol. Beih. Ergebn. Limnol. 43: 135-144.

Scully, N.M., Vincent, W.F., Lean, D.R.S., and Cooper, William J. 1997. Implications of ozone depletion for surface-water photochemistry: Sensitivity of clear lakes. Aquat. Sci. 59: 260-274.

Scully, N. M., McQueen, D.J.M. and Lean, D.R.S. 1996. Hydrogen peroxide formation: The interaction of ultraviolet radiation and dissolved organic carbon in lake waters along a 43-75° gradient. Limnol. Oceanogr. 41: 540-548.

Scully, N.M., Lean, D.R.S., McQueen, D.J. and Cooper, W.J. 1995. Photochemical formation of hydrogen peroxide in lakes: Effects of dissolved organic carbon and ultraviolet radiation. Can. J. Fish. Aquat. Sci. 52: 2675-2681.

Sellers, P., Kelly, C.A. and Rudd, J.W.M. 2001. Fluxes of methylmercury to the water column of a drainage lake: The relative importance of internal and external sources. Limnol. Oceanogr. 46(3): 623-631.

Sellers, P., Kelly, C.A., Rudd, J.W.M. and MacHutchinson, A.R. 1996. Photodegradation of methylmercury in lakes. Nature. 380: 694-697.

Seritti, A., Morelli, E., Nannicini, L., Giambelluca, A. and Scarano, G. 1994. *Fluorescence emission characteristics of naturally occurring organic matter in relation to metal complexation studies.* Sci. Total Environ. 148: 73-81.

Shtamm, E.V., Purmal, A.P., and Skurlatov, Y.I. 1991. The role of hydrogen peroxide in natural aquatic media. Russian Chemical Reviews. 60(11): 1228-1248.

Siciliano, S.D., and Lean, D.R.S. 2002. Methyltransferase: An enzyme assay for microbial methylmercury formation in acidic soils and sediments. Environ. Tox. Chem 21(6): 1184-1190.

Siciliano, S.D., O'Driscoll, N.J., and Lean, D.R.S. 2002. Microbial reduction and oxidation of mercury in freshwater lakes. Environ. Sci. Tech. 36: 3064-3068.

Skogerboe, R.K., and Wilson, S.A. 1981. Reduction of ionic species by fulvic acid. Analytical Chemistry. 53: 228-232.

Skurlatov, Yu.I. and Ernestova, L.S. 1998. The impact of human activities on freshwater aquatic systems. Acta Hydrochim. Hydrobiol. 26(1): 5-12.

Snodgrass, J.W., Jagoe, C.H., Bryan Jr., A.L., Brant, H.A. and Burger, J. 2000. Effects of trophic status and wetland morphology, hydroperiod, and water chemistry on mercury concentrations in fish. Can. J. Fish. Aquat. Sci. 57: 171-180.

St. Louis, V.L., Rudd, J.W.M., Kelly, C.A., Beaty, K.G., Bloom, N.S. and Flett, R.J. 1994. Importance of wetlands as sources of methyl mercury to boreal forest ecosystems. Can. J. Fish. Aquat. Sci. 51: 1065-1076.

Steinberg, C., and Muenster, U. 1985. "Geochemistry and Ecological Role of Humic Substances in Lakewater", in G.R. Aiken, D.M. McKnight, and R. L. Wershaw (eds), Humic Substances in Soil, Sediment and Water, John Wiley & Sons, New York, p 105-145.

Suda, I, Suda, M and Hirayama, K. 1993. Degradation of methyl and ethylmercury by singlet oxygen generated from sea water exposed to sunlight or ultraviolet light. Arch. Toxicol. 67: 365-368.

Sundh, I. Biochemical composition of dissolved organic carbon released from natural communities of lake phytoplankton. 24 Archivf. Hydrobiologie, Bd. 125. © 1992 E. Schweizerbart 'sche Verlagsbuch handlung, D-700 Stuttgart 1. p 347-369.

Thruman, E. M. 1985. "Humic substances in groundwater", in G.R. Aiken, D.M. McKnight, D.L. Wershaw, and P. MacCarthy (eds), Humic Substances in Soil, Sediment, and Water, J. Wiley and Sons, New York, p 87-103.

Vincent, W.F., and Roy, S. 1993. Solar ultraviolet-B radiation and aquatic primary production: Damage, protection, and recovery. Environ. Rev. 1: 1-12.

Voelker, B.M., Morel, Francois, M.M., and Sulzberger, B. 1997. Iron redox cycling in surface waters: Effects of humic substances and light. Environ. Sci. Technol. 31: 1004-1011.

Wallschlager, D., Madhukar V.M. D., and Wilken, R.-D. 1996. The role of humic substances from contaminated floodplain soils. Water, Air, and Soil Pollution. 90: 507-520.

Wang, G.-S., Liao, C.-H., and Wu, F.-J. 2001. Photodegradation of humic acids in the presence of hydrogen peroxide. Chemosphere. 42: 379-387.

Wang, G.-S., Hsieh, S.-T., andHong, C.-S. 2000. Destruction of humic acid in water by UV light-catalyzed oxidation with hydrogen peroxide. Wat. Res. 34(15): 3882-3887.

Wang, J. S., Huang, P.M., Liaw, W.K. and Hammer, U.T. 1991. Kinetics of the desorption of mercury from selected freshwater sediments as influenced by chloride. Water, Air, and Soil Pollution. 56: 533-542.

Wangersky, P.J. 1993. Dissolved organic carbon methods: A critical review. Marine Chemisty. 41: 61-74.

Watras, C.J., Morrison, K.A., and Bloom, N.S. 1995. Chemical correlates of Hg and methyl-Hg in northern Wisconsin lake waters under ice-cover. Water, Air and Soil Pollution. 84: 253-267.

Watras, C.J., Morrison, K.A., and Host, J.S. 1995. Concentration of mercury species in relationship to other site-specific factors in the surface waters of northern Wisconsin lakes. Limnol. Oceanogr. 40(3): 556-565.

Weber, J.H. 1993. Review of possible paths for abiotic methylation of mercury(II) in the aquatic environment. Chemosphere. 26(11): 2063-2077.

Westcott, K., and Kalff, J. 1996. Environmental factores affecting methyl mercury accumulation in zooplankton. Can. J. Fish. Aquat. Sci. 53: 2221-2228.

Wetzel, R.G., Hatcher, P.G., and Bianchi, T.S. 1995. Natural photolysis by ultraviolet irradiance of recalcitrant dissolved organic matter to simple substrates for rapid bacterial metabolism. Limnol. Oceanogr. 40(8): 1369-1380.

Willaimson, C.E. 1995. What role does UV-B radiation play in freshwater ecosystems? Limnol. Oceanogr. 40(2): 386-392.

Winfrey, M. R., and Rudd, J.W.M. 1990. Environmental factors affecting the formation of methylmercury in low pH lakes: A review. Environ. Tox. Chem. 9: 853-869.

Xiao, Z.F., Stromberg, D., and Lindqvist, O. 1995. Influence of humic substances on photolysis of divalent mercury in aqueous solution. *Water, Air and Soil Pollution. 80:* 789-798.

Zepp, R. G., Faust, B. C. and Hoigne, J. 1992. Hydroxyl radical formation in aqueous reactions (pH 3-8) of iron (II) with hydrogen peroxide: The photo-Fenton reaction. Environ. Sci. Technol. 26 : 313-319.

Zepp, R.G., Schlotzhauer, P.F., and Sink, R. M.. 1985. Photosensitized transformations involving electronic energy transfer in natural waters: Role of humic substances. Environ. Sci. Technol. 19(1): 74-81.

APPENDICES

Appendix 1. Trends in DOC fluorescence vs. concentration for the six lakes examined in this study (Data courtesy of Susan Winch).

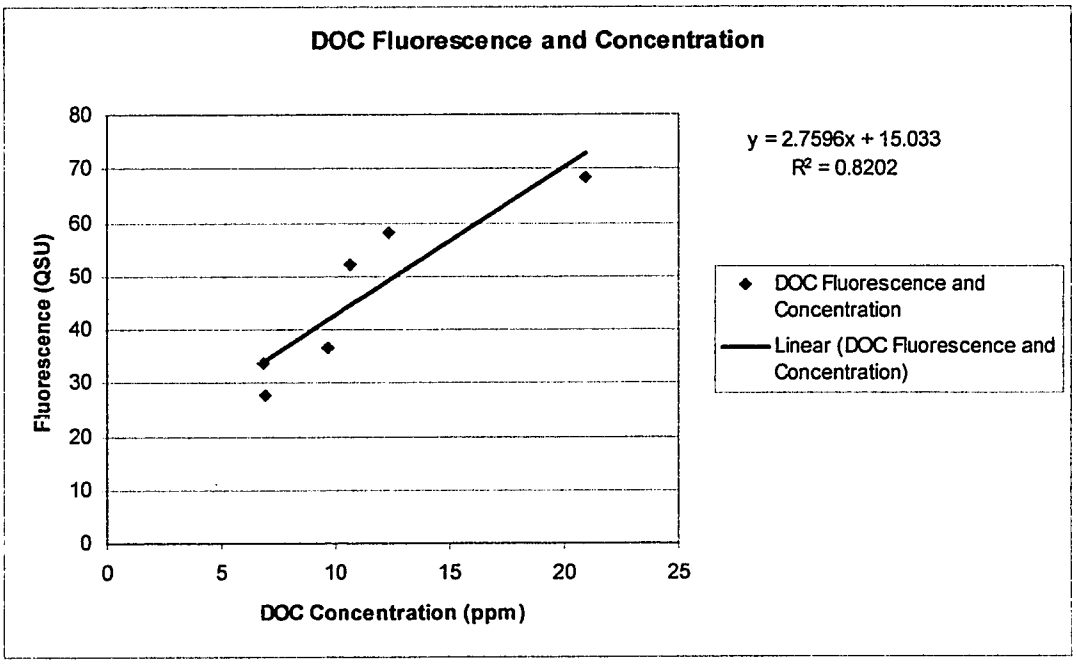

Appendix 2. Average ultraviolet intensities for field incubations, with readings taken every 15 minutes ($\mu W/cm^2$).

Lake	Morning Incubation		Afternoon incubation	
	UV-A	UV-B	UV-A	UV-B
DA9	666.3	123.6	1276.1	96.5
DF9	1374.7	105.0	1067.8	88.4
DF9 (Amb)	804.4	66.3	779.5	54.4
N55	1576.3	129.6	1124.6	83.7
N70	1609.9	124.5	1371.3	106.4

Appendix 3. UV radiation intensity trends for N70 incubations.

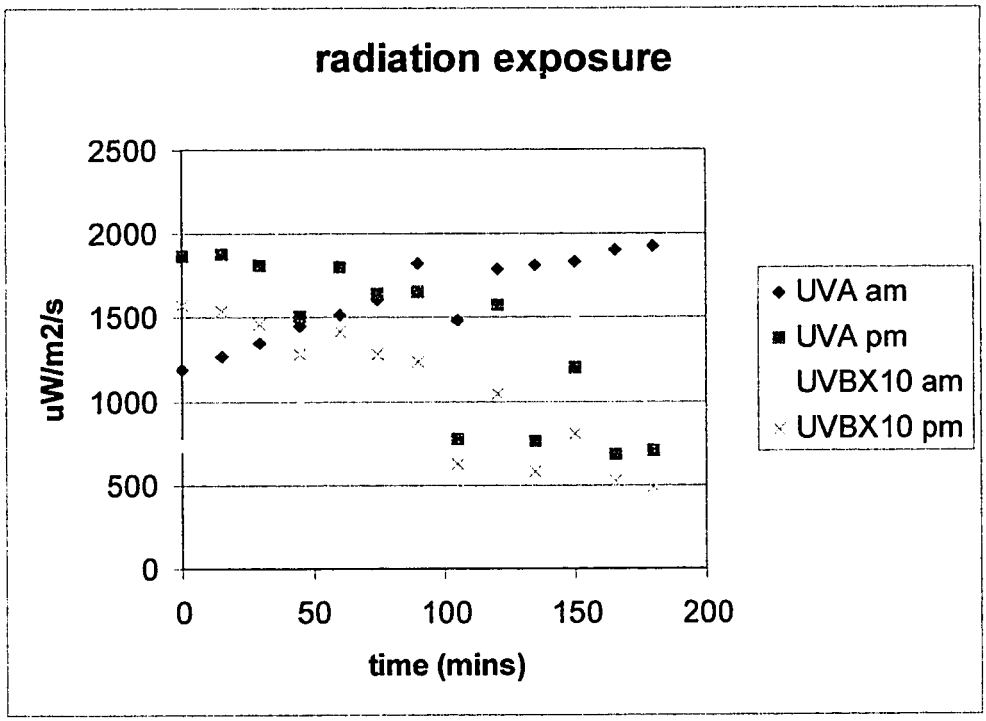

Appendix 4. 5 kDa DOC permeability experiment of Lake Berthelot

Volume Retentate/ Filtrate (mL)	Ratio	DOC in filtrate (mg/L)
900/100	9	5.59
800/200	4	5.12
700/300	2.333	4.91
600/400	1.5	5
500/500	1	5.39
400/600	0.666667	5
300/700	0.428571	5.12
200/800	.0.25	5.65

No values for retentate due to coagulation of DOC

Appendix 5. 30 kDa DOC permeability experiment of Lake Berthelot.

30kDa filter volume retentate/ filtrate (mL)	ratio	DOC in retentate (mg/L)	DOC in filtrate (mg/L)	DOC in filt/reten (mg/L)	DOC in retent/filt (mg/L)	log10 DOC filt/retent (mg/L)	log10 DOC retent/filt (mg/L)	volume filtrate (mL)
900/100	9.00	18.79	24.01	1.28	0.78	0.11	-0.11	100
800/200	4.00	16.16	20.26	1.25	0.80	0.10	-0.10	200
800/200	4.00	16.16	19.75	1.22	0.82	0.09	-0.09	200
800/200	4.00	15.49	20.01	1.29	0.77	0.11	-0.11	200
700/300	2.33	14.87	19.59	1.32	0.76	0.12	-0.12	300
700/300	2.33	14.99	19.88	1.33	0.75	0.12	-0.12	300
700/300	2.33	15.92	19.39	1.22	0.82	0.09	-0.09	300
600/400	1.50	15.69	14.81	0.94	1.06	-0.03	0.03	400
600/400	1.50	15.78	14.8	0.94	1.07	-0.03	0.03	400
600/400	1.50	17.52	15.65	0.89	1.12	-0.05	0.05	400
500/500	1.00	18.61	16.73	0.90	1.11	-0.05	0.05	500
500/500	1.00	18.53	16.11	0.87	1.15	-0.06	0.06	500
500/500	1.00	19.04	15.46	0.81	1.23	-0.09	0.09	500
400/600	0.67	21.57	16.15	0.75	1.34	-0.13	0.13	600
400/600	0.67	21.26	15.36	0.72	1.38	-0.14	0.14	600
400/600	0.67	22.14	14.73	0.67	1.50	-0.18	0.18	600
300/700	0.43	25.54	16.06	0.63	1.59	-0.20	0.20	700
300/700	0.43	25.22	16	0.63	1.58	-0.20	0.20	700
300/700	0.43	25.42	16.59	0.65	1.53	-0.19	0.19	700
200/800	0.25	28.34	17.17	0.61	1.65	-0.22	0.22	800

Appendix 6. 300 kDa DOC permeability experiment of Lake Berthelot.

300 kDa filter volume retentate/ filtrate (mL)	Ratio	DOC in filtrate (mg/L)	log transformed DOC in filtrate (mg/L)	volume filtrate (mL)
900/100	9.00	138.6	2.14	100
800/200	4.00	22.3	1.35	200
700/300	2.33	12.2	1.09	300
700/300	2.33	11.92	1.08	300
600/400	1.50	13.49	1.13	400
600/400	1.50	9.9	1.00	400
500/500	1.00	7.62	0.88	500
500/500	1.00	9.23	0.97	500
500/500	1.00	5.34	0.73	500
500/500	1.00	8.75	0.94	500
400/600	0.67	11.45	1.06	600
400/600	0.67	7.93	0.90	600
300/700	0.43	12.07	1.08	700

No values for retentate due to coagulation of DOC.

Appendix 7. DF9 ambient experiment (morning) data.

time (min)	UVA (uW/cm2)	UVB (uW/cm2)	Visible (microeinsteins/ m2/s)	treatment code	Temp (deg C)	pH before HCl	pH after HCl	vol HCl added (uL)
0	684.5	56	400	1-30		6.29	2.99	350
15	608.7	52.8	390	2-30		6.51	2.92	350
30	752.1	57	420	3-30		4.82	2.91	350
45	682.5	54.3	385	1-45		6.19	2.91	350
60	0	0	0	2-45		5.84	2.91	350
75	726.1	58.8	470	3-45		6.05	2.95	350
90	662.6	53.8	425	1-60	21.5	6.27	2.98	350
105	539.2	43.7	340	2-60		6.44	2.90	350
120	528	43.5	350	3-60		6.26	2.89	350
135	571.3	52.1	430	1-1.5	21.8	6.32	2.96	350
150	1253.7	99.5	910	2-1.5		6.50	2.95	350
165	1406.4	118.8	1000	3-1.5		5.78	2.88	350
180	1238.2	105.3	870	1-2	21.8	6.20	2.99	350
				2-2		6.49	2.94	350
				3-2		6.24	2.89	350
				1-3		6.29	2.94	350
				2-3		6.51	2.95	350
				3-3		6.18	2.92	350
				1-dark		6.18	2.99	350
				2-dark		6.48	2.94	350
				3-dark		6.24	2.94	350

Appendix 8. DF9 ambient experiment (afternoon) data.

time (min)	UVA (uW/cm2)	UVB (uW/cm2)	visible (microeinsteins/ m2/s)	treatment code	temp (Deg C)	pH before HCl	pH after HCl	vol HCl added (uL)
0	1444.9	106.5	1350	1-0 B	21.8	6.2	2.93	350
15	1374	101.6	1250	2-0 B	21.7	6.31	2.91	350
30	1261	87.9	1200	3-0 B	22.7	6.17	2.96	350
45	1199.4	85.4	1100	1-15 B	22.9	6.22	2.9	350
60	1113.2	75.3	1050	2-15 B	23.1	6.26	2.9	350
75	644	56.9	420	3-15 B	22.6	6.16	2.94	350
90	452.3	32	415	1-30 B	23.7	6.23	3.03	300
105	624.4	39.9	430	2-30 B	23.2	6.34	2.99	300
120	525.9	31.9	290	3-30 B	23.1	6.16	2.98	300
135	411.3	25.5	200	1-45 B	24	6.32	3.04	300
156	380.1	22.4	151	2-45 B	23.7	6.29	2.97	300
165	374.7	20.5	210	3-45 B	23.5	6	2.98	300
180	327.6	21.5	150	1-60 B	23.6	6.34	2.94	300
				2-60 B	23.8	6.31	2.97	300
				3-60 B	24.2	6.1	2.96	300
				1-1.5 B	23.3	6.17	3.02	300
				2-1.5 B	23.3	6.39	2.98	300
				3-1.5 B	23.3	6.24	2.97	300
				1-2 B	23.3	6.13	2.96	300
				2-2 B	23.1	6.4	2.96	300
				3-2 B	23.1	5.96	2.97	300
				1-3 B	22.6	6.17	3.04	300
				2-3 B	22.4	6.31	2.98	300
				3-3 B	22.5	5.89	2.95	300
				1-Dark (3hrs)	22.6	6.33	3.01	300
				2-Dark	22.7	6.23	3.01	300
				3-Dark	22.7	5.97	2.99	300

Appendix 9. DF9 2 ppt MeHg spike test (morning) data.

time (min)	UVA (uW/cm2)	UVB (uW/cm2)	Visible (microeinsteins/m2/s)	Temp (deg C)
0	1261.5	75.4	1350	18.5
15	908.9	68.9	1350	20.8
30	943.1	77.5	1400	23.3
45	1221	84.9	1475	
60	1289	93.5	1500	23.1
75	1404.3	103	1500	
90	1492.1	113.2	1650	24
105	1578.2	120.6	1650	
120	1572.8	124	1700	24.8
135	974.7	91.5	550	
156	1733.2	133.8	1725	
165	1616.5	132.2	1750	
180	1875.4	145.9	1850	24.8

Appendix 10. DF9 2 ppt MeHg spike test (afternoon) data.

time (min)	UVA (uW/cm2)	UVB (uW/cm2)	visible (microeinsteins/m2/s	Temp (deg C)
0	1224	165.2	1350	24.7
15	1801	144.6	1300	24.8
30	1358	113.8	750	25.7
45	851.3	76.4	330	26.1
60	1620	124.6	1050	26.1
75	803.6	70.3	37.5	
90	775.7	65.8	360	26.2
105	849.6	69.8	450	
120	1128	82.4	720	26.4
135	1175.9	80	730	
150	672.1	51	260	
165	798	53.4	490	
180	824.1	51.2	430	26

Appendix 11. DA9 2 ppt MeHg spike test (morning) data.

time (min)	UVA (uW/cm2)	UVB (uW/cm2)	visible (microeinsteins/ m2/s)	Sample Code	pH before HCl	pH after HCl	vol added (uL HCl)	temp (deg C)
0	329.3	25.3	150	1-0	7.09	2.97	250	0
15	190.5	14.7	90	2-0	6.9	2.9	250	0
30	328.1	24	145	3-0	6.85	2.92	250	0
45	277.2	19.8	130	1-15	7.09	2.96	250	23.8
60	314.2	24.8	140	2-15	6.89	2.97	250	23.7
75	348.1	28.1	150	3-15	6.91	3.01	250	23.7
90	348.4	0	155	1-30	7.15	3.02	250	23.6
105	0	0	0	2-30	6.86	2.98	250	23.4
120	228.3	35.7	125	3-30	6.88	2.99	250	23.3
135	775.5	373.2	400	1-45	7.14	2.94	250	23.4
150	1556.9	390.6	1050	2-45	6.62	2.89	250	23.1
165	1948	276.8	630	3-45	6.86	2.97	250	23.2
180	1351	146.6	1675	1-60	7.08	3.01	250	23
				2-60	6.96	2.98	250	22.9
				3-60	6.89	3.02	250	22.8
				1-1.5	7.16	2.94	250	22.8
				2-1.5	6.9	2.92	250	23
				3-1.5	6.84	2.76	250	23
				1-2	7.03	3.02	250	22.7
				2-2	6.89	2.98	250	22.8
				3-2	6.86	2.98	250	22.9
				1-3	7.07	2.89	250	25.1
				2-3	6.87	2.86	250	24.8
				3-3	6.9	2.85	250	24.6
				1-dark	6.96	2.89	250	25.1
				2-dark	6.85	2.91	250	25.6
				3-dark	6.87	2.93	250	25.3

Appendix 12. DA9 2 ppt MeHg spike test (afternoon data)

time (min)	UVA uW/cm2)	UVB (uW/cm2)	visible (microeinsteins/ m2/s)	Sample Code	pH before HCl	pH after HCl	vol added (mL HCl)	temp (Deg C)
0	2037	157.7	1750	1-0	7.07	2.94	250	25.1
15	1784.2	146.8	1675	2-0	6.78	2.98	200	25.2
30	785.4	65.1	340	3-0	6.85	2.99	200	25
45	1630.4	132.6	1650	1-15	6.88	2.97	250	26.3
60	1576.6	126.3	1650	2-15	6.79	3.01	200	26.4
75	1566.5	119.3	1750	3-15	6.79	3.06	200	26.5
90	1030.5	74.2	650	1-30	6.93	2.96	250	25.8
105	1420.3	103.8	1700	2-30	6.72	2.96	200	25.6
120	1039.2	71.5	1300	3-30	6.79	3.04	200	25.8
135	1198.6	84.4	1550	1-45	6.8	2.85	250	26.1
150	1165	76.5	1650	2-45	6.74	2.94	200	26.2
165	502.5	41.3	210	3-45	6.76	2.97	200	25.9
180	853.3	54.4	1400	1-60	6.97	2.96	250	27
				2-60	6.72	2.93	200	27.1
				3-60	6.79	2.95	200	26.8
				1-1.5	6.9	2.95	200	26.3
				2-1.5	6.71	2.96	200	26.3
				3-1.5	6.76	2.98	200	26.1
				1-2	6.95	3.01	200	26.5
				2-2	6.75	2.99	200	26.4
				3-2	6.84	3	200	26.2
				1-3	6.96	3.02	200	25.3
				2-3	6.7	2.92	200	24.8
				3-3	6.84	2.96	200	24.9
				1-dark	6.9	2.98	200	24.7
				2-dark	6.76	2.95	200	24.3
				3-dark	6.82	2.95	200	24.1

Appendix 13. N55 2 ppt MeHg spike test (morning) data.

time (min)	UVA (uW/cm2)	UVB (uW/cm2)	visible (microeinsteins/ m2/s	Sample Code	pH before HCl	pH after HCl	vol added (uL HCl)	temp (deg C)
0	1258.2	89.5	1065	1-0	7.62	2.97	200	21.3
15	1239.2	86.3	1275	2-0	7.19	2.95	200	21
30	1110.4	82.8	1150	3-0	6.83	3.05	200	20.7
45	1261.3	98.2	1350	1-15	8.61	3.03	200	22.5
60	1388.6	111	1450	2-15	7.11	3.04	200	22.4
75	1590.2	124.9	1600	3-15	6.72	3.08	200	22.1
90	1715.7	180.7	1950	1-30	8.5	3.07	200	23
105	1853.3	151.6	1750	2-30	7.25	3.03	200	22.9
120	1734.8	145.8	1550	3-30	7.02	3.02	200	22.8
135	1536.7	121.1	1050	1-45	8.48	2.97	200	24
150	1869.8	156.5	1600	2-45	7.11	2.95	200	23.6
165	1958.4	166.8	1600	3-45	6.8	2.93	200	23.4
180	1975.8	169.1	1500	1-60	8.21	3.02	200	23.5
195	2013	170.7	1400	2-60	6.98	3.02	200	23.6
210	2025	172.6	1375	3-60	6.9	3.05	200	23.3
225	2026	172	1300	1-1.5	8.34	2.98	200	24.2
				2-1.5	7.06	2.93	200	24.3
				3-1.5	6.77	2.94	200	24.2
				1-2	8.35	3.03	200	24.8
				2-2	7.02	2.97	200	24.2
				3-2	6.85	0	250	24.3
				1-3	7.81	2.93	200	25.8
				2-3	7.09	2.91	200	25.6
				3-3	6.88	2.91	200	0
				1-dark	7.57	2.9	200	26.6
				2-dark	6.46	2.92	200	26.5
				3-dark	6.89	2.95	200	0

Appendix 14. N55 2 ppt MeHg spike test (afternoon) data.

time (min)	UVA (uW/cm2)	UVB (uW/cm2)	visible (microeinsteins/ m2/s)	Sample Code	pH before HCl	pH after HCl	vol added (mL HCl)	temp (deg C)
0	1848.2	147.5	1700	1-0	8.05	3.02	200	22
15	1801.9	140.9	1700	2-0	7.28	2.95	200	22.3
30	1750	134.3	1650	3-0	6.96	2.94	200	22.2
45	1636.6	123.8	1700	1-15	7.58	3.07	200	23.6
60	1544.2	113.7	1750	2-15	7.17	3.01	200	23.8
75	675.2	58.7	470	3-15	6.66	3.05	200	23.4
90	1088.5	77.9	1175	1-30	7.59	3.08	200	24.8
105	789.8	63.2	560	2-30	7.18	3.02	200	23.6
120	669.1	48.2	390	3-30	6.96	3.03	200	24.9
135	699.1	47.4	1600	1-45	7.62	3	200	25.5
150	814.8	53.6	865	2-45	7.18	2.93	200	25.7
165	620.4	38.7	1300	3-45	6.95	2.93	200	25.6
180	681.3	39.6	900	1-60	7.55	3.1	200	25.7
				2-60	7.07	3	200	25.6
				3-60	6.92	3.01	200	25.8
				1-1.5	7.63	3	200	25.8
				2-1.5	7.13	2.92	200	25.6
				3-1.5	6.93	2.92	200	25.3
				1-2	7.55	3.08	200	25
				2-2	7.18	3	200	25
				3-2	6.96	3	200	25
				1-3	7.48	3.04	200	23.8
				2-3	7.18	3.01	200	23.8
				3-3	6.96	2.94	200	23.8
				1-dark	7.26	2.98	200	24.2
				2-dark	6.95	2.94	200	24.1
				3-dark	6.93	2.95	200	24.1

Appendix 15. N70 2 ppt spike test (morning) data.

time (mins)	UVA (uW/cm2)	UVB (uW/cm2)	visible (microeinsteins/ m2/s)	Sample Code	pH before HCl	pH after HCl	vol added (uL HCl)	temp (deg C)
0	1192.9	73.9	1600	1-0	6.7	3.04	150	16.4
15	1264.5	81.9	1700	2-0	6.71	2.96	150	16.2
30	1342.8	90.7	1650	3-0	6.14	3.04	150	16.7
45	1442.8	99.6	1650	1-15	6.6	3.06	200	20.1
60	1518.7	107.4	1650	2-15	6.51	3.07	150	20
75	1609	116.1	1640	3-15	5.88	3.07	150	19.8
90	1821.3	136	1800	1-30	0	3.06	150	21.8
105	1482.5	114.5	1350	2-30	0	3.05	150	21.6
120	1789.4	135.5	1450	3-30	0	3.04	150	21.6
135	1809.1	144.4	1700	1-45	6.34	2.96	150	22.7
150	1831.9	150.8	1650	2-45	6.57	2.97	150	22.4
165	1901.6	155.5	1650	3-45	6.53	2.96	150	22.6
180	1921.5	161.3	1725	1-60	6.61	3.05	150	23.6
195	2012	167.4	1775	2-60	6.6	3.06	150	23.2
210	2020	167.8	1700	3-60	6.56	3.05	150	23.4
225	2011	167.9	1700	1-1.5	6.43	3.04	150	24.6
240	2042	169.9	1700	2-1.5	6.58	2.99	150	24.6
255	1780.1	153.6	1450	3-1.5	6.51	2.97	150	25
270	1979	165.1	1650	1-2	6.63	3.07	150	25.5
285	1931.2	162.5	1675	2-2	6.38	3.05	150	25.4
300	1864.7	157	1650	3-2	5.55	3.06	150	25.2
315	1874.5	154.4	1650	1-3	6.67	3.01	150	26.4
330	1805.9	146	1650	2-3	6.59	2.97	150	26.3
345	1502.4	128.2	1350	3-3	6.52	2.96	150	26.2
360	1801.9	141	1750	1-dark	6.23	2.97	150	27.1
375	1644.7	128.1	1600	2-dark	5.76	2.99	150	27.8
390	1654.3	123.8	1750	3-dark	5.23	2.97	150	26.9

Appendix 16. N70 2 ppt MeHg spike test (afternoon) data.

time (mins)	UVA (uW/cm2)	UVB (uW/cm2)	visible (microeinsteins/ m2/s)	Sample Code	pH before HCl	pH after HCl	vol added (uL HCl)	temp (deg C)
0	1864.7	157	1650	1-0	6.63	3.03	150	20.8
15	1874.5	154.4	1650	2-0	6.62	3.02	150	20.5
30	1805.9	146	1650	3-0	6.56	3.03	150	20.8
45	1502.4	128.2	1350	1-15	6.51	3.09	150	23.7
60	1801.9	141	1750	2-15	6.55	3.08	150	23.9
75	1644.7	128.1	1600	3-15	6.5	3.07	150	24.5
90	1654.3	123.8	1750	1-30	6.56	3.1	150	25.4
105	767.8	62.3	395	2-30	6.56	3.08	150	25.8
120	1575.4	104.2	1800	3-30	6.51	3.06	150	26.4
135	759.5	57.5	1300	1-45	6.51	3.06	150	26.2
150	1196.7	80.7	1675	2-45	6.53	2.99	150	26.3
165	680.5	51.6	1300	3-45	6.5	2.99	150	26.6
180	698.7	48.1	630	1-60	6.52	3.09	150	26.9
				2-60	6.14	3.07	150	27.1
				3-60	6.46	3.07	150	27.1
				1-1.5	6.51	3.05	150	27.5
				2-1.5	6.55	3	150	27.7
				3-1.5	6.52	2.99	150	27.7
				1-2	6.58	3.09	150	27.6
				2-2	6.55	3.06	150	27.6
				3-2	6.5	3.04	150	27.3
				1-3	6.36	3.09	150	26.5
				2-3	6.54	2.94	150	26.4
				3-3	6.5	3.03	150	26.4
				1-dark	6.45	3	150	27
				2-dark	4.64	3.04	150	26.9
				3-dark	6.24	3.04	150	26.7
				1-6.5	6.55	3.03	150	27.3
				1-6.5 drk	6.36	3.07	150	27.9

Appendix 17. MeHg values for DF9 ambient test.

Fraction	time (mins)	1st test MeHg conc (ppt)	1st test MeHg conc (ppq)	log10 conc (ppq)	2nd test MeHg conc (ppt)	2nd test MeHg conc (ppq)	log10 conc (ppq)
5 kDa	0	0.0774	77.37	1.889	0.0661	66.11	1.82
	15	0.0746	74.63	1.873	0.0611	61.14	1.786
	30	0.0686	68.59	1.836	0.0370	37.02	1.568
	45	0.0465	46.51	1.668	0.0371	37.09	1.569
	60	0.0490	49.04	1.691	0.0436	43.63	1.64
	90	0.0367	36.74	1.565	0.0370	37.04	1.569
	120	0.0434	43.4	1.638	0.0588	58.75	1.769
	180	0.0477	47.73	1.679	0.0665	66.47	1.823
	dark	0.0728	72.81	1.862	0.0674	67.39	1.829
30 kDa	0	0.0392	39.23	1.594	0.0562	56.15	1.749
	15	0.0437	43.69	1.64	0.0458	45.8	1.661
	30	0.0337	33.73	1.528	0.0500	49.98	1.699
	45	0.0386	38.56	1.586	0.0376	37.64	1.576
	60	0.0255	25.52	1.407	0.0326	32.56	1.513
	90	0.0100	10	1	0.0301	30.13	1.479
	120	0.0346	34.56	1.539	0.0496	49.65	1.696
	180	0.0372	37.15	1.57		44.22	1.646
	dark	0.0496	49.61	1.696	0.0534	53.36	1.727
300 kDa	0	0.0755	75.53	1.878	0.0636	63.63	1.804
	15	0.0597	59.65	1.776	0.0586	58.57	1.768
	30	0.0367	36.74	1.565	0.0583	58.29	1.766
	45	0.0535	53.5	1.728	0.0302	30.18	1.48
	60	0.0515	51.52	1.712	0.0436	43.64	1.64
	90	0.0462	46.21	1.665	0.0391	39.09	1.592
	120	0.0610	61.01	1.785	0.0654	65.39	1.815
	180	0.0767	76.73	1.885	0.0678	67.76	1.831
	dark	0.0733	73.32	1.865	0.0384	38.45	1.585

Appendix 18. MeHg values for DF9 2 ppt spike test

Fraction	Time (mins)	1st test MeHg conc (ppt)	log10 conc (ppt)	2nd test MeHg conc (ppt)	log10 conc (ppt)
5kDa	0	0.951	-0.022	0.648	-0.188
	15	0.722	-0.142	0.739	-0.131
	30	0.730	-0.136	0.653	-0.185
	45	0.834	-0.079	0.515	-0.289
	60	0.820	-0.086	0.657	-0.182
	90	0.716	-0.145	0.460	-0.337
	120	0.687	-0.163	0.451	-0.346
	180	0.540	-0.268	0.397	-0.402
	dark	0.536	-0.270	0.675	-0.171
30kDa	0	0.832	-0.080	0.582	-0.235
	15	0.820	-0.086	0.711	-0.148
	30	0.808	-0.093	0.696	-0.157
	45	0.833	-0.079	0.560	-0.252
	60	0.835	-0.078	0.590	-0.229
	90	0.809	-0.092	0.543	-0.265
	120	0.761	-0.119	0.604	-0.219
	180	0.670	-0.174		
	dark	0.715	-0.146	0.631	-0.200
300kDa	0	0.749	-0.125	0.567	-0.247
	15	0.650	-0.187	0.606	-0.218
	30	0.612	-0.213	0.605	-0.218
	45	0.545	-0.264	0.478	-0.321
	60	0.594	-0.226	0.502	-0.299
	90	0.603	-0.220	0.460	-0.337
	120	0.541	-0.267	0.543	-0.265
	180	0.506	-0.296	0.326	-0.486
	dark	0.580	-0.236	0.491	-0.309

Appendix 19. MeHg values for DA9 2 ppt spike test.

Fraction	time (mins)	1st test MeHg conc (ppt)	log10 1st test (ppt)	2nd test MeHg conc (ppt)	log10 2nd test (ppt)
5 kDa	0	2.43	0.385	2.16	0.335
	15	2.09	0.319	2.15	0.333
	30	2.06	0.313	2.02	0.306
	45	1.94	0.289	2.27	0.356
	60	1.88	0.275	2.17	0.335
	90	2.08	0.318	2.13	0.327
	120	2.08	0.318	1.46	0.163
	180	1.34	0.128	1.68	0.225
	dark				
30 kDa	0	2.20	0.342	1.97	0.294
	15	2.52	0.401	2.04	0.309
	30	2.35	0.371	1.95	0.290
	45	2.41	0.381	2.12	0.326
	60	4.53	0.656	2.06	0.314
	90	2.10	0.323	1.57	0.195
	120	1.60	0.204	1.35	0.131
	180	1.99	0.300	1.52	0.183
	dark				
300 kDa	0	2.16	0.333	1.95	0.291
	15	1.96	0.292	2.12	0.327
	30	2.06	0.314	2.14	0.330
	45	2.32	0.366	2.00	0.301
	60	1.51	0.180	2.07	0.316
	90	1.98	0.297	1.36	0.134
	120	1.78	0.249	1.35	0.131
	180	1.63	0.212	1.86	0.269
	dark				

Appendix 20. MeHg values for N55 2 ppt spike test.

Fraction	time (mins)	1st test MeHg conc (ppt)	log10 1st test (ppt)	2nd test MeHg conc (ppt)	log10 2nd test (ppt)
5 kDa	0	1.34	0.128	1.59	0.200
	15	1.42	0.151	1.11	0.045
	30	1.74	0.241	1.36	0.132
	45	1.13	0.053	1.49	0.172
	60	1.46	0.165	1.43	0.156
	90	1.48	0.170	1.39	0.141
	120	1.47	0.168	1.34	0.128
	180	1.34	0.128	1.28	0.107
	dark				
30 kDa	0	1.40	0.146	1.71	0.232
	15	1.26	0.102	1.04	0.017
	30	0.60	-0.223	1.16	0.066
	45	2.04	0.309	1.39	0.144
	60	1.50	0.176	1.20	0.078
	90	1.53	0.184	1.51	0.179
	120	1.61	0.206	1.56	0.193
	180	1.38	0.140	1.16	0.064
	dark				
300 kDa	0	1.35	0.131		
	15	1.08	0.032	1.09	0.039
	30	0.67	-0.177	1.07	0.029
	45	1.28	0.108	1.16	0.063
	60	1.61	0.207	1.21	0.082
	90	1.77	0.247	1.25	0.096
	120	1.03	0.012	1.22	0.088
	180	1.25	0.098	1.22	0.086
	dark				

Appendix 21. MeHg values for N70 2 ppt spike test.

Fraction	time (mins)	1st test MeHg conc (ppt)	log10 1st test (ppt)	2nd test MeHg conc (ppt)	log10 2nd test (ppt)
5 kDa	0	1.56	0.193	2.37	0.375
	15	1.25	0.097	2.18	0.338
	30	1.25	0.097	2.84	0.453
	45	1.41	0.148	1.62	0.209
	60	1.18	0.070	2.61	0.417
	90	1.33	0.123	2.57	0.410
	120	1.42	0.152	2.30	0.361
	180	0.83	-0.083		
	dark				
30 kDa	0	1.19	0.075	2.37	0.375
	15	1.10	0.041	2.25	0.352
	30	1.23	0.089	2.16	0.334
	45	1.44	0.159	2.50	0.398
	60	1.06	0.025	2.72	0.435
	90	1.32	0.122	2.22	0.346
	120	1.18	0.070	2.14	0.331
	180	1.01	0.006		
	dark				
300 kDa	0	1.04	0.018	2.73	0.436
	15	1.05	0.023	2.41	0.383
	30	1.12	0.051	1.08	0.033
	45	1.06	0.026	1.96	0.293
	60	0.97	-0.011	2.76	0.441
	90	1.20	0.077	2.06	0.314
	120	0.98	-0.009	2.40	0.380
	180	0.87	-0.059		
	dark				

Appendix 22 . Inorganic Hg^{2+} spike experiment.

sample	time (hrs)	MeHg conc (ppt)	MeHg conc (ppq)
drk spike	0	0.219	219
DA9 blank	0	0.211	211
DA9 blank B	0	0.143	143
spike	0	0.166	166
spike B	0	0.124	124
spike	4	0.117	117
spike B	4	0.126	126
spike	12	0.081	81
spike B	12	0.069	69
ambient	12	0.098	98
ambient B	12	0.059	59
dark control	12	0.086	86
dark cntrl B	12	0.088	88

Appendix 23. Laboratory photodegradation experiment with Jack's Lake inflow water (ambient MeHg levels).

5 kDa			300 kDa		
time (hrs)	MeHg conc (ppt)	MeHg conc (ppq)	time (hrs)	MeHg conc (ppt)	MeHg conc (ppq)
0	0.23	235	0	0.22	215
4	0.21	214	4	0.21	207
8	0.11	107	8	0.23	233
10	0.15	150	10	0.25	254
10 B	0.06	61	10 B	0.22	223
avg 10	0.11	106	avg 10	0.24	239

Appendix 24. MeHg fractionation experiments (DF9)

time of incubation	UVA (uW/cm2)	UVB (uW/cm2)	visible (microeinsteins/m2/s)
0915	638.6	45.7	375
0930	708.6	51.9	430
0945	966.4	71.7	770
1000	821.4	63.7	520
1015	813.8	64	500
1030	920.4	72.8	550
1045	862.2	69.4	470
1100	901.8	74	520
1115	897.8	74.3	520
1130	1069.5	90.8	560
1145	1350	110.3	950
1200	1003.9	87	745
1215	1843.2	146.6	1450
1230	1974	160.4	1600
1245	2003	169.7	1675
1300	2078	165.3	1700
1325	1638.8	136	1275
1330	2045	158	1850
1345	1857.1	96.7	1750
1400	1556.4	153.1	1675
1415	1943.5	160.2	1675
1430	1419	123.5	1150
1445	1950.4	154.8	1325
1500	1201.3	101.1	740
1515	1586.6	117.7	1450
1530	1602.7	132.7	1250
1545	1722.2	133.1	1250
1600	1208.9	86	550
1615	1285	90.8	1400

sample code	vol for MeHg analysis (mL)	conc MeHg (ng/L)	MeHg/sample (ng)	DOC (mg/L)
300kDa/30/R1 T=0	500	3.19	1.60	18.04
300kDa/30/F1 T=0	500	0.24	0.12	20.83
300kDa/30/R2 T=0	500	0.17	0.09	20.15
300kDa/30/F2 T=0	500	0.54	0.27	13.6
300kDa/5/R1 T=0	350	2.09	0.73	19.13
300kDa/5/F1 T=0	350	0.40	0.14	24.86
300kDa/5/R2 T=0	350	2.92	1.02	
300kDa/5/F2 T=0	350	0.59	0.20	22.14
30kDa/5/F1 T=0	450	0.84	0.38	18.24
30kDa/5/R1 T=0	450	2.76	1.24	18.95
30kDa/5/R2 T=0	450	2.55	1.15	16.84
30kDa/5/F2 T=0	450	0.51	0.23	16.87
30kDa/5/F1 T=1	450	0.27	0.12	16.59
30kDa/5/R1 T=1	450	1.03	0.46	16.64
30kDa/5/F2 T=1	450	0.24	0.11	14.28
30kDa/5/R2 T=1	450	0.97	0.43	18.95
300kDa/30/R1 T=2	500	0.34	0.17	17.93
300kDa/30/F1 T=2	500	0.91	0.45	13.65
300kDa/30/R2 T=2	500	0.43	0.22	19.82
300kDa/30/F2 T=2	500	0.91	0.45	10.01
300kDa/5/R1 T=2	400	0.39	0.16	12.96
300kDa/5/F1 T=2	400	1.66	0.66	14.21
300kDa/5/R2 T=2	400	0.38	0.15	
300kDa/5/F2 T=2	400	1.53	0.61	15.27
30kDa/5/R1 T=2	450	0.38	0.17	15.06
30kDa/5/F1 T=2	450	1.07	0.48	17.21
30kDa/5/R2 T=2	450	0.32	0.14	14.88
30kDa/5/F2 T=2	450	1.16	0.52	15.68
30kDa/5/R1 T=3	450	0.27	0.12	17.34
30kDa/5/F1 T=3	450	0.27	0.12	16.43
30kDa/5/R2 T=3	450	0.37	0.17	15.42
30kDa/5/F2 T=3	450	0.49	0.22	15.85
300kDa/30/R1 T=1	500	0.27	0.14	21.53
300kDa/30/F1 T=1	500	1.07	0.54	22.65
300kDa/30/R2 T=1	500	0.33	0.16	21.76
300kDa/30/F2 T=1	500	1.12	0.56	13.68
300kDa/5/R1 T=1	400	0.30	0.12	20.91
300kDa/5/F1 T=1	400	0.46	0.18	22.8
300kDa/5/R2 T=1	400	0.40	0.16	15.16
300kDa/5/F2 T=1	400	0.30	0.12	16.69
300kDa/30/R1 T=3	500	0.32	0.16	20.93
300kDa/30/F1 T=3	500	1.27	0.63	17.65
300kDa/30/R2 T=3	500	0.30	0.15	20.88
300kDa/30/F2 T=3	500	0.88	0.44	12.12

300kDa/5/R1 T=3	280	0.61	0.17	18.14
300kDa/5/F1 T=3	450	0.27	0.12	17.49
300kDa/5/R2 T=3	450	0.27	0.12	17.68
300kDa/5/F2 T=3	450	0.39	0.17	15.71

Appendix 25. MeHg fractionation experiment (DA9, t = 0 hrs)

Sample Code	vol Hg analysis (mL)	vol DOC (mL)	vol MeHg (mL)	volume remaining (mL)	total volume (mL)	MeHg conc (ng/L)	MeHg in sample (ng/vol)
300K/30K/F	30	20	500	1000	1550	1.83	0.91
300K/30K/R	30	20	500	771	1321		
300K/5K/F	30	20	398	0	448	0.46	0.18
300K/5K/R	30	20	425	0	475	1.46	0.69
30K/5K/F	30	20	500	417	967	0.97	0.49
30K/5K/R	30	20	500	400	950	4.75	2.38

Appendix 26. MeHg fractionation experiment (N55, t = 0 hrs)

Sample Code	vol Hg analysis (mL)	vol DOC (mL)	vol MeHg (mL)	volume remaining (mL)	total volume (mL)	MeHg conc (ng/L)	MeHg in sample (ng/vol)	DOC (mg/L)
300K/30K/F	50	50	500	1080	1680	0.29	0.15	14.84
300K/30K/R	50	50	500	890	1490	1.82	0.91	10
300K/5K/F	30	20	460	0	510	0.24	0.11	21.38
300K/5K/R	30	20	470	0	520	0.48	0.23	
30K/5K/F	50	50	1000	340	1440	0.42	0.42	9.24
30K/5K/R	50	50	1000	360	1460	1.57	1.57	7.86

Appendix 27. MeHg fractionation experiment (N70, t = 0 hrs)

sample	Hg analysis (mL)	DOC (mL)	Vol MeHg analysis (mL)	Volume remaining (mL)	total volume (mL)	MeHg conc (ng/L)	MeHg in sample (ng)	DOC (mg/L)
300/30/F	30	20	500	1090	1640	0.55	0.28	10.47
300/30/R	50	50	1000	420	1520	missing	from field	10.55
300/5/F	30	20	450	0	500	0.29	0.13	13.49
300/5/R	30	20	500	0	550	0.57	0.29	11.43
30/5/F	50	50	870	0	970	0.46	0.40	8.92
30/5/R	50	50	860	0	960	1.51	1.30	8.76

Appendix 28. Jack's Lake pH and buffering trends with incubation in sunlight

5 kDa

Time (hrs)	pH (initial)	pH (final)	volume 3.6N HCL added (uL)	actual incr in H+ conc (moles/L)	Theor incr in H+ conc (moles/L)	Diff bet theor and actual
0	5.95	3.09	400	8.13E-04	1.52E-03	7.07E-04
0	5.8	2.94	400	1.15E-03	1.52E-03	3.70E-04
1	6.21	3.09	500	8.13E-04	1.90E-03	1.09E-03
1	6.47	3.08	500	8.32E-04	1.90E-03	1.07E-03
3	6.74	3.01	350	9.77E-04	1.33E-03	3.53E-04
3	6.7	3.07	550	8.51E-04	2.08E-03	1.23E-03
5	6.79	3.1	650	7.94E-04	2.46E-03	1.67E-03
5	6.83	3.09	550	8.13E-04	2.08E-03	1.27E-03
8	7.08	3.06	750	8.71E-04	2.84E-03	1.97E-03
8	6.97	3.07	700	8.51E-04	2.65E-03	1.80E-03

30 kDa

Time (hrs)	pH (initial)	pH (final)	Vol 3.6N HCl added (uL)	actual incr in H+ conc (moles/L)	Theor incr in H+ conc (moles/L)	Diff bet theor and actual
0	6.05	3	400	1.00E-03	1.52E-03	5.20E-04
0	5.79	3.03	400	9.33E-04	1.52E-03	5.87E-04
1	6.34	3.09	450	8.13E-04	1.71E-03	8.97E-04
1	6.48	3.07	450	8.51E-04	1.71E-03	8.59E-04
3	6.75	3.08	550	8.32E-04	2.08E-03	1.25E-03
3	6.82	3.06	600	8.71E-04	2.27E-03	1.40E-03
5	6.82	3.06	400	8.71E-04	1.52E-03	6.49E-04
5	6.89	3.09	650	8.13E-04	2.46E-03	1.65E-03
8	7.07	3.06	700	8.71E-04	2.65E-03	1.78E-03
8	6.89	3.08	750	8.32E-04	2.84E-03	2.01E-03

300 kDa

Time (hrs)	pH (initial)	pH (final)	Vol 3.6N HCl added (uL)	actual incr in H+ conc (moles/L)	Theor incr in H+ conc (moles/L)	Diff bet theor and actual
0	5.7	2.99	400	1.02E-03	1.52E-03	5.00E-04
0	5.76	3.07	350	8.51E-04	1.33E-03	4.79E-04
1	6.41	3.09	550	8.13E-04	2.08E-03	1.27E-03
1	6.28	3.07	500	8.51E-04	1.90E-03	1.05E-03
3	6.76	3.07	650	8.51E-04	2.46E-03	1.61E-03
3	6.78	3.1	550	7.94E-04	2.08E-03	1.29E-03
5	6.94	3.08	650	8.32E-04	2.46E-03	1.63E-03
5	6.86	3.09	650	8.13E-04	2.46E-03	1.65E-03
8	6.93	3.07	700	8.51E-04	2.65E-03	1.80E-03
8	6.85	3.07	700	8.51E-04	2.65E-03	1.80E-03

Appendix 29. DOC fluorescence (courtesy of Susan Winch)

'*' Denotes user modified

Sample Name	TOC Area (cts)	ppm	
	0	223	
	5	3062	
	10	5771	
	25	12823	
	50	24446	y = 479.78x + 628.92
AB34	4001	7.028388	
AB35	3931	6.882488	
AB40	2391	3.672683	
AB220	3067	5.081662	
CSL2	4663	8.408187	
CSL5	6318	11.85768	
DA2	5238	9.606653	
DA4	6255	11.72637	
DA9	6544	12.32873	
DF2	19481	39.29318	
DF4	6200	11.61174	
DF5	5572	10.30281	
DF7	6634	12.51632	
DF9	10663	20.91392	
K1	4759	8.608279	
K2	5746	10.66547	
K3	5277	9.68794	
K4	6581	12.40585	
K8	7296	13.89612	
N35	3524	6.034182	
N43	5941	11.07191	
N55	3935	6.890825	
N70	3898	6.813706	
N89	6839	12.9436	
25 ppm check	13737	27.32102	Note: check standard was after DF2 and before DF4+D16
25 ppm check	13563	26.95836	Note: check standard was after N35 and before N 43

Appendix 30. pH experiment of N55

pH	Time (hrs)	MeHg conc (ppt)	Log10 MeHg
4.5	0	1.33	0.12
	0	1.47	0.17
	4	0.13	-0.87
	4	1.03	0.01
	7	1.13	0.05
	7	1.23	0.09
6.5	0	1.52	0.18
	0	1.29	0.11
	4	1.43	0.15
	4	1.36	0.14
	7	1.17	0.07
	7	1.10	0.04
7.7	0	1.03	0.01
	0	1.58	0.20
	4	1.39	0.14
	4	1.45	0.16
	7	0.98	-0.01
	7	0.99	-0.01

Appendix 31. pH experiment of DA9.

pH	Time (hrs)	MeHg conc (ppt)	Log10 MeHg
4.4	0	1.39	0.14
	0	1.55	0.19
	4	0.95	-0.02
	4	0.96	-0.02
	6	0.94	-0.02
	6	0.65	-0.19
6.4	0	0.83	-0.08
	0	1.44	0.16
	4	0.97	-0.01
	4	1.09	0.04
	6	1.17	0.07
	6	1.03	0.01
7.6	0	0.85	-0.07
	0	1.14	0.06
	4	1.11	0.04
	4	1.02	0.01
	6	1.21	0.08
	6	0.88	-0.06

Appendix 32. pH experiment of K2.

pH	Time (hrs)	MeHg conc (ppt)	Log10 MeHg
4.46	0	1.51	0.18
	0	1.68	0.23
	4	1.44	0.16
	4	1.48	0.17
	6	1.47	0.17
	6	1.21	0.08
6.53	0	1.11	0.05
	0	1.23	0.09
	4	1.32	0.12
	4	1.37	0.14
	6	1.18	0.07
	6	1.25	0.10
7.44	0	1.30	0.12
	0	1.41	0.15
	4	1.57	0.20
	4	1.43	0.15
	6	1.28	0.11
	6	1.44	0.16

Appendix 33. pH experiment of K3.

pH	Time (hrs)	MeHg conc (ppt)	Log10 MeHg
4.06	0	2.86	0.46
	0	1.67	0.22
	4	0.89	-0.05
	4	1.10	0.04
	6	0.71	-0.15
	6	1.06	0.03
6.41	0	1.70	0.23
	0	1.87	0.27
	4	1.05	0.02
	4	0.73	-0.14
	6	0.82	-0.08
	6	1.49	0.17
7.5	0	1.40	0.15
	0	1.19	0.08
	4	0.96	-0.02
	4	0.73	-0.14
	6	0.87	-0.06
	6	1.01	0.00

Appendix 34. Ultraviolet radiation intensities for rooftop incubations of DA9, N55, K2 and K3

Lake	Time (hrs)	UVA (320-400 nm) (W/cm^2nm)	UVB (280-320 nm) (W/cm^2nm)
DA9	0	2.98×10^{-3}	4.95×10^{-5}
	4	3.72×10^{-3}	9.48×10^{-5}
	4(B)	2.18×10^{-3}	5.88×10^{-5}
	6	2.04×10^{-3}	4.58×10^{-5}
N55	0	2.29×10^{-3}	3.20×10^{-5}
	4	5.64×10^{-3}	1.31×10^{-4}
	7	3.84×10^{-3}	7.37×10^{-5}
K2	0	6.87×10^{-4}	8.87×10^{-6}
	1.5	2.51×10^{-3}	5.24×10^{-5}
	4	2.31×10^{-3}	6.37×10^{-5}
	5	4.58×10^{-3}	1.08×10^{-4}
K3	0	1.18×10^{-3}	2.80×10^{-5}
	2	3.74×10^{-3}	8.84×10^{-5}
	4	4.23×10^{-3}	1.08×10^{-4}
	6	3.29×10^{-3}	7.78×10^{-5}

Appendix 35. Dark incubation time course experiment

Sample	time (hrs)	conc MeHg (ng/L)
300K/30K/R	12	4.31
	24	1.63
	36	2.99
	48	3.37
300K/30K/F	24	0.41
	36	0.85
	48	0.77
300K/5K/R	12	1.33
	24	0.38
	48	1.56
300K/5K/F	12	0.53
	24	0.15
	48	0.81
30K/5K/F	12	4.33
	24	0.25
	48	0.54
30K/5K/R	12	2.62
	24	1.06
	48	2.22